NEW APPROACHES IN CALIBRATION FOR MULTI-ELEMENT LASER ABLATION INDUCTIVELY COUPLED PLASMA MASS SPECTROMETRY ANALYSIS

Kristina Mervič

Doctoral Dissertation
Jožef Stefan International Postgraduate School
Ljubljana, Slovenia

Supervisor: Dr. Vid Simon Šelih, National Institute of Chemistry, Ljubljana, Slovenia
Co-Supervisor: Dr. Martin Šala, National Institute of Chemistry, Ljubljana, Slovenia

Evaluation Board:
Prof. Dr. Tea Zuliani, Chair, Jožef Stefan Institute, Ljubljana, Slovenia
Asst. Prof. Paula Pongrac, Member, Biotechnical Faculty, University of Ljubljana, Ljubljana, Slovenia
Dr. Pascal Bohleber, Member, Alfred-Wegener-Institute Helmholtz Zentrum für Polar- und Meeresforschung, Bremerhaven, Germany

MEDNARODNA PODIPLOMSKA ŠOLA JOŽEFA STEFANA
JOŽEF STEFAN INTERNATIONAL POSTGRADUATE SCHOOL

Kristina Mervič

NEW APPROACHES IN CALIBRATION FOR MULTI-ELEMENT LASER ABLATION INDUCTIVELY COUPLED PLASMA MASS SPECTROMETRY ANALYSIS

Doctoral Dissertation

NOVI PRISTOPI H KALIBRACIJI ZA VEČELEMENTNE ANALIZE Z LASERSKO ABLACIJO Z INDUKTIVNO SKLOPLJENO PLAZMO V MASNI SPEKTROMETRIJI

Doktorska disertacija

Supervisor: Dr. Vid Simon Šelih

Co-Supervisor: Dr. Martin Šala

Ljubljana, Slovenia, May 2024

"Live as if you were to die tomorrow. Learn as if you were to live forever."

(Mahatma Gandhi)

Acknowledgments

First of all, I would like to thank my supervisors Dr. Martin Šala and Dr. Vid Simon Šelih for their guidance, support and encouragement throughout my doctoral studies. Especially for their patience in the beginning when I was still trying to find my footing in the field of laser ablation. Thank you for guiding me every step of the way, involving me in your research and providing me with some truly great opportunities.

I would like to thank the Department of Analytical Chemistry (D04) for providing me with an encouraging environment for my academic development. I would especially like to express my gratitude to Dr. Johannes Teun Van Elteren for his academic support, as well as all my current and former office colleagues for their encouraging "pep talks", coffee breaks, and positive energy.

I would also like to thank committee members Dr. Tea Zuliani, Dr. Paula Pongrac, and Dr. Pascal Bohleber for evaluating this dissertation.

Special thanks to Dalia for her assistance in designing graphical abstracts and figures that greatly enhanced our papers.

This work was made possible by the financial support of my doctoral studies by the Slovenian Research Agency. I was included in the core research funding No. P1-0034, which enabled me to pursue my research goals and contribute to the advancement of knowledge in my field.

Finally, I would like to thank my family and friends (those close and far away) who have stood by my side since day one. Their constant encouragement, and understanding have helped me get through the ups and downs of graduate school. A special thank you goes to my parents, whose support in all my endeavors has been invaluable. They taught me the important things in life and sparked my curiosity from day one. Without them, I would not be where I am today.

Abstract

One of commonly used analytical technique for direct elemental analysis of solid samples is Laser ablation inductively coupled plasma mass spectrometry (LA-ICP-MS). Although widely used for the analysis of various samples, obtaining accurate quantitative results remains a major challenge as matrix-matched standards are required. The aim of this thesis was to overcome these calibration issues by improving the quantitative capabilities of LA-ICP-MS through a comprehensive understanding of the factors affecting the processes and the introduction of a novel calibration approach based on ablated volume correction.

To understand the single pulse response (SPR) and the signal-to-noise ratio (S/N) of the measurement, it was essential to study the factors influencing the relationship between the stoichiometry of the sample and ablated and subsequently analyzed sample aerosol. We investigated the elemental fractionation during LA-ICP-MS analysis, focusing on the influence of fluence on the signal-to-noise ratio and the formation of double washout peaks. Systematic experiments and evaluation were used to gain deeper insight into these factors, allowing the development of strategies to mitigate their effects on the analysis results. An important contribution of this work was the introduction of a new calibration approach that eliminated the need for matrix-matched standards. By using 3D profilometry as a complementary tool, the morphology of the sample surface (e.g. ablated volume) was accurately determined after LA-ICP-MS analysis. This enabled the normalization of ICP-MS signals independent of matrix-matched standards or internal standardization methods and improved the accuracy and reliability of quantitative measurements.

The developed calibration approach was rigorously evaluated by bulk analysis and 2D mapping/imaging studies. All analytically relevant instrumental parameters were carefully optimized and the methods were partially validated and compared with existing techniques such as scanning electron microscopy. The results demonstrated the effectiveness of the new calibration approach in the accurate and precise quantification of elements in a wide range of sample types and matrices. Furthermore, the applicability of the developed calibration approach was demonstrated by the successful analysis of standard materials with different compositions. The thesis concludes with a discussion of the implications of these results for the wider field of elemental analysis and suggests avenues for future research to further develop LA-ICP-MS calibration methods.

Overall, this work represents an important step in overcoming calibration problematics in LA-ICP-MS analysis and sets the way for improved quantitative measurements in various scientific disciplines.

Povzetek

Ena od pogosto uporabljenih analitskih tehnik za neposredno elementno analizo trdnih vzorcev je masna spektrometrija z lasersko ablacijo in induktivno sklopljeno plazmo (LA-ICP-MS). Čeprav se pogosto uporablja za analizo različnih vzorcev, je pridobivanje natančnih kvantitativnih rezultatov še vedno velik izziv, saj so potrebni z matriko usklajeni standardi. To predstavlja velik izziv za kalibracijo in posledično za pridobitev natančnih in zanesljivih kvantitativnih rezultatov. Glavni cilj tega doktorata je bil odpraviti težave s kalibracijo in tako izboljšati kvantitativne zmogljivosti LA-ICP-MS preko boljšega razumevanja dejavnikov, ki vplivajo na procese, in z uvedbo novega kalibracijskega pristopa, ki je temeljil na korekciji abliranega volumna.

Za razumevanje odziva posameznega pulza in razmerja med signalom in šumom (S/N) je bilo bistveno raziskati dejavnike, ki vplivajo na razmerje med stehiometrijo vzorca ter abliranim in nato analiziranim aerosolom vzorca. Raziskali smo frakcioniranje elementov med analizo LA-ICP-MS, s poudarkom na vplivu fluence na razmerje med signalom in šumom ter na nastanek dvojnih vrhov. S sistematičnimi poskusi in vrednotenjem je bil pridobljen globlji vpogled v te dejavnike, kar je omogočilo razvoj strategij za ublažitev njihovega vpliva na rezultate analize.

Pomemben prispevek tega dela je bila uvedba novega pristopa kalibracije, ki odpravlja potrebo po uporabi matrično ujemajočih standardov. Z uporabo 3D profilometrije kot dopolnilnega orodja je bilo mogoče po analizi LA-ICP-MS natančno določiti morfologijo površine vzorca (npr. ablirani volumen). To je omogočilo normalizacijo signalov ICP-MS neodvisno od matrično ujemajočih se standardov ali metod notranje standardizacije in s tem izboljšalo natančnost in zanesljivost kvantitativnih meritev.

Razviti kalibracijski pristop je bil natančno ovrednoten s pomočjo analize osnovnega vzorca in 2D oslikovanja z LA-ICP-MS. Vsi analitično pomembni instrumentalni parametri so bili skrbno optimizirani, metode pa so bile delno potrjene in primerjane z obstoječimi tehnikami, kot je vrstična elektronska mikroskopija. Rezultati so dokazali učinkovitost novega kalibracijskega pristopa pri natančni in precizni kvantifikaciji elementov v številnih vrstah vzorcev in matric. Poleg tega je bila uporabnost razvitega kalibracijskega pristopa dokazana z uspešno analizo standardnih materialov z različnimi sestavami. Delo se zaključi z razpravo o posledicah teh rezultatov za širše področje elementne analize trdnih vzorcev in predlaga možnosti za prihodnje raziskave za nadaljnji razvoj kalibracijskih metod LA-ICP-MS.

Ta disertacija predstavlja pomemben korak pri premagovanju težav s kalibracijo pri analizi LA-ICP-MS in utira pot za boljše kvantitativne meritve v različnih znanstvenih disciplinah.

Contents

List of Figures

List of Tables

Abbreviations

2D	. . . two-dimensional
3D	. . . three-dimensional
AI	. . . artificial intelligence
CMG	. . . Corning Museum of Glass
CRM	. . . certified reference material
EPMA	. . . electron probe microanalyzer
HI-RES	. . . high resolution
GeoReM	. . . Geological and Environmental Reference Materials
ICP	. . . inductively coupled plasma
IDA	. . . isotope dilution analysis
IPS	. . . International Postgraduate School
JSI	. . . Jožef Stefan Institute
LA	. . . laser ablation
MS	. . . mass spectrometry
MS/MS	. . . tandem mass spectrometry
Nd:YAG	. . . neodymium:yttrium-aluminum-garnet
NIST	. . . national Institute of Standards and Technology
PM	. . . particulate matter
PMMA	. . . poly(methyl methacrylate)
Q	. . . quadrupole
QMS	. . . quadrupole mass spectrometry
SEM-EDXS	. . . scanning electron microscopy coupled with energy dispersive X-ray spectroscopy
S/N	. . . signal to noise ratio
SPR	. . . single pulse response
SRM	. . . standard reference material
TOF	. . . time-of-flight
TOFMS	. . . time-of-flight mass spectrometry
UV	. . . ultraviolet

Glossary

Acquisition time is the total amount of time needed for the acquisition of all elements per one data point.

Dwell time is the amount of time ICP-MS uses within acquisition time to measure specific element.

Single pulse response time/Washout time is the time needed to transfer 99% of ablated particles produced by a single shot out of the ablation chamber.

Fluence is the energy density of laser expressed in J cm^{-2}.

Dosage is the number of overlapping laser pulses per pixel. In this dissertation, mapping was achieved by measuring lines with continuous movement of the stage, meaning the dosage refers to laser pluses that are partially overlapped. The smear that is produced in this measurement mode is compensated with the drastic improvement in time required for the analysis. Using a higher dosage also increases the signal-to-noise ratio.

Chapter 1

Introduction

The commercialization of inductively coupled plasma mass spectrometry (ICP-MS) began in 1984, followed by the very early integration of laser ablation (LA) as a sampling and sample introduction device in 1985 when it was used for analyzing the elemental and Pb isotopic composition of granites [1]. However, its full potential wasn't recognized until the early 1990s, mostly for microanalysis of trace element composition and U-Pb isotopic age determination of geological samples [2, 3]. Since then, laser ablation inductively coupled plasma mass spectrometry (LA-ICP-MS) has gained importance and is now a widely used method for direct elemental analysis of solid samples. The technique is characterized by high analytical sensitivity, excellent detection limits and a very wide linear dynamic range of up to twelve orders of magnitude. LA-ICP-MS also provides information on major, minor and trace elements and enables microanalysis, two-dimensional elemental mapping and depth profile analysis. Through microdestructive direct sampling, the technique also avoids the loss of analytes or contamination during preparation procedures. In contrast to other techniques, LA-ICP-MS introduces the sample into the ICP under "dry plasma" conditions, which improves atomization and ionization and reduces matrix effects [4, 5]. Laser ablation has also undergone some important developments in recent years, such as the development of fast washout cells, which significantly increase the speed of analysis by reducing the response time of a single pulse to as little as 1 ms, compared to the typical 500 ms for conventional systems [6]. This advance enables much faster mapping, allowing either a larger area to be covered or smaller measurement points to be used without increasing the duration of the experiment. In addition, rapid aerosol transport has increased sample throughput, resulting in higher signals and a better signal-to-noise ratio, thereby improving sensitivity [7-9]. In addition, significant improvements in instrument hardware and a better understanding of the effects of operating conditions on image quality have made LA-ICP-MS mapping not only faster but also more powerful. Optimization of laser ablation parameters to avoid mapping artifacts such as smearing, noise, blurring, and aliasing have led to the creation of high-quality 2D LA-ICP-MS (multi-)element maps [10-12]. Moreover, the introduction of ICP time-of-flight (TOF) MS instruments represents a significant advance in this field. In contrast to conventional sequential quadrupole mass analyzers, ICP-TOF-MS enables simultaneous analysis of the entire elemental spectrum. This technology has found diverse applications ranging from thin biological tissue samples to meteorites. When combined with laser ablation, LA-ICP-TOF-MS becomes a powerful tool for comprehensive sample characterization, enabling the simultaneous detection of ions over the entire elemental m/z range while minimizing sample consumption [8, 13-16]. Due to the many advantages of laser ablation, the number of reported applications has vastly increased over the last decade and the range of applications is becoming wider and wider.

However, the calibration of LA-ICP-MS requires a specific approach. Despite advances in quantification techniques and laser technology, commercial calibration standards are still of limited availability. Therefore, the matrix dependence of the signal remains a major challenge. Various strategies have been proposed for calibration, with solid matrix-matched standards often recommended. However, the preparation of such standards can be time-consuming and lead to unknown homogeneity, which can affect the precision of the analysis. In addition, unrecognized matrix interferences can affect the accuracy of laser ablation, especially when non-matrix matched standards are used. Nevertheless, such standards are still commonly used [17]. It is crucial to understand the design and operation of the LA-ICP-MS in order to properly assess these calibration challenges.

1.1 LA-ICP-MS

The core components of a basic LA-ICP-MS setup include a pulsed laser source, beam delivery optics, an airtight sampling cell, an aerosol transport line (LA part of the setup) and an ICP-MS detector, as shown in Figure 1. To achieve accurate analysis, certain conditions must be met, such as representative aerosol composition, high transport efficiency and complete decomposition, atomization and ionization of particles inside the ICP and reaching the MS due to the heterogeneity and size structure of aerosols generated by laser ablation. LA-ICP-MS can be divided into three main phases: Sampling (laser ablation), particle decomposition, atomization and ion production (inductively coupled plasma) and ion separation (mass spectrometer). In the sampling phase, the sample introduction system consists of an airtight cell, a laser with associated optics and tubes for transporting the gas stream to the ICP. In the cell, the laser converts the sample into aerosol particles, which are then transported to the ICP via a helium gas flow. Upon entering the ICP, the sample aerosol is further vaporized, atomized and ionized in the plasma. The ions are then separated in the mass spectrometer (MS) on the basis of their mass-to-charge ratio. Finally, the intensity of the ion beam, which indicates the concentration, is converted into an electrical signal which is measured and recorded [18-20]. Each step of this process is explained in more detail below.

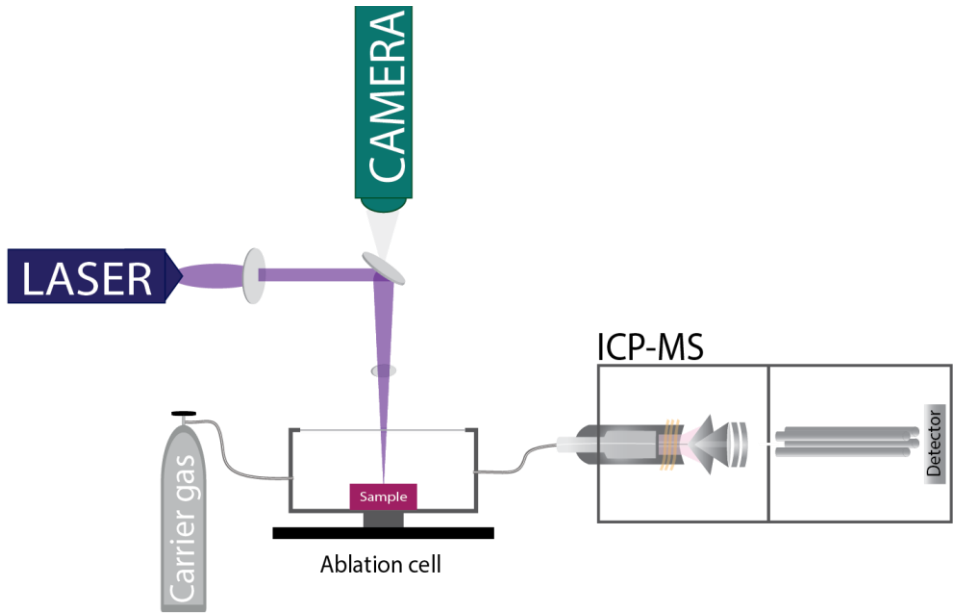

Figure 1: A fundamental configuration of an LA-ICP-MS setup designed for sampling solid materials, illustrating its primary elements.

1.1.1 Laser ablation

Laser ablation is a complicated sampling system that consists of a series of special mirrors and/or prisms and lenses that direct, shape and form the laser beam and then focus it on the sample. It all starts with the laser source itself (so called laser head), which must have sufficient power. There are various lasers on the market. In the past, Nd:YAG (neodymium:yttrium-aluminum-garnet) solid state lasers in the nanosecond (5 – 10 ns) pulse duration range were generally used for representative sampling. Their fundamental wavelength is 1064 nm, but by using suitable non-linear optics, the frequency of the laser can be multiplied, resulting in 532 nm, 355 nm, 266 nm or 213 nm wavelengths, out of which 266 nm and 213 nm were most commonly used. Nowadays, however, excimer ArF lasers with a higher energy wavelength of 193 nm are mainly used, as the shorter wavelengths couple better with the materials and utilize the energy more efficiently, as only a small fraction is transformed into heat. They also offer several advantages over solid state lasers, such as very high energy density and stability, also as the laser emits at fundamental wavelength, there is no need for special non-linear optics. In contrast, longer wavelengths couple worse with the materials, and more energy is transformed into heat, which besides ablation also leads to melting of the sample and contributes to elemental fractionation. This has been observed with nanosecond laser sources and leads to preferential evaporation, especially when analyzing metals and semiconductors. Furthermore, due to the “long” duration of the laser pulse event, part of the pulse energy is absorbed by the plasma formed above the irradiated area, which can change the composition of the aerosol particles formed during the expansion. Zone heating and plasma shielding are influenced by the duration of the laser pulse, which in turn affects the dynamics of the laser ablation process. To mitigate the "heating" effect" and improve the ablation properties, the use of even shorter laser pulses in the femtosecond range has been proposed. Extensive studies have shown that the aerosols generated by femtosecond laser ablation consist mainly of mesoscopic particles with a size of around 10 nm to 100 nm and form fractal aggregates whose composition varies depending on the particle size [18, 19, 21-24].

1.1.2 Aerosol formation and transportation

The generation of aerosols during laser ablation is due to a variety of mechanisms, following the transfer of the energy from the laser to the sample surface, including condensation from supersaturated vapor, phase separation at the critical point, phase explosion, and hydrodynamic instabilities. Of these mechanisms, condensation growth is thought to be the primary process, where particles smaller than 100 nm are mainly formed due to the rapid cooling of the expanding material [25]. However, microscopic examination of the images of ablated material deposited on filters using scanning electron microscopy has revealed the presence of particles significantly larger than 100 nm, particularly when laser ablation is performed in an ambient atmosphere with energy densities above the LA threshold ($>>1$ J/cm^2) or in an argon environment. These larger particles can result from simultaneous processes such as aggregation of already solidified particles, coalescence or phase explosion and serve as a source for smaller and larger particles. As a result, aerosols generated by femtosecond (fs) and nanosecond (ns) laser ablation have heterogeneous composition, which can lead to material loss during transport due to various factors such as diffusion, electrostatic forces, inertial effects and gravitational forces (inertial and gravitational settling). Extensive research has focused on understanding these compositional changes as they can affect the accuracy of the analysis. While older studies indicated inconsistent transport efficiency values, ranging from 10% to 60% depending on

the method, more recent evidence suggests higher efficiencies of > 70-90%, which appear to be less dependent on flow conditions, cell geometry and volume. This means that most common transport systems and laser ablation cells are suitable for analysis as they differ only minimally in their overall throughput and resulting sensitivity [19, 25]. The selection criteria for the optimal system are primarily based on practical considerations, such as ease of sampling and the degree of aerosol dispersion within the transport tube, which influences precision and accuracy to some extent. While a high degree of aerosol dispersion is usually desirable, for certain applications, such as large area mapping or 3D analysis, minimal dispersion may be required. Traditionally, the design of laser ablation cells and transport lines has relied on time-consuming trial-and-error methods, but in recent years computer modeling has emerged as a promising alternative approach [26].

1.1.3 Inductively coupled plasma mass spectrometry system

In the field of ICP-MS, the analysis process is based on a dynamic interaction of components that outline its essential areas. The ions of the analyte materialize in the atmospheric pressure environment of the ICP torch and then require a vacuum environment for their detection in the mass spectrometer itself. This task is assigned to the differential vacuum system comprising of sampler-skimmer cones system, which is strategically located immediately after the ICP torch, then a set of various electrostatic lenses shape and form the ion beam, entering the mass analyzer. Mass analyzer then discriminates ions based on their mass-to-charge ratio (m/z) while an ion detector measures the intensity of the ions. The landscape of ICP-MS analysis unfolds through different modalities, each tailored to specific sensitivity, precision and resolution requirements. There are a variety of options ranging from the versatile quadrupoles (Q) to the precision-driven high-resolution magnetic sectors (HI-RES) to the fast throughput of time-of-flight (TOF) instruments. Table 1 gives a comprehensive overview of the available configurations and illustrates the different analysis methods. With the exception of TOF detectors, today's detectors have a wide linear dynamic range that allows the simultaneous detection of major and trace elements in up to twelve orders of magnitude. In routine analysis, ICP-Q-MS is the preferred choice as it offers a good balance between affordability, robustness and rapid data acquisition [27].

Table 1: Types of currently available configurations for ICP-MS instruments.

	Time of flight (TOF)	Quadrupole (Q)	HI-RES single collector	HI-RES multi collector
Sensitivity (signal per unit concentration	Low	Medium to high	High	High
Speed – time to change from one selected mass to another	Simlutaneous measurement (no time)	Fast	Depends upon the magnitude and number of jumps	No mass jumps are usually implemented
Cost	€€	€	€€	€€€
Applications	Extremely fast scanning capabilities	General use for elemental and isotopic analysis	General use for elemental and isotopic analysis	High precision isotope ratio

1.2 LA-ICP-MS Application

In the beginning, LA-ICP-MS has been mostly used in geology to analyze the isotopic composition of rocks, study the formation of mineral deposits and investigate the evolution of magma [28-31]. Since then its application range has spread to a variety of scientific fields (e.g. biological, environmental, material and forensic sciences) due to its high sensitivity, spatial resolution and minimal/no sample preparation [32, 33]. Marine research in particular benefits greatly from LA-ICP-MS, as chemical archives of environmental changes can be created by analyzing marine samples such as shells, corals and fish otoliths [34, 35]. For example, elemental analysis of corals provides information on natural and anthropogenic changes in reef environments, as observed in the Great Barrier Reef in Australia [34]. In addition, elemental analysis of fish otoliths helps to assess migration patterns and environmental conditions [35]. Beyond marine research, the utility of LA-ICP-MS also extends to ornithology, where it helps to determine elemental profiles of feather shafts that provide information on environmental pollution in bird habitats [36]. Plant material is also often analyzed with LA-ICP-MS to evaluate the distribution of elements in relation to pollution sources and to gain insight into contaminant levels [37, 38]. LA-ICP-MS also proves useful in the analysis of soils, sediments, particulate matter and ice samples, facilitating the measurement of trace metal concentrations and elemental analysis [39-42]. Another field for LA-ICP-MS application is forensic science, where it is utilized for analysis of trace elements in forensic samples such as hair and tissue as well as the analysis of gunshot residue in criminal investigations [43-46]. This technique is also applied for characterization of various materials (ceramics, polymers, metals and coatings) to investigate material properties, determining elemental composition and identifying impurities. For example, LA-ICP-MS has been used to evaluate the purity of semiconductor materials, investigate corrosion processes and analyze trace elements in archeological artifacts [32, 47-53]. A more recent area where LA-ICP-MS is being used is in the analysis of nanoparticles to better understand their behavior in light of increasing concerns about their impact on the environment. Through size characterization, spatial distribution and elemental composition analysis using LA-ICP-MS, the transport of nanoparticles in aquatic systems is assessed, their uptake and distribution in biological tissues is investigated and their interactions with organisms are explored [54-58]. Another pressing issue is the presence of microplastic particles, especially concerning their sources and environmental spread. Consequently, LA-ICP-MS has recently been employed to examine microplastic particles in biological, water, and sediment samples. This analysis aims to determine their elemental composition and size range, enhancing our understanding of the impact of microplastic pollution on ecosystems [59-62]. Overall, LA-ICP-MS proves to be a versatile analytical tool with numerous applications across various scientific disciplines.

1.3 Quantification Methods

As mentioned above, LA-ICP-MS is widely appreciated for its many advantages, such as minimal or no sample preparation, high sample throughput, access to isotopic information, and the ability to analyze both conductive and non-conductive, opaque and transparent materials. Nevertheless, the laser ablation process is influenced by various phenomena that need to be carefully considered during the analysis. Factors such as the sample physical and chemical properties, its homogeneity as well as methods to compensate for signal fluctuations or ablated mass must be considered [17, 63]. A comprehensive review of several research papers shows several "ideal" conditions for analyzing solid samples with LA-ICP-MS. First and foremost, minimizing evaporation (in contrast to ablation) and melting of

sample constituents in the crater region is critical. It is important that the removed aerosols have a stoichiometric composition that matches the original solid sample. In addition, the generation of uniformly sized particles during the ablation process is critical to ensure efficient transport to the ICP without losses. Finally, the particles must be sufficiently small to ensure complete decomposition, atomization and ionization in the ICP torch and thus avoid fractionation effects [64-66]. From the preceding discussion, it is clear that the effectiveness of LA-ICP-MS as a universal technique for the direct analysis of solid samples depends on two main conditions.

First, the abundances of the detected ions after m/z separation often do not fully correspond to the composition of the original sample. This phenomenon is commonly referred to as "elemental fractionation" and includes various effects such as particle size-dependent fractionation, preferential evaporation of volatile elements and isotope-specific fractionation. In addition to the transport of the aerosol particles into the ICP and the subsequent evaporation, atomization and ionization processes in the ICP, the ablation process itself also contributes significantly to fractionation. The literature review shows that the efficiency of laser ablation depends on factors such as pulse length, laser wavelength, fluence, ratio between crater depth and diameter and the composition of the sample. There are some strategies to minimize fractionation, such as creating well-defined craters, using short laser wavelengths for high absorption, fine-tuning the gas flow and flow dynamics of ablation cells in general, using short pulse duration lasers, and preventing redeposition of particles on the sample surface.

Secondly, differences in the interaction between the laser beam and the sample surface for various matrices lead to changes in the analyte mass ablated per pulse. These differences in matrix properties, such as absorptivity, reflectivity and thermal conductivity, lead to variations in the size and geometry of aerosol particles which affect the efficiency of sample transport from the ablation cell to the plasma. Together, these limitations contribute to matrix effects that lead to variations in plasma mass loading. Consequently, sample-related matrix effects affect the accuracy of LA-ICP-MS analysis and pose a challenge for quantification. This complication is related to elemental fractionation and results in LA-ICP-MS signals that may not accurately reflect the elemental composition of the analyzed sample. Consequently, the absolute signal intensity or sensitivity may differ significantly for samples with identical analyte concentrations but different matrix compositions or physical properties. The growing interest in the application of LA-ICP-MS in various scientific disciplines has led researchers to attempt to overcome these limitations. Much of this work has focused on the influence of laser wavelength and pulse duration. For example, studies have shown that use of either shorter wavelengths or femtosecond lasers, significantly reduces element fractionation and attenuates matrix effects [63].

1.3.1 Signal correction approaches

Signal normalization protocols are often used in LA-ICP-MS analysis to obtain more accurate quantitative results, as the accuracy and precision of LA-ICP-MS are generally worse than those of conventional or solution mode ICP-MS. Several methods have been proposed to improve the precision of laser ablation ICP-MS: Monitoring of the signal emitted from the laser-induced plasma (LIP) or scattered light during sample transportation; shot-to-shot normalization; monitoring of acoustic waves generated during laser ablation; internal standardization, *etc.* [67-70]. These approaches take into account deviations caused by instrumental drift, matrix effects and element fractionation. Internal standards are mostly used to combat this problem and preferably also to correct for differences in mass removed and transported to the ICP-MS. In conventional ICP-MS,

internal standards are routinely used to improve the accuracy and precision of solution nebulization, similarly, they enable a more accurate determination in LA. The signals for quantitative LA-ICP-MS analysis are usually normalized using an isotope of the main matrix element that is homogeneously distributed over the sample and whose concentration is known. If no suitable elements are available, an additional standard can be used or a sum normalization procedure can be applied [71-73].

1.3.1.1 Internal standardization

LA-ICP-MS usually uses either intrinsic elements present in the sample and standard or additionally introduced non-intrinsic elements for signal normalization. Not many elements are suitable for use as internal standards, as they must be homogeneously distributed in the sample and standard and behave similarly to the analyte during ablation, transport and ICP detection. In addition, the internal standards must have a similar first ionization potential and/or a similar atomic mass as the analyte itself [74].

In biological samples, carbon is one of the most commonly used elements for signal normalization, as it was assumed to be homogeneously distributed and also has the ability to correct for differences in the water content of samples and reference materials. However, its suitability as an internal standard has been studied in detail over the years. Frick and Gunther discovered in their studies that ^{13}C in aerosols exhibits a two-phase, matrix-dependent formation containing particular and gaseous species [75]. The partial formation of gaseous carbon species can lead to inaccurate analysis of the target analyte, as most elements are transported exclusively in a particulate phase. On the other hand, Austin *et al.* found that despite its disadvantages ^{13}C can be used as an internal standard under certain conditions [74]. However, due to the complexity of biological matrices (*e.g.* plants, *etc.*) and the segmentation of elements in certain compartments of biological samples, carbon is still often used as an internal standard to improve quantitative analysis [76-81]. In addition, ^{34}S has been successfully used as an internal standard in various LA-ICP-MS studies of hair and nails, as it is one of their major constituents and theoretically evenly distributed [82-84]. In calcium-based samples (bones, teeth, *etc.*) and geological samples, ^{43}Ca is often used as an internal standard because it has a better signal intensity and signal-to-background ratio than ^{44}Ca and is homogeneously distributed [85-90]. When using glass standard reference materials (*e.g.* NIST SRM 61X series), ^{29}Si is often used as the internal standard [91]. In another study, ^{57}Fe and ^{60}Ni were used to compensate for the variations of signal in multi-elemental analysis of low-alloy steel samples [67].

As mentioned above, there are not many elements that are naturally present in the samples and fulfill all the criteria to serve as an internal standard. Therefore, non-intrinsic elements are sometimes used, which are introduced into standards and samples via various strategies. The non-intrinsic elements are usually not present in the sample or only present in trace amounts and are added to the sample/standard by different methods: direct addition to the sample (*e.g.* whole blood samples); addition of a thin polymer, metal or gelatin layer with internal standard element under the sample; deposition of the internal standard on the sample by sputtering techniques or inkjet printers, *etc.* The main goal of all strategies is to achieve a homogeneous distribution and to use elements that have no/low background signals, are not affected by spectral interferences and have a first ionization potential comparable to the analytes of interest [92-99].

1.3.1.2 Signal sum normalization

In signal sum normalization approach, signals from all elements (or as many as possible) are acquired and it is assumed that their sum or sum their oxides reflect the ablated mass. If these techniques are considered as independent methods for direct measurement of the ablated mass, only semi-quantitative information is obtained. However, if the entire sample matrix is used as a single internal standard, signal variations can be compensated and the precision of LA-ICP-MS analyzes can be improved. This normalization strategy, in which the individual element signals are treated as a function of the summed signals of all sample components, has been shown to be immune to matrix effects and enables the rapid determination of major, minor and trace elements with satisfactory precision and accuracy. For example, Chen *et al.* applied a normalization strategy together with an external calibration using reference silicate glasses to determine fifty-four major and trace elements in carbonate [100]. Similarly, van Elteren *et al.* used the sum normalization approach to overcome calibration challenges in the quantitative analysis of old glasses. Again, 54 elements were measured simultaneously and normalized to 100 % based on their oxide concentrations. Using SiO_2 as an internal standard, the algorithm adjusts its concentration until the cumulative concentrations of all 54 elemental oxides reach 100 % [w/w]. The accuracy of the results was confirmed by the agreement between found and reported values for major and minor oxides in synthetic glasses with typical medieval compositions [101]. On the other hand, the sum normalization strategy of Latkoczy *et al.* was applied to the analysis of magnesium-based alloys by LA-ICP-MS, where the results for Mg showed good agreement (2.2 %) with quantitative line scans from EPMA measurements [102].

1.3.2 Calibration approaches

Despite all the problems, there are some "general" quantification methods that can be applied to a variety of sample types with different matrix properties. In general, we can distinguish between calibration approaches that are based on matrix-matched standards and those that are not dependent on matrix-matched standards. In order to fully utilize the advantages of dry plasma when working with laser ablation, solid standards are usually used for quantification. Compared to liquid standards, which are readily available, easy to prepare and customizable in terms of elements and their concentration range, solid samples, with few exceptions (*e.g.* glass), are limited in availability and often inhomogeneous on the micrometer scale. As the scope of LA-ICP-MS has expanded from geological to biological samples and everything in between, the lack of commercially available reference materials for the variety of matrices to be analyzed has become increasingly apparent in recent years. This has led to the development of numerous new calibration techniques and the search for suitable matrix-matched standards that can be easily produced in-house. A brief summary of the calibration methods used for LA-ICP-MS analyzes is summarized in Figure 2.

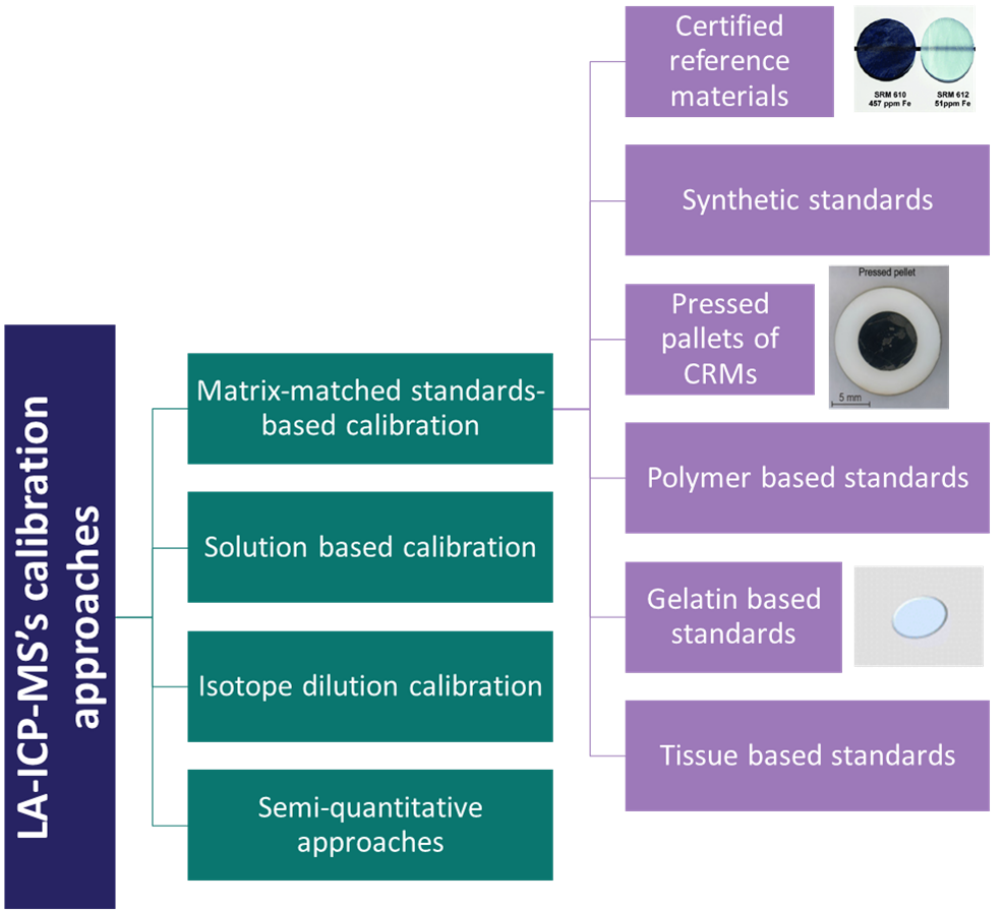

Figure 2: Different calibration strategies commonly used for quantitative LA-ICP-MS analysis.

1.3.2.1 External matrix-matched standards-based calibration

When quantitative analysis is required, the preferred method is external calibration, using a set of known standards to produce single or multi-point calibration curves. These curves allow linear regression analysis to be performed, ensuring accurate quantification. External calibration with matrix-matched standards can generally be divided into two areas: commercial matrix-matched standard reference materials and in-house manufactured matrix-matched standards.

The use of certified reference materials (CRMs) in external calibration is considered the most reliable method for accurate quantification in LA-ICP-MS [20, 22–24]. Ideally, these CRMs match the composition of the sample under investigation as closely as possible, if not exactly, in terms of physical properties, chemical composition and analyte concentration. If this requirement is met, the processes of ablation, transport, atomization and ionization can be considered almost identical for the sample and the standard, allowing reliable quantification. Each CRM is accompanied by a comprehensive certificate containing precise information on the concentrations of the components. In addition, preferred concentration values for non-certified sample components can often be found in the literature [25]. One of the most commonly used CRMs are the commercially available and well-characterized glass standards of the NIST SRM 61X series. They contain major, minor and trace elements with concentrations ranging from 5 to 500 g kg^{-1} depending on the series. Reference glasses are generally regarded as the "to-go" reference materials for LA-ICP-MS calibration, especially for the quantitative analysis of geological samples [66,

89, 103-112]. Due to their availability and ease of use, they are also often used as a reference for sensitivity. In some cases, however, they do not fulfill all the requirements for matrix matching or the actual required concentration range of the analyte. Therefore, various techniques have been developed to produce homogeneous standards that can be used as reference materials for glass and other geological standards (*e.g.* new series of glass standards, direct fusion of rocks, *etc.*) [73].

Another promising method for quantification is the use of matrix-matched calibration standards from materials that have the same/similar matrix as the sample itself to combat the lack of suitable CRMs, especially for environmental, biological or medical samples. Given the complex nature of fractionation, the analytical compatibility of quantitative LA-ICP-MS analysis can be significantly improved by ensuring that both samples and standards exhibit similar behavior during ablation. Various sample preparation techniques are described in the literature, including embedding in polymer resin, melting with borate and preparation of pressed disks in the presence of a binder [113-116]. Calibration with matrix-matched standards can be broadly divided into three types: Standards obtained from powdered matrix reference materials, synthetic standards obtained from the primary sample, and matrix-matched standards obtained from spiked sample materials. These sample preparation techniques offer several advantages, including the ability to incorporate one or more internal standards, known amounts of analytes of interest, or isotope-enriched spikes. They also facilitate the adjustment of analyte concentration as needed. However, it should be noted that this approach is only applicable for powdered samples and that additional sample preparation, *e.g.* by grinding or crushing, is required for samples in compact, native form. Furthermore, adapting the sample matrix in this way inevitably leads to a dilution of the analyte, which can reduce the detection sensitivity of the analytical method. This is particularly difficult with biological tissues with its complex and heterogeneous matrix composition, which makes it difficult to accurately mimic the sample matrix. Consequently, there are many different calibration approaches for biological samples, but none of the quantification methods are universally accepted and harmonized. Most of them focus on the development of in-house manufactured standards that best mimic the analyzed tissue. Over the years, different approaches have been developed using various matrices as a basis.

The production of standards from commercially available CRMs appears to be a practical approach in many cases. Although they are mainly available in powder form, depending on their initial state, some preparation is required prior to analysis, such as additional grinding/milling, pressing into pellets and/or addition of binders (*e.g.* polyethylene powder, *etc.*) to improve the homogeneity and stability of the pellets [104, 117-123]. In addition, the standards prepared based on CRM can be modified by adding selected elements, either to act as internal standards or to achieve the desired concentration range. Many studies have been conducted using different materials and techniques, *e.g.* powdered solid CRMs with binders for the analysis of sediments, ashes and soils [124], nanoparticulate pressed powder pellets from natural rock powder CRM [125], synthetic materials based on TiO2 matrices, *etc.* [126].

Another possibility for the preparation of matrix-matched standards is the use of synthetic standards based on the main component of the sample [127]. Artificial sulfide crystals were used by Dewaele *et al.* as matrix-matched external standards for the quantitative analysis of natural hydrothermal pyrite [128]. To mimic the hair matrix, extracted keratin proteins were also used to produce Pb-enriched keratin films to determine Pb in hair samples by LA-ICP-MS [129]. In another study, trace elements in mussel shells were determined using in-house solid multi-element standards based on $CaCO_3$ matrix [90]. While hydroxyapatite enriched standards were used to quantitatively analyze dorsal fish spine [130].

In addition, in-house produced polymer and gelatin-based standards are often used for the quantitative analysis of biological samples. Numerous LA-ICP-MS studies have explored the effectiveness of polymer and resin-based standards for calibration, as they are adaptable and can be easily customized. Various preparation methods have been developed, such as spin-coating with PMMA solutions spiked with metal standards, which allows careful control of thickness and homogenous elemental distribution [93, 131]. However, this method requires that the composition of the polymer under investigation is known and that the properties of the prepared standards match those of the original sample [93]. Alternatively, aqueous soluble polymers such as dextran have been used to extend the range of elements that can be included in the standards. These polymer-based calibration approaches have been validated using tissue samples and applied to human clinical samples, demonstrating their usefulness in real-world scenarios [132]. Another approach is the production of polymer-based section standards using cold-curing resins, such as Technovit 7100, mixed with metal solutions. These standards have been shown to quantify platinum distribution in tissues of mice treated with chemotherapeutic agents and demonstrate their potential in the evaluation of drug toxicity and efficacy [133]. Recently, an innovative method for the production of polymeric reference materials using 3D printing technology has been proposed, which offers higher concentration accuracy and homogeneity compared to conventional methods [134]. Another method is the dried droplet technique, in which liquid standards are applied directly to solid samples, allowing simultaneous analysis after evaporation of the solvent [135, 136]. Although this method is advantageous for calibration, it also has disadvantages such as the uneven deposition of residues due to the "coffee ring" effect and size discrimination during drying. Despite attempts to mitigate this by ablating the entire residue, the process is time consuming. In addition, dried droplet standards can only be analyzed once, making them impractical for LA-ICP-MS, which must be calibrated for each analysis. Recently, a different approach has been developed in which a commercial sprayer is used to homogeneously apply thin layers of standards of different concentrations onto the sample surface. In this way, the disadvantages of more conventional sample spiking techniques, such as dried droplets or standard addition quantification approaches, which also use the aforementioned sample spiking, are avoided [113]. These advances in polymer-based standards hold promise for improving the precision and reliability of LA-ICP-MS analysis in a wide range of research and clinical applications.

Gelatin has also been shown to provide a soft matrix that is very similar to proteinaceous biological tissue. Gelatin gels are generally readily available, easy to handle, non-toxic and customizable in terms of element selection and concentration range. However, the production of gelatin standards is not as easy as it may seem, and various approaches were developed to obtain highly homogeneous standards, *e.g.*, by printing gelatin standards, using high temperatures during the drying process, complete ablation, production of gelatin microdroplets, rapid drying, *etc.* [137, 138]. Several studies have demonstrated the effectiveness of gelatin-based standards for quantitative bioimaging applications using LA-ICP-MS. Studies comparing gelatin-based standards with tissue-based standards have shown their effectiveness in accurately quantifying elements such as copper. This validation was achieved through various approaches, including comparison of Cu quantification in spiked liver tissue homogenates using thin sections and gelatin droplet standards, as well as cross-validation of calibration approaches such as standard addition and external standardization on different tissue samples [139, 140]. The properties of gelatin allow easy modification and adjustment of analyte concentrations, although increasing the number of elements can lead to problems such as brittleness and precipitation. Gelatin-based calibration standards come in various forms, including microarrays [141], cryo-sections [142-144], molds [145], and bio-printed standards[146], which enable accurate quantification of elements such as gadolinium, iron, copper, and zinc in a medical context.

Gelatin microdroplet standards, produced manually or automatically, offer a high degree of precision and homogeneity and are therefore suitable for metal-based anticancer drug studies and nanoparticle analysis. These gelatin-based standards are commercially available and provide researchers with accessible tools for accurate analysis using LA-ICP-MS [138].

Finally, matrix-matched standards based on spiked sample material are also used in LA-ICP-MS, especially for animal and human tissue. The tissue section standards are usually homogenates of different tissue types, which are spiked with different concentrations of the target analytes depending on the analyte. These spiked homogenates are then dried and cut to the same thickness as the sample [147, 148]. By matching the standard preparation material to the sample, it is conventionally assumed that the interference from the sample matrix is eliminated. Compared to the preparation of gelatin standards, the preparation of tissue standards requires a large amount of labor, skilled professionals and access to a cryotome. In addition, the sample may consist of softer and harder material, which is lost when homogenizing the tissue in the standards. This, together with inaccuracies in thickness between sample and standards, can lead to biased quantitative LA-ICP-MS results, as removing the same amount of ablated material is one of the main requirements of this technique. The development of matrix-matched tissue standards has made considerable progress since the first protocol presented by Becker *et al.* in 2005 [147]. These standards, often derived from the same tissue type as the target species, have been produced using various matrices such as brain, liver, kidney, blood, bone and teeth. For example, in 2013, Hare *et al.* provided a comprehensive guide for the preparation of matrix-matched standards for the assessment of trace metal concentrations in brain tissue [148]. They used cortical tissue from sheep brains spiked with standard solutions of various elements and demonstrated their effectiveness in quantitative analysis. Similarly, matrix-matched standards were used for imaging Zn and Mg in rat brain tissue [149] and for assessing the feasibility of quantitative imaging using tissue homogenates spiked with Se and Fe [150]. In cancer research, liver-based tissue standards have been used to quantify Ru and Pt concentrations in organs and tumor tissues of mice treated with anticancer agents. These standards have also been used to investigate the quantitative distribution of Cu in liver tissue [151]. For hard tissues such as bones and teeth, bones have been evaluated as a matrix for the preparation of calibration standards to quantify tungsten and zinc deposits [152]. Teeth, which provide valuable bioindicators of metal exposure, have been calibrated using a variety of standards, including internally prepared matrix-matched standards from healthy teeth and synthetic hydroxyapatite standards doped with the elements of interest [88, 153, 154]. In hair analysis, spiked hair strands are often used as matrix-matched standards due to the limited availability of certified reference materials. These standards have been used to quantify the distribution of analytes along a single hair strand [155-157], *e.g.* to determine the As and Pb content in individual hair strands of leukemia patients [158]. In addition, as mentioned above, spiked keratin films have been used as calibration materials for hair analysis, offering better recovery and linearity compared to conventional methods [129]. Overall, the development of matrix-matched tissue standards has facilitated accurate and precise quantification in various analytical studies covering different tissue types and research areas.

1.3.2.2 Solution based calibration

In addition to solid-based calibration, LA-ICP-MS also uses solution-based calibration methods for quantitative analysis. These methods typically use dual flow-through systems to introduce both the laser ablated material and nebulized aqueous standard solutions simultaneously to the ICP torch. The two main advantages of solution-based calibration

are the ability to use aqueous elemental standards, which are readily available and easy to prepare, and the compensation of matrix-related differences. However, it requires correction for differences in ablation efficiency and elemental sensitivities between ICP-MS and LA-ICP-MS analysis [159]. Such a method involves the calculation of correction ratios based on the slopes of calibration curves obtained by calibration with both solution standard and solid standard. This correction ensures accurate quantification despite variations in instrument sensitivity and sample matrix composition. In addition, differences in ablation efficiency can also be corrected by using an internal standard. Despite challenges, such as increased formation of polyatomic ions due to water introduction and potential loss of analytes during nebulization, solution-based quantification has been successfully applied to various samples, including biological tissues and hair strands [103, 160-162]. These studies have demonstrated the effectiveness of solution-based calibration in LA-ICP-MS for accurate elemental quantification. In addition, solution-based calibration methods are promising for forensic isotope investigations and routine research applications as they provide valuable insights into the composition and distribution of elements in complex samples.

1.3.2.3 Isotope dilution calibration

The laser ablation sampling method, combined with Isotope dilution analysis (IDA) quantification in mass spectrometry, shows great potential for accurate and precise determination of trace elements. By measuring the isotopic ratios of the sample, spike, and their mixture, the analyte concentration can be accurately determined. IDA offers the advantage of being unaffected by matrix effects and instrument instabilities during LA-ICP-MS experiments. However, it requires costly isotopically-enriched spike solutions, cannot be applied to monoisotopic elements, and may involve laborious sample preparation compared to external calibration methods, thus reducing sample throughput. Additionally, knowing or calculating the exact mass or volume of the spike solution added to the sample is essential. The key requirement for IDA is the equilibration of isotopes between the spike and the sample to ensure similar behavior between the spike nuclide and the analyte nuclide in the sample. Recent applications include the work by Yang *et al.*, who used a dual-flow gas system and solution standard to quantify boron in silicon wafers, achieving accurate results with relative standard deviations below 14% [163]. Similarly, Pickhardt *et al.* proposed a rapid quantification method using a microflow nebulizer and an isotope-enriched standard solution and achieved a precision of about 1.90 % and 1.41 % RSD for different sample materials [164, 165]. In another study, an isotope-enriched solution was nebulized in parallel with laser ablation of platinum material and the Pb concentration in NIST 681 was determined with good accuracy compared to the certified value [162]. In addition, various strategies for the addition of spike solutions for LA-ICP-MS bioimaging experiments have been described, including solid spiking methods, online aerosol addition, inkjet printing, and microarray deposition [166-170]. These methods enable precise quantification of metal distributions in biological samples at both macroscopic and single-cell levels and provide valuable insights into various diseases and treatments.

1.3.2.4 Semi-quantification approaches

In addition to the standard external calibration methods described above, a variety of other techniques have been developed to support quantitative analysis by laser ablation ICP-MS. Furthermore, the increasing integration of AI in all scientific disciplines, including analytical chemistry, is inevitable. Although progress in this area is rather limited, recent discussions by Pan *et al.* have shed light on the potential impact [171]. As more laboratories adopt ICP-TOFMS systems with a focus on continuous measurement of all nuclides, the

need for their consistent quantification becomes apparent. Although the use of gelatin standards has facilitated quantification, the preparation of calibration standards that include all elements remains impractical. Metarapi *et al.* have developed gelatin-based microdroplet standards covering 72 elements and used them to create a library of response factors for semi-quantitative calibrations. In a two-step evaluation process that included bootstrapping with gelatin standards and analyzing real tissue sections, they found that using 10 to 15 elements as calibration standards yielded reasonable accuracy. This approach, which allows the determination of 136 nuclides from 63 elements with errors below 25%, represents a novel semi-quantification method. In addition, a web application was developed to facilitate the use of this method. This semi-quantitative approach differs from previous uses of the term and emphasizes the particular methodology described [172].

Chapter 2

Research Aims and Hypothesis

The aim of the thesis is, firstly, to gain a better understanding of the fundamentals of LA-ICP-MS by adapting and optimizing the operation of LA-ICP-MS to achieve minimal elemental fragmentation and thus improve the precision of elemental analysis. Secondly, the main objective of this research is to develop an advanced calibration method based on the consideration of ablated volume variations using 3D profilometry for LA-ICP-MS bulk analysis as well as for imaging. The volume-based calibration approach was tested by cross-calibrating different materials (standards) to develop an approach that allowed the use of different materials as standard and sample in LA-ICP-MS quantification. For confirmation, cross-calibration of 10 standards from different matrices (including glass, carbonates, zircon, plants, and proteinaceous materials) was performed using the newly developed volume-corrected calibration approach to achieve robust comparability across different sample types. In addition, the volume-corrected calibration approach was applied to correct for within-sample inhomogeneity in LA-ICP-MS imaging in real samples, contributing to a more nuanced and accurate representation of elemental distribution in complex materials.

Hypotheses:

1. The optimal choice of energy density (J cm^{-2}) is essential in LA-ICP-MS analysis to ensure accuracy and achieve a robust signal-to-noise ratio, thereby improving the precision of the results obtained.
2. Using an energy density well above the ablation threshold of the matrix can lead to the formation of a gaseous phase, potentially causing double peaks for certain elements during LA-ICP-MS analysis.
3. A non-matrix matched calibration can be used effectively by accounting for the mass/volume ablated and using a fluence just above the threshold.
4. By combining LA-ICP-MS and 3D profilometry, cross-calibration of different materials (*e.g.* glass, zircon, carbonates, plants, proteins, *etc.*) is possible. This combined approach allows precise determination of the ablated volume, enabling accurate comparisons between different sample types.
5. Without volume correction, non-matrix-matched calibration will lead to inaccuracies unless the standard and sample have similar properties. This emphasizes the importance of accounting for differences in ablated volume for reliable LA-ICP-MS results.

Chapter 3

Scientific Publications

The dissertation consists of three original scientific manuscripts and one review manuscript. Manuscript 1 (Section 3.1) investigates optimization of LA-ICP-MS instrumental settings to minimize quantification anomalies in single-pulse laser ablation analysis. This manuscript focuses on the effects of laser fluence and beam size on the signal as well as on the formation of double peaks and targets Hypothesis 1 and . Hypothesis 2 is then further explored in Appendix A.1, which was published in collaboration with colleagues from University of Ghent and University of Zagreb. This manuscript addresses in more detail the formation of double peaks upon ablation of soft materials, using gelatin as a proxy for soft biological samples. It is a continuation of Manuscript 1 as it further explores and explains how the unsuitable use of higher laser fluence can lead to two-phase sample transport, which affects the signal and therefore the accuracy of LA-ICP-MS. It also includes a comparison between a 213 nm laser and a 193 nm laser. Manuscript 2 (Section 3.2) presents the state of the art of calibration approaches currently used for the quantitative analysis of biological materials with LA-ICP-MS. In this manuscript, the quantification methods for biological samples are evaluated in detail and their advantages and disadvantages are highlighted. In addition, this manuscript provides a good introduction to the calibration issues of laser ablation techniques and confirms that further research and new methods are needed. Manuscript 3 (Section 3.3) focuses on the development of a non-matrix-matched calibration approach for bulk multielement LA-ICP-MS analysis. Laser ablation is combined with post-ablation 3D profilometry to measure the topography of the sample after ablation to determine the ablation volume. This corrects for ablation differences and thus "eliminates" the matrix effect, enabling successful cross-calibration of materials with completely different matrix properties. However, this only works if optimal laser parameters are used, as higher fluences lead to distorted signal results. Therefore, this manuscript is in line with Hypothesis 3 and 4. Furthermore, in Manuscript 4 (Section 3.4) the volume-aided calibration approach was also tested for LA-ICP-MS mapping analysis. Again, post-ablation volume was determined by 3D profilometry. The elemental maps were normalized based on the measured volume per pixel, which resulted in the concentration being defined as mass per volume (in $\mu g\ cm^{-3}$) rather than mass per mass (in $\mu g\ g^{-1}$). The approach was found to correct for ablation differences between/within standards and samples, supporting Hypothesis 5. In addition, the potential benefits of modifying the ablation grid in two-dimensional (2D) and three-dimensional (3D) LA-ICP-MS mapping to achieve a smooth surface after ablation and thus increase the precision of elemental distribution on the surface and improve image quality were investigated in Appendix A.2. Therefore, in this dissertation, the LA-ICP-MS fundamentals are investigated to gain a better understanding of the effects of the parameters on the obtained ICP-MS signal. Furthermore, this knowledge is used to develop

a new quantification approach based on the correction of ablation differences by using the ablated volume. This enables comparatively precise and usable “non-matrix matched” calibration, potentially enabling quantitative analysis of many samples for which matrix-matched standards are currently not available.

3.1 Manuscript 1: Quantification Anomalies in Single Pulse LA-ICP-MS Analysis Associated with Laser Fluence and Beam Size

Published: Jerše A., Mervič K., Van Elteren J.T., Šelih V. S., Šala M., (2022). Analyst, 31(1), doi: 10.1039/d2an01172g.

Laser ablation inductively coupled plasma mass spectrometry (LA-ICP-MS) is an important technique for the direct analysis of solid samples. With its growing popularity and wider range of applications in recent years, this technique has undergone some important developments over the last decade. Advances, such as the introduction of fast washout cells, have led to higher spatial resolution, improved sensitivity and a reduction in analysis time. Despite these improvements, obtaining accurate quantitative results still presents a challenge for LA-ICP-MS analysis. Quantification by laser ablation still mainly depends on matrix-matched standards and suitable internal standards. However, what makes the calibration processes even more complicated is the additional element fractionation and matrix-dependent ablation associated with laser fluence and beam size. Therefore, in order to improve the calibration methods, one needs to understand the influence of the different operating parameters on the obtained signal.

This work focuses on investigating the influence of fluence, beam size and aerosol transport on the quantification of single-pulse LA-ICP-MS analysis. This is done using approaches based on three factors - laser ablation spot volume, pulse intensity and noise characteristics for different elements (As, Gd, La, Ni, Te and Zn) as well as a wide concentration range (from 100 to 1000 $\mu g\ g^{-1}$) and different matrices (NIST SRM 612 glass standard and in-house prepared gelatin standards). Firstly, the study aimed to assess the impact of laser fluence and beam size on signal intensity, normalized to crater volume, in LA-ICP-MS analysis. To determine whether the ablated volume correlates linearly with the signal intensity, the accumulated counts of individual pulses were normalized to the crater volume. Furthermore, the relationship between the laser fluence and both signal intensity and noise contributions was also investigated. Finally, single pulse peaks were monitored to determine whether the two variables also influence the shape of the peak profiles.

The study determined that higher fluences, well above the ablation threshold of the material, and larger beam sizes significantly affect the results of the analysis. They can lead to signal reduction, a lower signal-to-noise ratio and the formation of double peaks for certain elements. The formation and characterization of double peaks is then further explored in Appendix A.1. These problems are attributed to factors such as particle size distribution and inefficient aerosol transport. The results show the importance of optimizing parameters tailored to the analyzed material to improve the accuracy and precision of LA-ICP-MS analysis.

Analyst

ROYAL SOCIETY OF CHEMISTRY

PAPER

View Article Online
View Journal | View Issue

Check for updates

Cite this: *Analyst*, 2022, **147**, 5293

Quantification anomalies in single pulse LA-ICP-MS analysis associated with laser fluence and beam size†

Ana Jerše,‡ Kristina Mervič,‡ Johannes Teun van Elteren, * Vid Simon Šelih and Martin Šala *

Received 19th July 2022,
Accepted 20th October 2022

DOI: 10.1039/d2an01172g

rsc.li/analyst

Laser ablation inductively coupled plasma mass spectrometry (LA-ICP-MS) has undergone major improvements in recent years which have led to reduction of the analysis time, higher spatial resolution, and better sensitivity. However, quantification and accurate analysis remain one of the bottlenecks in LA-ICP-MS analysis and so far satisfactory calibration solutions are restricted to well-documented matrices and suitable internal standards. Additional uncertainties associated with laser fluence and beam size *via* various ablation cells and interfaces make quantification even more challenging. This work is focused on the influence of fluence, beam size and aerosol transport on quantification in single pulse LA-ICP-MS analysis *via* approaches based on pulse intensity, LA spot volumes, noise characteristics, *etc.* for different elements (As, Gd, La, Ni, Te and Zn), concentrations (between 10 and 1000 μg g^{-1}), and matrices (gelatin standards and NIST SRM 612). The findings indicate that selection of the appropriate laser fluence, just above the ablation threshold, and beam size, depending on the interface of LA and ICP-MS, are critical for reliable quantification and should be properly adjusted to avoid excessive Poisson and Flicker noise, achieve maximum sensitivity, and prevent the formation of double peaks in single pulses.

Introduction

Laser ablation inductively coupled plasma mass spectrometry (LA-ICP-MS) is a technically advanced microanalytical method for direct sampling of solid materials and measurement of most elements of the periodic table. However, the processes involved from ablation to detection are complex; in particular, the interaction of the laser beam with the solid material, involving transient changes from solid, through liquid, into a plasma state, is not well-understood.

The provoking title of Hergenröder's presentation at the 9th European Workshop on Laser Ablation in Elemental and Isotopic Analysis (Prague, Czech Republic, 2008), "LA-ICP-MS: The astonishing story why it works (at least sometimes)", appropriately conveys these intricacies. Elemental quantification in LA-ICP-MS, either in bulk or imaging mode, requires that the stoichiometry of the ablated material is the same as the overall stoichiometry of the particles measured by the ICP-MS. However, non-stoichiometric conversion of elements leads to elemental fractionation, which may occur during ablation, transport and/or atomization/ionization in the ICP.[1] During transport from the LA cell to the ICP-MS, particle size-segregation may occur as a result of size-dependent impaction when particles collide with the surfaces of the laser ablation cell or the interface, or due to gravitational settling.[2–4] Once entering the plasma, larger particles may not be completely atomized and ionized, resulting in further elemental fractionation.[2,4–7]

Despite these drawbacks, under matrix-matched conditions, it is assumed that samples and standards with the same total elemental concentrations can be accurately quantified. However, matrix-matched standards are hardly ever available, especially for biological samples, hence a number of calibration strategies have emerged,[8] such as homogenization of tissue and standard addition of element(s) of interest,[9] spiking of the samples by soaking in solution (*e.g.* for hair samples),[10] preparation of external standards in gelatin that mimic the tissue matrix,[11,12] including microdroplet standards,[13] (in-cell or in-torch) aspiration of a standard solution during laser sampling,[14–16] and application of a "film" standard on/under a biological sample combined with total consumption (*i.e.* ablation of the entire depth) of the assembly.[17] In addition, internal standardization protocols have been developed to compensate for instrumental drift and possible

Department of Analytical Chemistry, National Institute of Chemistry, Hajdrihova 19, 1000 Ljubljana, Slovenia. E-mail: elteren@ki.si, martin.sala@ki.si

† Electronic supplementary information (ESI) available. See DOI: https://doi.org/10.1039/d2an01172g

‡ These authors contributed equally to this work.

ablation differences between matrices of sample and calibration standards. These include, *e.g.*, the use of homogeneously distributed elements in the sample[18,19] and labeling of tissue components with a metallo-intercalator.[20]

Generally, better precision in single pulse LA-ICP-MS can be obtained by increasing signal intensity, *i.e.*, generating more counts, implying a higher laser fluence, and/or larger beam size. In imaging applications, signal intensity can also be increased using more laser shots per measurement or pixel (=dosage). The effects of laser shot dosage on LA-ICP-MS imaging and image quality were recently discussed,[21] while the influence of laser fluence and beam size on noise still has to be investigated.

Precision in LA-ICP-MS measurements can be evaluated by the total standard deviation (SD_t) of the signal intensity (*i.e.*, number of counts, A), and can be divided into two components, *i.e.*, Poisson noise (SD_P) and Flicker noise (SD_F). Poisson noise, which originates in counting statistics, is proportional to the square root of signal intensity ($\sqrt{A}$) and is important at lower signal intensities. Flicker noise is proportional to the signal intensity ($q \times A$, where q is a factor between 0 and 1) and is associated with LA-ICP-MS settings (laser fluence, beam size, ...).[22] The factor q is only constant for the same settings used. Hence, when we change any of the parameters influencing the Flicker noise *vide supra*, the factor q also changes as this is the actual variable in the propagation of noise that we can affect and try to minimize. Total noise can therefore be expressed as

$$SD_t^2 = SD_P^2 + SD_F^2 = A + q^2 \cdot A^2. \quad (1)$$

Careful selection of operational settings can improve the precision of LA-ICP-MS analysis. A series of experiments was conducted to investigate the effects of laser fluence and beam size on the single pulse response, signal intensity, and noise. This study will help to better understand the issues that may occur if the experimental parameters (laser fluence and beam size in this case) are not optimized and how these may affect the precision of the obtained LA-ICP-MS results. The study was conducted on gelatin standards, commonly used as a standard of choice in studies of biological samples,[23–25] and NIST glass standards, commonly used in geological studies[26–28] as appropriate "general" reference standards. As and Gd were selected to be measured in all experiments, and for single peak profiles some additional elements were measured, namely La, Ni, Te and Zn.

Experimental

Materials and standards

Gelatin gels and glass standards were used as target matrices in the experiments. Silicate glass NIST SRM 612 (trace elements in glass, nominal concentration of 50 μg g^{-1}; National Institute for Standards and Technology, Gaithersburg, MD, USA) was used as a glass standard. Gelatin standards were prepared in-house following the procedure previously described by Šala *et al.*[12] In brief, 10% (m/v) gelatin solution was prepared by suspending gelatin (porcine-skin gelatin, type A, bloom strength 300, Sigma-Aldrich, St Louis, MO, USA) in ultra-pure water (18.2 MΩ cm), supplied by a Milli-Q water purification system and heating it up to approximately 55 °C. Subsequently, the desired amount of selected elemental ICP standard solution(s) from Merck or Sigma Aldrich was added. The mixture was then dropped onto a microscope glass slide using a micropipette and dried in a convection oven at 95 °C for one hour.

Instrumentation

In all experiments, an Analyte G2 193 nm ArF* excimer laser ablation system (Teledyne Photon Machines Inc., Bozeman, MT, USA) was used. It was equipped with a standard two-volume ablation cell HelEx II (aerosol washout time 0.5 s, full width at 1% of the maximum (FW 0.01 M)). The LA system was coupled to an ICP-MS instrument Agilent 7900x (Agilent Technologies, Santa Clara, CA, USA), either *via* the standard HelEx II aerosol delivery system[29] (HelEx in further text) or using the Aerosol Rapid Introduction System[30] (ARIS) for fast aerosol washout (FW 0.01 M, *ca.* 20 ms). Ablation cell and both aerosol delivery systems are commercially available from Teledyne Cetac Technologies. Similar behavior is expected from ablation cells and aerosol delivery systems by other vendors. A 3D interference optical profilometer (Zegage PRO HR, Zygo Corporation, PA, USA) was used to determine the volume of craters after laser ablation. The 3D information was recorded using a 50× magnification lens with a lateral resolution of 0.173 μm, and a surface topography repeatability better than 3.5 nm.

Signal intensity and noise contributions as a function of laser fluence

We investigated how the single pulse intensities and generation of Flicker and Poisson noise correlate with increasing laser fluence. In-house prepared gelatin standards and the NIST SRM 612 glass standard were used in the ARIS setup. As and Gd (10, 50, 100 and 150 μg g^{-1} each) were measured in gelatin and NIST SRM 612[31] (certified value for As 37.4 ± 2.2 μg g^{-1}, informative value for Gd 39 μg g^{-1}). These elements were selected as highly homogeneous standards and can be prepared in gelatin.[12] Gd also exhibits minimal polyatomic interferences and low background in ICP-MS analysis. As was chosen as a toxic element that may be of interest for determination in tissues. Laser fluences between 0.5 and 9 J cm^{-2} were used for gelatin standards and between 1 and 9 J cm^{-2} for glass standards. The data were obtained in line scanning mode with a fixed dosage of 1 (non-overlapping laser shots/craters), and integration of counts for single peaks by matching the integration time to the particle washout time and the inverse of the repetition rate. Detailed instrumental conditions used in the experiments are summarized in Table S1† (ESI). Raw data were processed with OriginLab software (OriginPro 2018, OriginLab Corporation, Northampton, MA, USA).

Influence of laser fluence and beam size on the signal intensity normalized to crater volume

To investigate whether or not the ablated volume is linearly proportional to the measured signal intensity, the accumulated counts for LA-ICP-MS single pulses, obtained at different fluences and beam sizes, were normalized to their crater volume. To enable accurate determination of the crater volumes, the scanning speed was selected in such a way that ablation craters for each laser shot were nonadjacent, *i.e.*, scanning speed (μm s^{-1})/repetition rate (Hz) > 2 × beam size (μm). Three different laser fluences were compared (0.5, 4 and 8 J cm^{-2}) and three different beam sizes for each setup (5, 10 and 20 μm square with ARIS, 35 and 80 μm square, and 65 μm circle with HelEx). Data acquisition was performed similarly to the previous experiment. The data obtained with both setups cannot be directly compared; only data obtained with different parameters using the same setup are comparable. Other instrumental conditions used for ablation of gelatin (containing 1000 μg g^{-1} As or Gd) are listed in Table S2† (ESI). OriginLab software was used to process the raw data.

Effect of fluence and beam size on single pulse peak profiles

Single pulse peak profiles were monitored by ablation of single spots, generated by one laser shot per spot for individual elements. Gelatin standards containing different elements (As, Gd, La, Ni, Te, and Zn) at a concentration level of 1000 μg g^{-1} were ablated in this experiment. Additionally, As and Gd gelatin standards were prepared (20 and 100 μg g^{-1}) to evaluate if the shape of the peak profile is also influenced by the concentration or only by the ablation conditions. Laser fluences of 0.5 and 4 J cm^{-2} were used with 5, 10 and 20 μm beam sizes (square) with ARIS, and 35 and 80 μm (square), and 65 μm (circle) with HelEx. Detailed conditions used are summarized in Table S3† (ESI). OriginLab software was used for data processing and peak profile depiction. Again, data using different setups cannot be compared and the experiments with both setups were performed to see if trends are similar or not.

Results and discussion

Signal intensity and noise contributions as a function of laser fluence

A major characteristic of the analytical performance is related to the signal intensity and noise as a function of the laser fluence which was investigated by single pulse LA-ICP-MS of *ca.* 50 μg g^{-1} Gd in both the gelatin standard and the NIST SRM 612 glass standard, followed by retrieval of the Flicker and Poisson noise using eqn (1). From Fig. 1 it follows that for both the gelatin and NIST 612 the Flicker noise determines the overall noise as by quadratically summing the Flicker and Poisson noise, the low levels of Poisson noise negligibly affect the overall noise. Although one would expect the signal intensity to linearly increase with fluence, this is only seen in the case of the NIST 612 above an ablation threshold of *ca.* 3 J cm^{-2}, whereas for the gelatin standard we can see that for laser fluences well above the ablation threshold of approx. 0.2 J cm^{-2}, the signal intensities of Gd reach a plateau. The fact that the measured volumes ablated per shot as a function of the fluence for the NIST 612 (Fig. 2) follow a very similar trend as the Gd intensities *vs.* fluence graphs (Fig. 1), is an indication that signal intensities for the NIST are likely linked

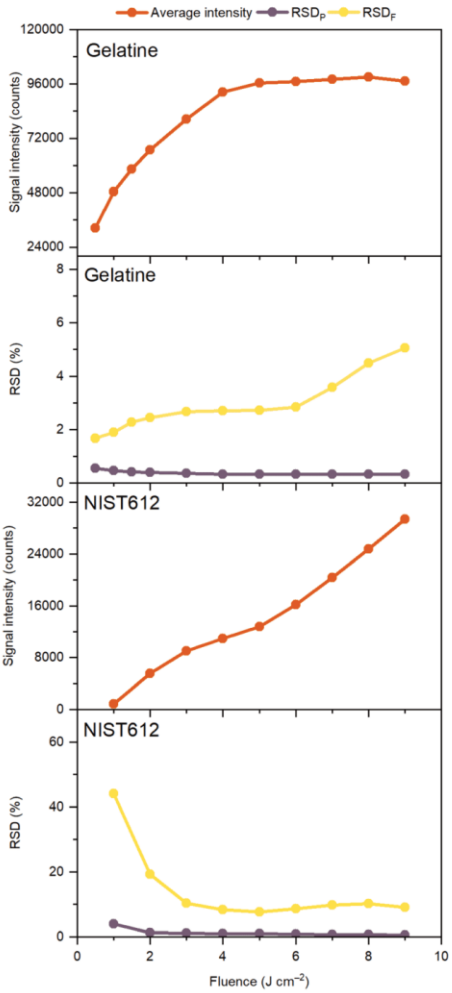

Fig. 1 Average line intensity, Poisson noise and Flicker noise as a function of fluence for single dosage experiments with *ca.* 50 μg g^{-1} Gd in gelatin and NIST SRM 612 glass standards (see Table S1† for operational conditions).

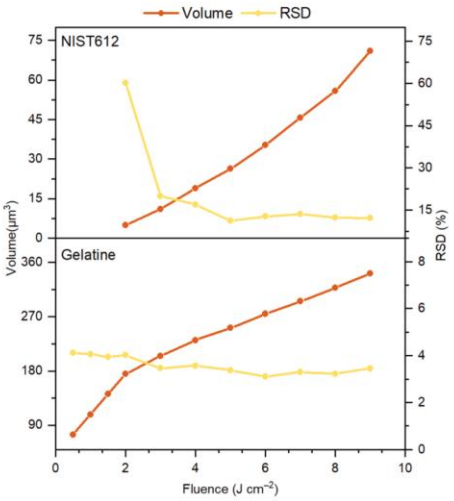

Fig. 2 Average crater volumes and RSDs (based on 50 measurements) for 5 μm LA shots in gelatin and NIST 612 as a function of the fluence.

to LA processes and to a lesser extent to transport and detection phenomena for these particular LA-ICP-MS conditions.

From Fig. 2 is can be seen that gelatin ablates much better than NIST 612 (5–20 times better, depending on the fluence), potentially leading to plasma shielding[32] at higher fluences, resulting in lower signal intensities and plateauing as we may see in Fig. 1. The higher Flicker noise for NIST 612 compared to gelatin is most likely associated with more erratic ablation of the NIST 612, resulting in less reproducible craters, evident from the calculated RSDs in the volumes ablated per laser shot (Fig. 2). The fact that the Flicker noise for the NIST 612 is so high at low fluences is due to ablation below the ablation threshold as it levels off to *ca.* 10% off above 3 J cm^{-2}, similar to the RSDs levels for the volumes ablated. In our experiments for gelatin, ablation always took place above the ablation threshold, implying that no irregular ablation (on the account of lower fluence than ablation threshold used) took place as for the NIST 612. Nevertheless, the Flicker noise slightly increased to *ca.* 5% at the highest fluence, whereas the RSDs in the volumes ablated were more or less constant, slightly above 3%. This discrepancy might be caused by the much higher particle generation and throughput compared to NIST 612, suggesting that for ablation of gelatin besides LA processes also other processes play a role in determination of the Flicker noise. Similar to above experiments with Gd (Fig. 1), from Fig. S1† (ESI) we can see that for *ca.* 50 μg

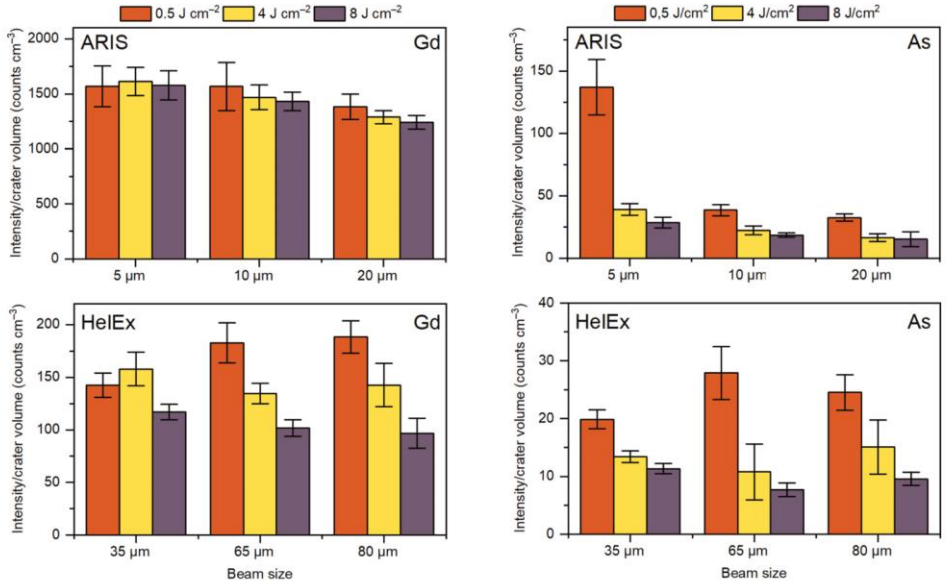

Fig. 3 Signal intensity to crater volume ratios for single pulse LA-ICP-MS of Gd and As in gelatin at different beam sizes (4, 10 and 20 μm for ARIS and 35, 65 and 80 μm for HelEx), fluences (0.5, 4 and 8 J cm^{-2}) and aerosol transport setups (ARIS or HelEx) (see Table S2† for operational conditions).

g^{-1} As in gelatin and NIST 612 almost identical results were obtained. Additional ablation of a range of As concentrations in gelatin (10, 100 and 150 μg g^{-1}) as a function of the fluence (Fig. S2, ESI†) showed that concentration affects the signal intensity as expected, *i.e.*, signal intensity ≈ concentration, with plateauing for all concentrations, whereas Poisson and Flicker noise are minimally affected.

Previous studies on LA-ICP-MS analysis of glass,[4–7,33] metals,[6] and gelatin[2] have shown that the laser wavelength, fluence, and ablation mode are the key parameters influencing the particle size (range) generated. Using a fluence well above the material's ablation threshold considerably alters the particle size distribution, resulting in the formation of proportionally larger particles that undergo significantly more gravitational settling.[33] Additionally, it has been shown that larger particles are less likely to be completely vaporized, atomized, and ionized in the ICP.[7] Studies have shown that the plasma source is not capable of sufficiently atomizing particles above

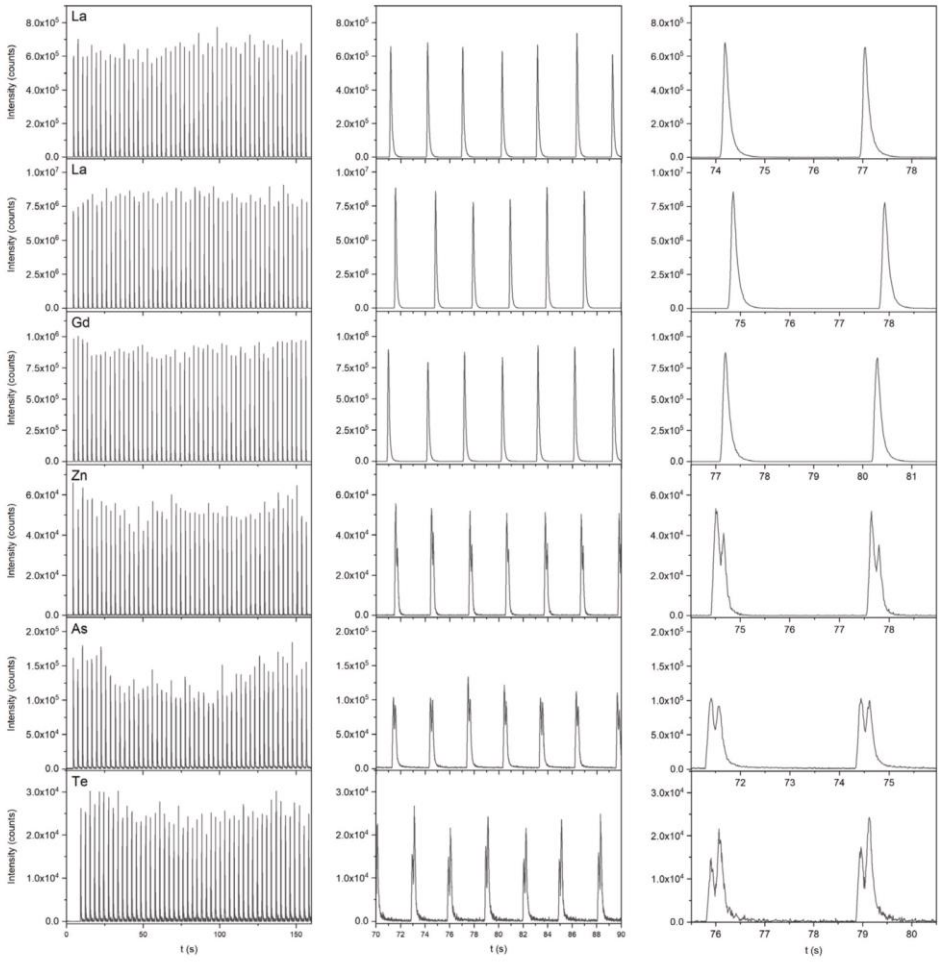

Fig. 4 Single pulse peak profiles for Ni, La, Gd (single peaks), Zn, As and Te (double peaks) – 50 pulses [left] and two zoom ins (20 [middle] and 5 s [right]) for each element that show the repeatability of the peak shape. Data were obtained using the HelEx aerosol delivery system at a fluence of 4 J cm^{-2} and a beam size of 80 μm (square mask) (see Table S3† for operational conditions).

150 nm.[7] If standards and samples are matrix-matched, this would merely result in lower sensitivity; however, if the matrix is not ideally matched, the concentrations in the samples may be under- or overestimated. In the remainder of the text, we will only focus on the irregular laser ablation behaviour of gelatin as an approximation for elemental quantification of biological tissues.

Influence of laser fluence and beam size on the signal intensity normalized to crater volume

We expect larger beam sizes to ideally only affect the number of particles generated, whereas higher fluences may not only result in higher particle number concentrations but also in a changed particle size distribution. Generation of larger particles may potentially result in gravitational settling and/or incomplete atomization/ionization.[2,4–7] To investigate how the fluence and beam size affect the signal intensity, we measured single pulse intensities of Gd and As in gelatin as a function of the ablation volume–normalized intensity in the ARIS and HelEx setups (Fig. 3). A constant intensity/volume ratio would imply that no analysis anomalies exist. However, Fig. 3 shows that the average intensity/volume ratio at different fluences and beam sizes is not constant in either the ARIS or HelEx setup. Regardless of the setup used or the element measured, there is a trend that the highest intensity/volume ratios are obtained for the lowest fluence, implying that some of the particles "disappear" due to transport losses or detection problems, potentially as a result of generation of larger particles or agglomeration of smaller particles. However, larger beam sizes do not necessarily lead to lower intensity/volume ratios as can be seen from the Gd and As measurements in the HelEx setup. In the ARIS setup, there is an indication of decreasing intensity/volume ratios with beam size, presumably due to overloading the ICP plasma and insufficient time for ionization due to because of much faster aerosol transport than in the HelEx cell.[30]

Effect of fluence and beam size on single pulse peak profiles

Ablation of gelatin standards containing various elements (As, Te, Zn, Au, Gd, or La, 1000 μg g^{-1}) in the HelEx setup, using a fluence of 4 J cm^{-2} and a beam size of 80 μm (square mask), led to a single pulse response showing differences in peak profiles – either single or double peak profiles were obtained, depending on the element (Fig. 4). It can be seen that the occurrence of single and double peaks was very reproducible. However, the occurrence of double peaks for As, Te, and Zn was very dependent on the fluence and beam size as with a lower fluence (0.5 J cm^{-2}) and a smaller beam size (35 μm, square mask) single peaks were recorded for all measured elements in the HelEX setup, although some shouldering was observed for As (Fig. S3, ESI†), Te and Zn (data not shown). Differences seem to be the result of an excess of material ejected upon ablation since for the ARIS setup in Fig. S3† (ESI), having a much smaller overall internal volume, similar results were obtained for As at scaled-down settings (beam size 5, 10 and 20 μm), square mask at the same fluences. Consequently, at 5 and 10 μm and 0.5 J cm^{-2} in the ARIS setup, a single peak was obtained for As, while at 20 μm and 0.5 J cm^{-2} as well as 4 J cm^{-2}, regardless of the beam size, split peaks were observed. Additional Gd and As gelatin standards (20 and 100 μg g^{-1}) were used to assess whether the peak shape in the HelEx setup is affected by the concentration. The results (Fig. S4, ESI†) showed no differences in peak shape with different concentrations, which suggests that splitting of peaks is merely affected by the parameters used in the LA-ICP-MS experiment.

Nováková *et al.*[5] demonstrated the influence of the beam size on the particle size distribution upon ablation of glass. They showed a bimodal particle size distribution, most probably related to small primary particles and large coagulates/agglomerates, regardless of the beam size, although the larger beam sizes produced proportionally more large particles than the smaller beam sizes. However, if this is the case in the present study, one would expect all elements to showcase similar behavior resulting in double peaks for every element. Niehaus *et al.*[2] on the other hand reported that at higher fluences larger particles are generated for gelatin and the embedding polymer resin Technovit (used for fixation of biological materials). Also, the efficiency/speed of the transport from the ablation cell to the ICP might be affected by the particle size. If the distribution of different elements over the particle size range varies, double peaks can appear for elements that are distributed in small and large particles, while single peaks can appear for elements that are primarily present in particles of similar size.

Conclusions

This paper is focused on quantification anomalies in single pulse LA-ICP-MS analysis caused by non-optimized laser fluence and beam size. The results from this study stress the importance of selecting the appropriate ablation parameters to minimize noise and improve the precision of the analytical results caused by differences in particle size distribution, particle agglomeration, inertial impact, gravitational settling, laminar and/or turbulent diffusion, electrostatic attraction, ion yield, degree of ionization, *etc.* In a series of experiments, we investigated the influence of laser fluence and beam size on signal and noise, single pulse intensity profiles, LA spot volumes, *etc.* The results from this study suggest that through the appropriate choice of instrumental parameters, we can circumvent (i) LA-generation of a large particle size range, (ii) elements distributing differently over the particle size range generated, (iii) issues related to particle size and transportation of generated aerosol (*e.g.* gravitational settling) and (iv) particle size-related ionization in the ICP.

It was shown that ablation with higher fluences (*i.e.*, fluences well above the material's threshold) and large beam sizes (depending on the interface associated with the HelEx or ARIS setup) result in issues such as lowering the signal/ablated volume ratio, increasing the RSDs, splitting of peaks in single pulse response mode, *etc.* The results from the present study

support the previously published findings stating that with higher fluences, larger particles are formed, whereas too large beam sizes generate an excess of aerosol particles. This can lead to impaired transport efficiency from the ablation cell into the ICP as well as poor atomization and/or ionization of the elements present in large particles, which result in the partial loss of signal. By selecting optimal parameters for the investigated material, one can considerably improve the precision and accuracy of the obtained results.

Author contributions

Ana Jerše: investigation, formal analysis, writing – original draft, visualization. Kristina Mervič: investigation, formal analysis, writing – original draft, visualization. Johannes Teun van Elteren: conceptualization, writing – review & editing, visualization. Vid Simon Šelih: writing – review & editing, funding acquisition. Martin Šala: investigation, conceptualization, writing – review & editing, visualization, data curation, supervision.

Conflicts of interest

There are no conflicts to declare.

Acknowledgements

The authors acknowledge the financial support from the Slovenian Research Agency ARRS (research core funding no. P1-0034). K. M. thanks the Slovenian Research Agency for funding her PhD research.

References

1 S. Zhang, M. He, Z. Yin, E. Zhu, W. Hang and B. Huang, *J. Anal. At. Spectrom.*, 2016, **31**, 358–382.
2 R. Niehaus, M. Sperling and U. Karst, *J. Anal. At. Spectrom.*, 2015, **30**, 2056–2065.
3 H. R. Kuhn and D. Günther, *Anal. Chem.*, 2003, **75**, 747–753.
4 M. Guillong and D. Günther, *J. Anal. At. Spectrom.*, 2002, **17**, 831–837.
5 H. Nováková, M. Holá, M. Vojtíšek-Lom, J. Ondráček and V. Kanický, *Spectrochim. Acta, Part B*, 2016, **125**, 52–60.
6 M. Holá, J. Ondráček, H. Nováková, M. Vojtíšek-Lom, R. Hadravová and V. Kanický, *Spectrochim. Acta, Part B*, 2018, **148**, 193–204.
7 H. R. Kuhn, M. Guillong and D. Günther, *Anal. Bioanal. Chem.*, 2004, **378**, 1069–1074.
8 A. Limbeck, P. Galler, M. Bonta, G. Bauer, W. Nischkauer and F. Vanhaecke, *Anal. Bioanal. Chem.*, 2015, **407**, 6593–6617.
9 D. J. Hare, J. Lear, D. Bishop, A. Beavis and P. A. Doble, *Anal. Methods*, 2013, **5**, 1915–1921.
10 D. La Rosa Novo, T. Van Acker, J. Belza, F. Vanhaecke and M. F. Mesko, *J. Anal. At. Spectrom.*, 2022, **37**, 775–782.
11 D. Gholap, J. Verhulst, W. Ceelen and F. Vanhaecke, *Anal. Bioanal. Chem.*, 2012, **402**, 2121–2129.
12 M. Šala, V. S. Šelih and J. T. Van Elteren, *Analyst*, 2017, **142**, 3356–3359.
13 A. Schweikert, S. Theiner, D. Wernitznig, A. Schoeberl, M. Schaier, S. Neumayer, B. K. Keppler and G. Koellensperger, *Anal. Bioanal. Chem.*, 2022, **414**, 485–495.
14 D. Günther, H. Cousin, B. Magyar and I. Leopold, *J. Anal. At. Spectrom.*, 1997, **12**, 165–170.
15 J. J. Leach, L. A. Allen, D. B. Aeschliman and R. S. Houk, *Anal. Chem.*, 1999, **71**, 440–445.
16 C. O' Connor, B. L. Sharp and P. Evans, *J. Anal. At. Spectrom.*, 2006, **21**, 556–565.
17 C. Austin, D. Hare, T. Rawling, A. M. McDonagh and P. Doble, *J. Anal. At. Spectrom.*, 2010, **25**, 722–725.
18 J. S. Becker, R. C. Dietrich, A. Matusch, D. Pozebon and V. L. Dressler, *Spectrochim. Acta, Part B*, 2008, **63**, 1248–1252.
19 M. S. Jiménez, M. T. Gomez, L. Rodriguez, L. Martinez and J. R. Castillo, *Anal. Bioanal. Chem.*, 2009, **393**, 699–707.
20 D. A. Frick, C. Giesen, T. Hemmerle, B. Bodenmiller and D. Günther, *J. Anal. At. Spectrom.*, 2015, **30**, 254–259.
21 M. Šala, V. S. Šelih, C. C. Stremtan, T. Tămaș and J. T. Van Elteren, *J. Anal. At. Spectrom.*, 2021, **36**, 75–79.
22 J. T. Van Elteren, V. S. Šelih and M. Šala, *J. Anal. At. Spectrom.*, 2019, **34**, 1919–1931.
23 M. Birka, K. S. Wentker, E. Lusmöller, B. Arheilger, C. A. Wehe, M. Sperling, R. Stadler and U. Karst, *Anal. Chem.*, 2015, **87**, 3321–3328.
24 M. Costas-Rodríguez, T. Van Acker, A. A. M. B. Hastuti, L. Devisscher, S. Van Campenhout, H. Van Vlierberghe and F. Vanhaecke, *J. Anal. At. Spectrom.*, 2017, **32**, 1805–1812.
25 M. Cruz-Alonso, B. Fernandez, A. Navarro, S. Junceda, A. Astudillo and R. Pereiro, *Talanta*, 2019, **197**, 413–421.
26 J. B. H. Andersson, L. Logan, O. Martinsson, D. Chew, E. Kooijman, M. Kielman-Schmitt, T. C. Kampmann and T. E. Bauer, *Precambrian Res.*, 2022, **372**, 106613.
27 K. Drost, D. Chew, J. A. Petrus, F. Scholze, J. D. Woodhead, J. W. Schneider and D. A. T. Harper, *Geochem., Geophys., Geosyst.*, 2018, **19**, 4631–4648.
28 H. C. Yu, K. F. Qiu, D. Chew, C. Yu, Z. J. Ding, T. Zhou, S. Li and K. F. Sun, *Ore Geol. Rev.*, 2022, **140**, 104612.
29 S. M. Eggins, R. Grün, M. T. McCulloch, A. W. G. Pike, J. Chappell, L. Kinsley, G. Mortimer, M. Shelley, C. V. Murray-Wallace, C. Spötl and L. Taylor, *Quat. Sci. Rev.*, 2005, **24**, 2523–2538.
30 T. Van Acker, S. J. M. Van Malderen, T. Van Helden, C. Stremtan, M. Šala, J. T. Van Elteren and F. Vanhaecke, *J. Anal. At. Spectrom.*, 2021, **36**, 1201–1209.
31 NIST, *Certificate of Analysis Standard Reference Material 612 Trace Elements in Glass*, Gaithersburg, MD, 2012.
32 X. Mao and R. Russo, *Appl. Phys. A*, 1997, **64**(1), 1–6.
33 S. H. Jeong, O. V. Borisov, J. H. Yoo, X. L. Mao and R. E. Russo, *Anal. Chem.*, 1999, **71**, 5123–5130.

3.2 Manuscript 2: Calibration Approaches in Laser Ablation Inductively Coupled Plasma Mass Spectrometry for Bioimaging Applications

Published: Mervič K., Šala M., Theiner S., (2024). Trends in analytical chemistry, 172, 117574, doi: 10.1016/j.trac.2024.117574.

As already mentioned, laser ablation inductively coupled plasma mass spectrometry is a microanalytical technique used for direct sampling of solid materials. It enables the determination of major, minor and trace elements from the periodic table and requires minimal sample preparation. It also provides the spatial elemental composition of samples in 2D and 3D. Initially, it was mainly used for analyzing geological materials as it allows direct sampling and is microdestructive. With the expansion of the application range, it is now also used for elemental analysis of biological samples, especially for bioimaging applications. LA-ICP-MS has undergone some important improvements that have led to a reduction in analysis time, better sensitivity, higher image quality/spatial resolution and a better signal-to-noise ratio. Despite the progress, the challenges discussed in Articles 1 and 2, together with others, lead to a lack of validated and reliable quantification approaches in LA-ICP-MS bioimaging. Therefore, the focus of this dissertation was to better understand the basic operations of LA-ICP-MS and to develop a new calibration approach that does not rely on matrix-matched standards.

This review addresses a detailed assessment of the quantitative methods currently used to obtain quantitative results when analyzing biological samples by LA-ICP-MS, critically evaluating their advantages and disadvantages in terms of analytical capabilities. With the advent of LA-ICP-MS applications in bioimaging, various quantification strategies have been developed, most of which still rely on matrix-matched standards. Commonly used calibration techniques are external calibrations based on standards that mimic the sample matrix, such as homogenized and spiked tissue, polymers and gelatin. Gelatin-based standards have proven to be a good matrix match for most biological samples and are widely used as they can be easily prepared in different concentrations and elemental compositions. This has even led to the development of commercially available gelatin microdroplets. In addition, alternative quantification approaches using standard addition, isotope dilution or semi-quantitative calibration have been developed in recent years. Originally, elemental calibration standards for bioimaging using LA-ICP-MS relied on manual preparation and complicated procedures, often requiring trained personnel and the handling of biological material, which can lead to inaccuracies in thickness. Modern quantification methods favor automated, reproducible processes such as spin-coating and robotic dispensing, which increases throughput and the potential for mass production and commercialization. The use of easily controllable matrices such as polymers and gelatin that mimic biological samples while mitigating issues such as background element abundance has become prevalent. Certified materials such as NIST 61X glasses remain essential for bioimaging applications. In contrast, quantification of nanoparticles is still in the early stages and requires multi-point calibration standards due to the reliance on single-point calibration. The quantification of metal-conjugated antibodies is similar, although the reliability of matrix-matched standards improves with increasing application of the methodology. The rise of ICP-TOFMS technology requires highly multiplexed standards or semi-quantitative approaches to quantify as many elements as possible, reflecting the need for improved quantification methods as technology advances.

Trends in Analytical Chemistry 172 (2024) 117574

Contents lists available at ScienceDirect

Trends in Analytical Chemistry

journal homepage: www.elsevier.com/locate/trac

Calibration approaches in laser ablation inductively coupled plasma mass spectrometry for bioimaging applications

Kristina Mervič [a,b], Martin Šala [a], Sarah Theiner [c,*]

[a] National Institute of Chemistry, Hajdrihova 19, 1000, Ljubljana, Slovenia
[b] Jožef Stefan International Postgraduate School, Jamova cesta 39, 1000, Ljubljana, Slovenia
[c] Institute of Analytical Chemistry, Faculty of Chemistry, University of Vienna, Waehringer Strasse 38, 1090, Vienna, Austria

ARTICLE INFO

Keywords:
Laser ablation
ICP-MS
LA-ICPMS
Calibration
Internal standardization
Bioimaging

ABSTRACT

Laser ablation (LA) in combination with inductively coupled plasma mass spectrometry (ICP-MS) is a technically advanced micro-analytical method for direct sampling of solid materials and allows the determination of a majority of elements from the periodic table. In recent years, the technology has undergone major improvements in hardware, software and the methodology, which have led to a significant reduction of the analysis time, higher spatial resolution/image quality, better sensitivity and signal to noise ratios. Reliable and validated quantification procedures remain one of the bottlenecks in LA-ICPMS bioimaging. This review provides a comprehensive overview on different quantification strategies commonly used for bioimaging applications by LA-ICPMS. The advantages and drawbacks of existing quantification approaches in terms of analytical capabilities will be critically discussed and showcases of their application to biological samples will be presented. Recent developments and future perspectives of the field will be discussed.

1. Introduction

Since the introduction of laser ablation inductively coupled plasma mass spectrometry (LA-ICPMS) for the analysis of solid samples by A. Gray in 1985 [1], it has become an established elemental and mapping technique that is characterized by low limits of detection, high spatial resolution, a wide linear dynamic range and limited sample preparation. The first publication describing the LA-ICPMS analysis of biological sample material was published by Durrant and Ward in 1992 [2]. This feasibility study focused on biological reference materials to demonstrate the potential of the method for multi-element analysis of biological samples. The concept of bioimaging by LA-ICPMS to study the spatial elemental distribution in biological tissue was first introduced by Wang et al., in 1994 [3]. Since then, the range of bioimaging applications for the technique has been expanded towards studies in the fields of metallomics, proteomics, nanotechnology, clinical/medical research and immuno-mass spectrometry imaging/imaging mass cytometry [4–6]. Bioimaging studies by LA-ICPMS have focused on the distribution of drugs or nanoparticles and metal-tagged markers in biological tissue sections and single cells, and on the visualization of the metallome within biological tissue (e.g. in the brain) to compare e.g. diseased vs. non-diseased tissue [6]. Metal homeostasis within biological systems is critical for the immune response, metabolism and intracellular signaling. Moreover, elevated and unregulated concentrations of certain elements have been linked to different diseases. Therefore, dedicated analytical workflows based on elemental imaging are required to quantitative assess their levels within biological samples.

The hardware significantly contributing to the advancements in LA-ICPMS imaging is the introduction of low-dispersion laser ablation cell setups [7,8], providing pulse response durations for a single laser shot of <5 ms [9–12]. This results in better signal to noise ratios, higher throughput and the ability to map at high spatial resolution down to the single-cell level. Understanding of fundamental imaging parameters [13] and the effect of different parameters and imaging strategies have also contributed significantly to the improvement in image quality [14,15]. Beside the laser parameter settings directly connected to the S/N via beam size and dosage, the effects of laser fluence was also studied. It was shown that keeping the energy as low as possible (but still exceeding the ablation threshold) results in lower relative standard deviations [16]. Moreover, the use of higher fluences leads to irregular peak shapes and can result in element-dependent image quality deterioration [17].

One of the main challenges for LA-ICPMS analysis of biological samples is the possibility for accurate, reliable and harmonized quantification. One of the reasons is fractionation that occurs during the

* Corresponding author.
E-mail address: sarah.theiner@univie.ac.at (S. Theiner).

https://doi.org/10.1016/j.trac.2024.117574
Received 3 November 2023; Received in revised form 30 January 2024; Accepted 1 February 2024
Available online 2 February 2024

ablation process, the aerosol transport and the ionization in the ICP source and the potential for signal drifts over the course of an imaging experiment [18,19]. Fractionation is a term describing a wide array of causes that reflect in non-stoichiometric signal response in ICP-MS in comparison with the analyzed material, which can be caused by matrix itself, the wavelength used, the design of the experiment (e.g. down-hole fractionation) etc [20]. Where these phenomena are matrix-dependent, usually matrix-matched standards (laboratory-produced or prepared with reference materials) are required for quantitative analysis by LA-ICPMS. Certified reference materials (CRMs) provide one-point calibration with a high degree of traceability and should match the sample in terms of analyte concentrations as well as chemical composition and physical properties. An example of such CRMs are the NIST SRM 61X series glasses, which are often used for LA-ICPMS calibration. Although they are used for the calibration of different matrices, they are often not well matched to the sample matrix. This is also true for biological samples, so they are rarely used for calibration purposes, but at best as a reference for sensitivity. Therefore, other CRMs are available for biological samples, which are usually provided in the form of freeze-dried powders that are not directly comparable to fresh tissue samples. The limited availability of suitable CRMs for the quantitative LA-ICPMS analysis of different tissue types and single cells have led to the development of a variety of alternative calibration strategies [21–24]. However, the complexity and heterogeneity of biological tissue makes it difficult to closely mimic the sample matrix and to develop appropriate calibration strategies that provide the desired accuracy, precision and robustness. Generally acceptable and harmonized quantification procedures for bioimaging applications by LA-ICPMS have still not been established. In most cases, matrix-matched standards are prepared in-house and undergo internal characterization and validation procedures. For this purpose, the exact elemental concentrations of LA-ICPMS calibration standards are determined by solution-based ICP-MS analysis after acid-assisted digestion. Moreover, their figures-of-merit are reported including linearity of the calibration curve, limits of detection/quantification, precision and long-term stability. Due to the lack of suitable biological CRMs, external and in the ideal case also independent validation procedures are a prerequisite for reliable and accurate quantification workflows for LA-ICPMS bioimaging. Complementary imaging modalities have been used in several studies to benchmark quantitative LA-ICPMS results. Ideally, interlaboratory comparison studies are carried out to prove the validity of newly introduced quantification concepts.

The first protocol for matrix-matched tissue standards was presented by Becker et al., in 2005 [25] and was based on the homogenization of brain tissue samples. These tissue-type standards are often sourced from the same tissue type of the target species (e.g. brain [26], liver [27] or blood [28]), spiked with varying concentrations of the analytes and sectioned to the same thickness as the sample. In this context, the use of polymer-based standards as spin-coated polymer films [29], epoxy resin-embedded standards [30] and printed standards using an inkjet printer [31] have been described. The use of gelatin as matrix for the calibration of elements in soft biological tissue and cells provides several advantages due to the possibility to easily fine-tune the properties of gelatin. Gelatin standards for biological applications by LA-ICPMS have been reported as sections, as micro-arrays [32], filled into defined molds [33] and as (micro-)droplets using manual pipetting [34,35] or a robotic micro-dispensing device [36]. Due to the growing interest in nanotechnology and immuno-mass spectrometry, methods for the quantitative assessment of nanoparticles and metal-conjugated antibodies in biological samples with LA-ICPMS will be critically discussed. A comprehensive overview of different quantification strategies used for biological samples by LA-ICPMS analysis is given in Fig. 1 and Table 1 (summarizes the advantages and disadvantages of the calibration strategies). In terms of quantification concepts for LA-ICPMS analysis, external calibration, isotope dilution analysis, standard addition approaches and semiquantitative analysis as well as internal standardization strategies will be discussed.

1.1. *Tissue-type calibration standards*

Several LA-ICPMS studies have focused on the development of tissue-type section standards, using homogenates of different tissue types (e.g. liver or brain tissue) that are spiked with varying concentrations of the target analyte and cryo-sectioned to the same thickness as the sample [26,27,37]. The exact concentrations of the analytes within the tissue homogenates are then determined by solution-based ICP-MS analysis following acid-assisted digestion. By matching the material for the standard preparation with the samples, this is considered to eliminate the interferences arising from the sample's matrix. However, the homogenization step can lead to a potential change of the biological material's integrity and the achievement of homogeneous elemental distribution is a must for this type of standards. A general disadvantage associated with section-type calibration standards is the occurrence of thickness inaccuracies and anomalies. The sectioning process and other

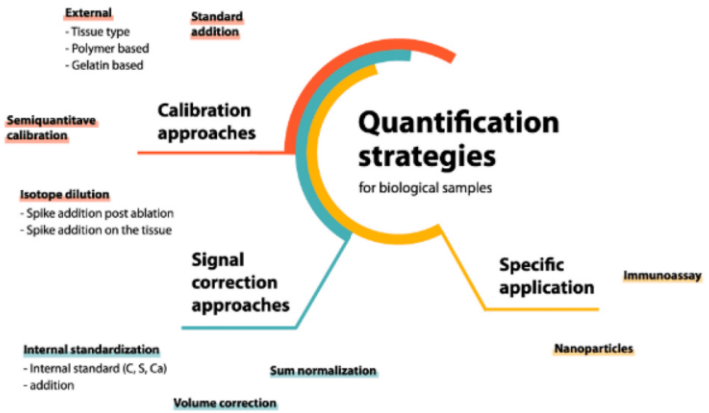

Fig. 1. Overview of different quantification strategies (including signal normalization) used for biological samples by LA-ICPMS imaging.

Table 1
Overview of different quantification and internal standardization concepts for bioimaging applications by LA-ICPMS.

Quantification type	Matrix	Advantages	Disadvantages
External calibration			
Tissue-type sections	Brain, liver kidney, blood	Can be considered as 'true' matrix-matched calibration standards	Access to a microtome Demanding workflow Handling of biological material Homogenization step required Accuracy of the section thickness High elemental background levels Matrix-matching
Polymer-based sections	Polymers	Low elemental background levels Properties of the polymers can be easily modified	Accuracy of the section thickness Access to a microtome Homogenous elemental distribution required
Spin-coating of polymer standards	Polymers	Low elemental background levels Properties of the polymers can be easily modified Can be used as internal standard layer	Matrix-matching Homogenous elemental distribution required
Gelatin sections	Gelatin	No biological material required Low elemental background levels	Access to a microtome Accuracy of the section thickness Homogeneous distribution of the analytes required
Gelatin micro-droplets	Gelatin	Defined volume Low elemental background levels	Availability/access to a micro-array spotter, ink-jet printer No homogeneous distribution of the analytes required
Gelatin micro-arrays	Gelatin	Defined volume Low elemental background levels	Fabrication of micro-arrays No homogeneous distribution of the analytes required
Gelatin molds	Gelatin	Defined thickness and surface roughness Low elemental background levels Good signal precision Easy preparation	Fabrication of molds
Solution-based	Aqueous	Use of aqueous elemental standards	Need to correct for differences in ablation efficiency Requires desolvation
Isotope dilution			
Spike addition post-ablation	–	Traceable to SI units Accurate single-point calibration	Cost intensive Applicable to one analyte
Spike addition on the tissue/cells	Tissue, cells	Traceable to SI units Accurate single-point calibration Matrix-matched	Cost intensive Applicable to one analyte Low count rates per pixel base Applicable for regions of interest
Semiquantification	Gelatin	Simultaneous (semi) quantification of all elements Allows higher concentration ranges	Small number of elements quantified, others semiquantified Applicable to biosamples for now Requires a library of response factors
Standard addition			
Standard addition of droplet standards	Tissue	Can be considered as matrix-matched calibration	High elemental background levels
Internal standardization			
Intrinsic elements (C, P, S, Ca)		Corrects for elemental fractionation and matrix effect Naturally present in sample/standard	Not actual quantification Lack of appropriate elements for IS Matrix-depending partitioning of C
Non-intrinsic elements		Corrects for elemental fractionation, matrix effect and differences in ablation mass	Binding to DNA – not present in the same extent in all cell types
Ablated volume normalized calibration	Any	No need for matrix-matched standards	Additional cost for instrumentation (to determine ablated volume)

preparation steps involved for cryo-sectioned standards can induce artefacts and various types of deformation, which are difficult to control [38]. The main requirement for this type of standards is the quantitative ablation of the standard and the sample (removal of the sample down to the substrate) to ensure that the amount of ablated material is the same. In case the biological sample is heterogenous with regions containing 'softer' and 'harder' material, complete ablation might be difficult to achieve and some residual material from harder parts of the sample can be observed after ablation. These phenomena together with potential thickness inaccuracies between standards and sample can potentially lead to biased LA-ICPMS results. Moreover, another disadvantage for the use of spiked tissue-type standards is the natural presence of endogenous elements contributing to high blank values.

1.2. Tissue-type section standards

The first protocol for matrix-matched tissue standards was presented by Becker et al., in 2005 [25] and was based on the homogenization of brain tissue samples spiked with elemental standard solutions of P, S, Cu and Zn. These tissue-type standards are often sourced from the same tissue type of the target species and subsequently, protocols for standards that are based on brain, liver, kidney or blood as matrix were developed. A general guide for producing matrix-matched standards for assessing the concentrations of trace metals in brain tissue was presented by Hare et al., in 2013 (Fig. 2A) [26]. For this purpose, cortical tissue from sheep brains was homogenized and spiked with varying concentrations of standard solutions of Co, Cu, Fe, Mg, Mn, Sr, Se and Zn. Cryo-sections were prepared and the elemental standard concentrations were determined by solution-based ICP-MS analysis. With the exception of Co and Se, the limits of detection were suitable for quantifying the analytes in a mouse brain sample [26]. The same principle of homogenizing, spiking with elemental standard solutions, freezing and cryo-cutting thin sectioned standards was used as matrix-matched standards for imaging Zn and Mg in rat's brain tissue [39]. True

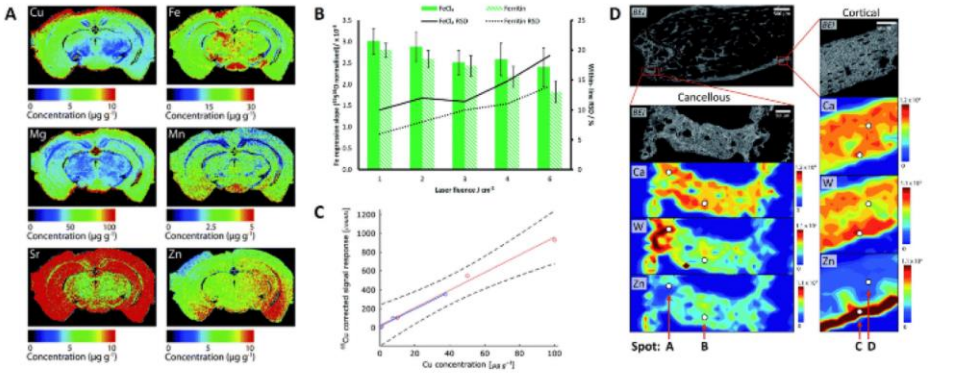

Fig. 2. (A) LA-ICPMS images of the quantitative Cu, Fe, Mg, Mn, Sr and Zn distribution in mouse brain using spiked and homogenized brain tissue standards [26]. (B) Species-dependent sensitivity using either the inorganic spike (Fe) or the species-specific spike (ferritin) in the standard, using different laser fluences [40]. (C) Comparison of calibration curves for spiked sections of liver tissue homogenates and spiked gelatin droplet standards, obtained by LA-ICPMS analysis [37]. (D) LA-ICPMS quantification of Ca, W and Zn deposits in bone samples using hydroxy-apatite collagen standards [44]. Figures adapted from the references [26,37,40,44] with permission from the publishers.

concentrations of Mg and Zn were determined in homogenized tissue by flame atomic absorption spectrometry (FAAS). Furthermore, a methodology for the production of matrix-matched tissue homogenates spiked with Se and Fe was described and its feasibility as calibration standards for quantitative imaging was examined [40]. The effect of elemental species-specific calibration on the quality of quantitative LA-ICPMS results was investigated by comparing tissue-matched standards spiked with inorganic Se and Fe with those spiked with specific-species, i.e. ferritin or selenoproteins (Fig. 2B). Homogeneity of the standards and correlation of the calibration graph slopes were monitored over a laser energy range of 1.0–6.0 J cm^{-2}. For Fe, the slopes were found to agree well, whereas, for Se the choice of the calibrant had an impact on the results [40]. Similarly, the development of durable standards was described for quantitative LA-ICPMS analysis by grinding rat brain tissue and spiking it with aqueous solutions with known concentrations of trace elements (Li, Co, Cr, Cu, Fe, Mn, Pb and Zn). The spiked tissue was then encapsulated in sol-gel pellets by adding it to a prepared xerogel solution. The mixture was poured into molds and dried. The results showed good linearity for all elements, repeatability, homogeneity and long shelf-life due to the stabilization of the standards by the sol-gel matrix [41]. Alternatively, homogenized sheep brain tissue sections mounted on slides were submerged into solutions with varying Fe concentrations rather than spiked with them [42]. In addition, the solutions contained a constant Rh concentration, which was used as an internal standard. To investigate tissue-matched standards for their suitability as calibration standards for quantitative LA-ICPMS imaging, their homogeneity and stability was characterized. Tissue-matched standards showcased homogenous distributions of both Fe and Rh with RSDs of 8.3 % and 4.7 % respectively, stability at room temperature to up to 50 days, and a good linear calibration. The accuracy of the LA-ICPMS data was evaluated against micro-XRF analysis [42]. Tissue-type sections standards based on liver were also employed in the context of cancer research to quantify Ru and Pt concentrations in organs and tumor tissue of mice after treatment with Ru- and Pt-based anticancer compounds [27]. Method validation relied on parallel solution-based analysis of biological samples by ICP-MS after acid-assisted digestion. In another study, the quantitative distribution of Cu in cryo-sections of liver tissue was examined via LA-ICPMS with both matrix-matched thin sections of spiked liver tissue homogenates as well as spiked gelatin droplet standards (Fig. 2C) [37]. No statistical differences were observed between the two approaches. However, low cost, simplicity and availability make spiked gelatin standards the favored choice. Thus, one of the main drawbacks of tissue-type standards is the laborious preparation, which requires access to a cryotome and skilled personnel. Additionally, an accurate estimation of the tissue thickness may be challenging in some cases as well. For single-cell analysis by LA-ICPMS, this approach is unsuitable as the assumption that the volume can be directly derived from the quantitative removal of the irradiated material may underestimate the mass removed, especially for smaller spot sizes. In this case, *a posteriori* surface characterization would be required to precisely define the volume removed [32].

One study reported the use of egg yolk as matrix for the preparation of calibration standards for tissue samples [43]. For this purpose, egg yolk was spiked with the analyte of interest, homogenized, heated up to 90 °C, and cooled down to generate a solid structure similar to tissue. The egg yolk standards were sectioned by cryo-cutting and fixed on a glass slide. In a proof-of-principle study, the quantification method was applied to investigate the delivery of therapeutic cells to the target organs. The quantitative distribution of tumor cells and macrophages labelled with a Tm-complex were tracked in different mouse tissue samples and benchmarked to information obtained by magnetic resonance imaging (MRI) [43].

1.3. Bone and teeth samples

Moreover, several LA-ICPMS studies have also focused on the development of tissue-type calibration standards for hard tissues. In this context, bone was evaluated as matrix for the preparation of matrix-matched calibration standards to quantify tungsten and zinc deposits in bone with LA-ICPMS [44]. Mouse bone samples were dried under vacuum, grounded using a ball mill and spiked with appropriate volumes of multi-element standard solutions. After mixing, the standards were evaporated to dryness, manually homogenized and compressed into a 1.0 mm thick pellet with a manual hydraulic press. The analytical performance (linearity, limits of detection and accuracy) of the pressed bone powder standard was tested alongside hydroxyapatite:collagen (HC) (mimics the composition of bone) and hydroxyapatite (HA) synthesized pressed powder standards (Fig. 2D). While, bone standards showed a good linearity for tungsten ($R^2 > 0.995$), the linearity was less for zinc ($R^2 > 0.90$). The accuracy was tested by quantifying zinc in NIST

SRM 1486 through external calibration and comparing the results to the known reference value of zinc. Both matrix-matched standards (bone and HC pellets) provided accurate quantification of zinc in NIST SRM 1486 without correction for the calcium content [44].

Teeth are another commonly analyzed mineralized tissue as they provide a valuable chronological bioindicator of toxic metal exposure [45] and as they can be used to reveal past human/animal migration. Recently, studies have used various standards from in-house prepared matrix-matched standards made from healthy teeth to synthetic hydroxyapatite (HA) standards doped with the elements of interest to calibrate tooth samples instead of the usual single-point calibration with NIST glass-SRM [46]. One study used matrix-matched standards prepared by grinding healthy teeth, sieving the powder, spiking with known volumes of elemental solutions, and then drying, homogenizing, and pressing into disks [47]. This quantification method, using matrix-matched laboratory standards, proved effective in determining element concentrations in thin cross-sections of both healthy and filled teeth. The use of these standards ensured accurate and precise results in the quantitative determination of Al, Ba, La and Sr in dental tissues with LA-ICPMS [47].

In another study, three synthetic HA materials (i.e., amorphous HA crystals, pelletized HA powder, and pelletized HA powder that was subsequently sintered) were prepared and evaluated for their suitability as external calibration standards for human teeth. The pelletized HA powder showed the best ablation properties compared to the previous materials HA and NIST glass-SRM, especially in tooth analysis. The metals were integrated uniformly, and the calibration curves showed excellent linearity. Detection limits ranged from 0.1 to 2 μg kg^{-1} for Mg, Al, Ni, Cu, Zn, Cd, Ba and Pb [45].

1.4. Hair samples

Spiked hair strands served as matrix-matched tissue standards for external calibration due to the limited availability of certified reference materials from human hair and their powder nature, which makes them not ideal as matrix-matched standards. Therefore, to quantify the distribution of analytes along a single hair strand, element-enriched hair strand standards were prepared in-house by immersing human hair in solutions with different bromine and iodine concentrations [48]. The exact elemental concentrations in the hair standards were determined by digestion followed by pneumatic nebulization (PN-)ICP-MS analysis. The method was successful in achieving homogenous standards and generating highly linear calibration curves [48]. Similarly, As and Pb levels were determined in individual hair strands of leukemia patients by LA-ICPMS [49]. The calibration method was based on matrix-matched hair standards spiked with the analytes of interest and the exact metal concentrations were determined in a portion of the spiked hair standards by ICP-MS analysis [49]. A similar principle was applied to the LA-ICPMS analysis of mummy hair samples, using three contemporary hair samples with known As concentrations as matrix-matched standards [50]. In another study, both metal-enriched hair powder standards and hair strand standards immersed in metal solutions were used for quantification [51]. Method development focused on arsenic with the use of sulphur as internal standard element. While a good linear correlation and LOD was obtained, the binding of As to keratin in hair has proven to be a slow process [51]. In-house prepared spiked hair strands were also used as calibration standards to quantify the platinum concentration along a single hair strand from a patient who had received cisplatin as a cytostatic drug [52]. Complete ablation of the hair cross-section increased the sensitivity of the method. A lownoise-intensity ratio was obtained along the hair strand, and the variation of the Pt signal as a function of the respective cisplatin dose was clearly visible [52]. An alternative calibration strategy for hair analysis by LA-ICPMS was based on spiked keratin films as calibration materials [53]. For this purpose, the keratin films were prepared by extracting keratin from human hair followed by the formation of films through self-assembly, self-aggregation, and cross-linking activities. The doped keratin films showed better recovery and linearity for Pb quantification compared to the traditional method of soaking hair in a solution with the element of interest. This is because hair strands have limited surface area for Pb adsorption and not the right physiology to retain it, whereas keratin films were able to retain high quantities of Pb on their surface [53].

1.5. Polymer-based standards

The use of polymer- and resin-based standards that are spiked with different metal-containing solutions has been described in several LA-ICPMS studies for calibration purposes. The standards are based on materials with characteristics that can be easily modified, however, a homogeneous thickness and elemental distribution are essential in the preparation of polymer-based standards.

For the preparation of polymer-based standards, different strategies were reported in the literature. One early study developed a method based on spin-coating with solutions of polymethylmethacrylate (PMMA, 10 %), xylene (40 %) and chlorobenzene (50 %) that were spiked with organometallic Cu and Zn standards [29]. Ruthenium phthalocyanine dye and an organometallic yttrium standard were added to be used as internal standards. After spin-coating, substrates were baked on a hot plate at 130 °C for 2 min. The thickness of the PMMA thin films was characterized by profilometry and the surface roughness evaluated by atomic force microscopy (AFM). UV–Vis spectroscopy was used to determine the change in concentration of the dye and a ten-fold increase in analyte concentration in the film was observed, compared to the spin-coating solution due to solvent evaporation. The polymer-based calibration standards were evaluated using the elements Cu and Zn and their analytical figures-of-merit were benchmarked to homogenized brain tissue standards that were spiked with the same analytes and prepared as cryo-sections. The proposed approach also allowed for internal standardization and drift correction by employing internal standard elements (Y and Ru) in the underlying thin film. For this purpose, the biological sample was placed on top of the thin film and co-ablation of the tissue sample and the internal standard layer required careful optimization of the laser fluence to enable selective and quantitative/-full ablation of both layers (down to the substrate) [29]. A similar calibration approach was developed that was based on an aqueous soluble polymer (dextran) to increase the number of elements that can be spiked into the polymer standards [54]. For this purpose, a dextran solution was prepared in water and spiked with different amounts of metal solutions (in total 11 elements) and internal standards solution. Solutions were spin-coated onto glass slides and dried with a light N_2 gas stream. The average mass of the polymeric films was determined for each calibration point using an ultra-high precision balance by weighting glass slide before and after film deposition. The film thickness was determined by optical profilometry. The LA-ICPMS quantification method was validated using in-house prepared kidney homogenates spiked with known amounts of metals and applied to clinical human samples [54].

As alternative to spin-coating, another quantification strategy is based on the preparation of polymer-based section standards. One study used a cold-curing resin based on 2-hydroxyethylmethacrylate (Technovit 7100) that was used as infiltration solution and embedding medium. For preparation of the standards, the infiltration solution was spiked with different amounts of platinum(II) acetylacetonate, which is well soluble in organic solvents [30]. Subsequently, dimethyl sulfoxide was added to the infiltration solution to heat up the mixture and initiate the polymerization. After hardening, the resin standards were sectioned to a thickness of 5 μm. The same resin/infiltration solution was also used for embedding of the tissue samples to simulate ‘matrix-matching’. The standards were characterized using ICP-MS analysis after microwave-assisted acid digestion to assess the elemental concentrations. As proof-of-principle, the platinum distribution was quantified by

LA-ICPMS at different time intervals in tissues of mice treated with the chemotherapeutic drug cisplatin. The tissue samples (testis, cochlea and kidney) were selected with regard to potential side effects and toxicity of cisplatin-treatment towards these tissue types [30]. In a subsequent study, the same calibration approach was used to quantify platinum in major functional units of testicle, cochlea, kidney, nerve and brain sections from cisplatin-treated mice [55]. Regarding the potential applicability of this standard type for 'hard' biological material, the quantitative platinum distribution was evaluated in tibia samples of mice treated with a platinum(II) anticancer compound [56]. Platinum was quantified in the hard bone samples upon resin-embedding to unravel potential targeting options of platinum chemotherapeutics in the treatment of bone metastases. Platinum levels were set in relation to the phosphorus and calcium distribution and correlative micro-XRF analysis was performed [56].

Recently, a new method for preparing polymeric reference materials for microanalysis using a 3D printing technique was proposed [57]. The elemental standard solutions were doped in polyacrylate resin by mixing with dispersant and then printed, layer by layer using a 3D printing technique at room temperature. The amount of dispersant in the mixture was optimized to achieve homogeneity of the printed polymer reference materials. The homogeneity was evaluated using LA-ICPMS analysis in line scan mode. The results showed that the printed sample was homogeneous on the 50-μm scale, and for some elements also on the 14-μm scale. Furthermore, the mass concentration of the doped elements was determined using ID-ICP-MS and proved to be equivalent to the nominal concentrations determined by the gravimetric method. Overall, compared to conventional preparation methods for polymer calibration standards, the 3D printing approach showed improved concentration accuracy and homogeneity of the prepared standards [57].

1.6. Gelatin-based standards

Gelatin was proposed as biological matrix mimic for the preparation of calibration standards for LA-ICPMS imaging. The main advantages of the use of gelatin are that it is easy to handle, readily available, inexpensive, non-toxic and provides a soft matrix similar to biological tissue. The matrix is considered to partially resemble fibrous protein collagen and its protein content is supposed to match the protein-rich cellular matrix. The fabrication of highly homogenous gelatin standards is not straight-forward and different approaches were used including total ablation, fast drying, the employment of high temperatures during the drying process, printing of gelatin standards and the production of gelatin micro-droplets.

In order to prove the matrix-matching capabilities of gelatin for biological tissue, several studies were performed. For this purpose, Cu quantification was compared using thin sections of spiked liver tissue homogenates and gelatin droplet standards [37]. No statistical differences were obtained between the results using the two calibration approaches and therefore, both were considered suitable for quantitative Cu bioimaging of liver cryo-sections [37]. In another approach, the calibration concept of standard addition on different mouse tissue samples was compared to external standardization based on gelatin micro-droplet standards. Cross-validation revealed consistent quantitative results between the two calibration approaches and matrices [58]. Both studies provided proof that gelatin-based standards could serve as matrix-matched calibrations for bioimaging applications by LA-ICPMS. One LA-ICPMS study evaluated the suitability of gelatin and the cold-curing resin Technovit as standard materials for bioimaging applications by investigating their particle transport and ionization characteristics using an optical particle counter inserted in-line between a 213 nm LA system and the ICP-MS instrument [59]. The size of the particles generated by the gelatin standards was smaller (sizes in the nm-range) than those of the Technovit standards (sizes in the low μm-range) resulting in higher signal intensities during ICP-MS analysis. Increasing the laser fluence resulted in a larger number of μm-sized particles for both materials, whereas the ionization efficiency of gelatin aerosols proved to be superior compared to aerosols produced from Technovit standards [59].

The properties of gelatin can be easily modified and the number and concentrations of analytes can be adjusted. For the latter, it has to be considered that with an increasing number of elements in gelatin as matrix, the gelatin becomes brittle, precipitation can occur and it becomes difficult to handle, especially at higher elemental concentrations. Whereas the working range of tissue-type section standards is determined by the natural abundance of endogenous elements and/or elements artificially introduced during sample preparation, gelatin shows comparably lower elemental background levels. One study compared gelatin standards prepared from a variety of animal sources and presented a method based on chelating resins to remove background metals in gelatin in order to increase the dynamic calibration range [33].

For quantification by LA-ICPMS, gelatin-based calibration standards in form of cryo-sections [60–62], micro-arrays [32], molds [33], bio-printed standards [63] and (micro-)droplets [35,36,64] were described. The use of gelatin sections was introduced as a calibration concept similar to tissue-type section standards. For this purpose, gelatin was doped with the analytes of interest and mixtures of gelatin and aqueous standard solutions were heated to 45–60 °C to ensure homogeneity of the analyte distribution. Gelatin cryo-sections were prepared with the same thickness as the biological samples and ablated using the same laser ablation parameters. Most studies verified the analyte concentrations within the gelatin standards performing acid digestion followed by bulk ICP-MS analysis. Gelatin-based section calibration was employed in several LA-ICPMS bioimaging studies in the medical context. As examples, this type of calibration was used to quantify the gadolinium deposition in the brain of patients that obtained with Gd-based contrast agents [65], to quantify the amounts of Fe, Cu and Zn in the brains of Alzheimer's disease and control mice [62] and to evaluate the iron and copper levels in liver needle biopsy specimens of patients suffering from Wilson's disease [60]. One LA-ICP-TOFMS study evaluated gelatin-based sections for the quantification of Mg, Mn, Fe, Cu and Zn in tissue cryo-sections [66]. The impact of variable thickness of gelatin sections on the signal intensity was studied and gelatin standards spiked with acidified single-element solutions and with solutions prepared from metal salts were compared. The developed method was used for the quantification of essential metals and molybdenum in kidney sections of rats dosed with bis-choline tetrathiomolybdate [66].

Recently, the production of bio-printed gelatin standards using a 3D printing device was proposed [63]. The gelatin was doped with lanthanide up-conversion nanoparticles and the bio-printed gelatin standards were compared with gelatin section standards and proved to be superior with regard to throughput, batch-to-batch repeatability and elemental signal homogeneity at 5 μm pixel size. For comparison and characterization, the thickness of the gelatin sections and the bio-printed gelatin standards was determined using multiphoton fluorescence microscopy. Bio-printing of gelatin standards provided a high level of automation, well-controlled spatial distribution in all three axes and the ability to control the temperature of the printing ink/gelatin and the printer bed [63]. The latter features prevented migration of material within the printed gelatin standards and allowed avoiding the occurrence of coffee-stain effects [67]. In a subsequent study, the same approach was adopted to prepare bio-printed gelatin standards for surface enhanced Raman scattering (SERS) [68]. Gelatin standards were spiked with SERS nanotags, which consisted of gold nanoparticles and a Raman reporter. The developed standards were characterized by single particle ICP-MS analysis and LA-ICP-TOFMS imaging [68].

In order to overcome the limitations associated with section-type standards (e.g. thickness inaccuracy, access to a cryotome and required homogenous distribution of the analytes), different quantification concepts based on gelatin as matrix were developed. For this purpose, a high-density gelatin micro-array was developed and characterized for calibration purposes by LA-ICPMS (Fig. 4C) [32].

Micro-machining of the micro-array was achieved by the laser ablation system itself and the method was cross-validated by synchrotron radiation (SR)-XRF analysis. Since all of the necessary instrumentation is already available in LA-ICPMS labs, the proposed micro-array standards are an attractive alternative to micro-dispensed droplet arrays, where a dedicated micro-droplet dispenser or micro-pipetting system is required. As a case study, the Cu uptake was studied in a model organism resulting from transition metal exposure at the sub-cellular level by LA-ICPMS and SR-XRF analysis [32]. The features of these microarrays could be especially attractive in high-throughput single-cell analysis. Alternatively, gelatin molds were evaluated as LA-ICPMS standards and benchmarked to gelatin sections and homogenized brain tissue standards (Fig. 4D) [33]. Compared to tissue-type standards, they proved to be superior in terms of thickness accuracy, signal precision and robustness for reproducible quantification and with regard to their analytical figures of merit. The latter ones depended on the levels of elements that were naturally abundant in the gelatin, which deviated significantly between different animal sources of gelatin. Therefore, an additional metal extraction step based on various resins was used to reduce the elemental backgrounds in gelatin and to improve the limits of detection [33].

One gelatin-based calibration strategy is based on the use of (micro-) droplet standards that are either pipetted manually or automated via an ink-jet device or a robotic micro-droplet dispenser. In droplet-based approaches, heterogeneous elemental distributions can occur on the microscale due to the coffee stain and/or Maragoni effect shown in Fig. 3 [69,70].

On the macroscale, this problem can be overcome by quantitative/full ablation of the entire droplet. However, this process can be time-consuming due to the dimensions of each droplet, especially when the droplet deposition is performed manually. For gelatin-based droplets, volumes of around 1–300 μL and droplet areas of up to 4.5–6 mm^2 have been reported, in case manual pipetting was performed by micro-pipettes and a micro-balance was used to record the exact amounts of the deposited droplet standards [35,71]. Reduction of the droplet size can be achieved, e.g. by drying the droplets on a hydrophobic surface. Alternatively, the analysis time can be decreased by ablating a representative part of the droplet, e.g. by ablating a cross-section or by spot analysis, provided that the elemental distributions are homogenous. One LA-ICPMS study systematically evaluated different parameters in the preparation of gelatin droplet standards in order to achieve a homogenous elemental distribution within the droplets and to avoid the occurrence of the coffee stain and/or Maragoni effect [67]. The latter

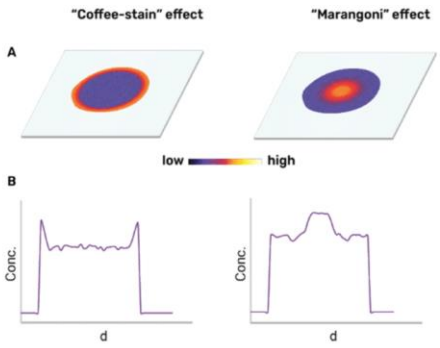

Fig. 3. Scheme of elemental distributions (A) on the surface and (B) in depth laterally through the center of the sample, showing the heterogeneous distribution of elements in the formation of gelatin droplets, which can result from the coffee stain or Maragoni effect.

ones proved to be element dependent and it was shown that the optimization of the drying/setting conditions of gelatin-based droplets was essential to provide homogenous elemental distributions. Increased temperatures improved the three-dimensional homogeneity of elements within the droplets and a drying temperature of 100 °C was recommended by using a mechanical convection oven to ensure a temperature-controlled environment (Fig. 4A) [67]. A subsequent LA-ICPMS study compared the quantitative ablation of entire gelatin-based droplet standards and spot ablation of highly homogenous dried gelatin gels spiked with different analytes [35]. For the second approach, the ablation volume was precisely determined using atomic force microscopy (AFM). Both calibration methods were applied to quantify membranous receptors in breast cancer cell lines using receptor-specific hybrid tracers for fluorescence confocal microscopy and high-resolution LA-ICPMS analysis (Fig. 4E) [35].

Gelatin-based droplet standards were further employed in LA-ICPMS studies in the context of metal-based anticancer drug research. One study addressed the platinum uptake in individual cells in the kidney of monkeys treated with cisplatin to evaluate possible mechanisms for cisplatin-induced nephrotoxicity [64]. In another study, the quantitative platinum distribution was studied by LA-ICPMS in ovarian cancer peritoneal xenografts after intraperitoneal chemoperfusion of oxaliplatin [72]. Quantification was accomplished by the use of gelatin droplet standards spiked with elemental platinum standards. Platinum accumulation was mainly observed in the extracellular matrix and results were correlated with results obtained by SR-XRF analysis [72].

One study developed a single particle detection method based on LA-ICPMS analysis for nanoparticle (NP) analysis in biomaterials [73]. Custom-made gelatin standards containing commercial or synthesized gold NPs of various sizes and with different number concentrations were used to optimize the conditions for the measurement of gold NPs. The optimized LA-ICPMS method was employed to study the size, number concentration and localization of Au NPs in roots of sunflower plants grown hydroponically with Au NPs added [73]. Gelatin droplet standards were evaluated for the quantification of iron oxide nanoparticles in gelatin microspheres containing $CaCO_3$ crystals by laser ablation in combination with ICP-MS/MS tandem technology [74]. Method development focused on resolving interferences ($^{40}Ar^{16}O^+$) on the signal of $^{56}Fe^+$ by relying on chemical resolution using a gas mixture of NH_3 and He. Fe-spiked gelatin droplet standards were prepared on a high-purity single-side polished silicon wafer and used as external calibration standards. Their corresponding Fe concentrations were determined by pneumatic nebulization ICP-MS/MS analysis after acidic digestion [74].

The dispensing of small-sized droplet standards in a precise and automated way can be achieved by the use of a commercial inkjet device or a robotic micro-spotting/arraying system. A modified dosing device based on a commercial ink cartridge was developed for the precise deposition of pL-droplets onto samples [75]. The method was applied to characterize the elemental composition of thin-layered materials via standard addition [75]. Another study describes the use of a MicroFab Jetlab micro-dispensing unit to create a rectangular grid of gold standard solutions [76]. The quantitative uptake of Au nanoparticles and of an Au-peptide cluster into single cells was studied by LA-ICPMS via this approach [76,77]. A micro-array spotter was used to print ICP-MS standard solutions onto nitrocellulose membranes [78] and on target glass slides [79] with volumes in the pL-range. This method was introduced for single-cell analysis by LA-ICP(-TOF)MS to quantify an Ir-DNA intercalator and an mDOTA-Ho dye in adherent 3T3 fibroblast cells [78,79]. A similar approach was employed to study the quantitative uptake of Ag nanoparticles in a multicellular tumor spheroid model by the use of droplet standards based on Ag nanoparticle suspensions [80].

Multi-element calibration standards for LA-ICP-(TOF)MS bioanalysis were introduced based on gelatin micro-droplets that were generated by a micro-spotter (Fig. 4B) [36]. This approach provided the robotic dispensing of droplets with volumes in the pL-range with high precision (around 5–10 %). The small size of the droplets with a diameter of

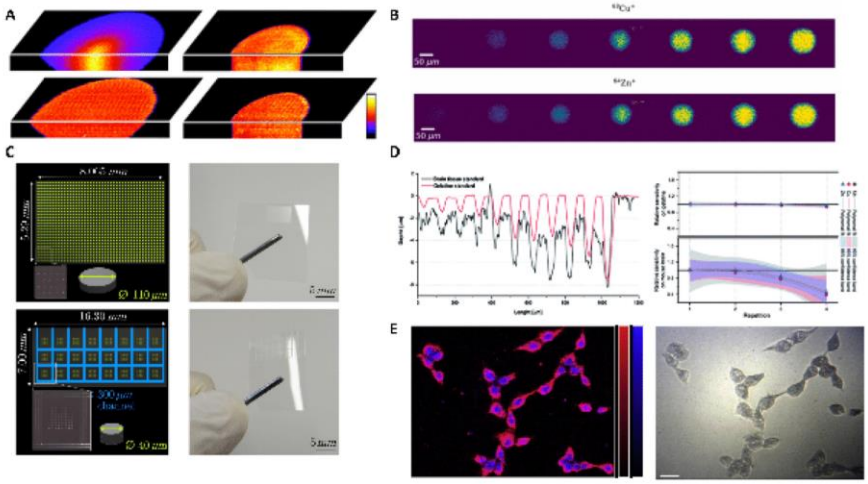

Fig. 4. (A) Effect of drying temperature (room temperature vs. 100 °C) on elemental distributions in gelatin-based droplet standards [67]. (B) Calibration sequence of multi-element gelatin micro-droplet standards prepared by a micro-dispensing device [36]. (C) Micro-array standards based on gelatin for single-cell analysis. The micro-array was machined by the laser ablation system [32]. (D) Profilometry data of standards that were ablated several times with increasing laser power and relative sensitivities for Mn, Cu and Zn derived from repeated ablation of calibration standards [33]. (E) Two channel LA-ICP-MS image (left) and brightfield microscopic image (right) of cells stained with receptor-specific hybrid traces, channels representing ^{89}Y and ^{193}Ir signal response [35]. The Figures were adapted from the references [32,33,35,36,67], with permission from the publishers.

100–200 μm and the use of a low-dispersion LA setup resulted in an analysis time of less than 10 min for a calibration blank and a series of 5 calibration standards. This is in a similar time regimen as a calibration sequence for solution-based ICP-MS analysis. The quantitative LA-ICPMS imaging method was validated by solution-based flow injection ICP-MS/MS analysis [36]. In a subsequent study, the calibration method was further validated by standard addition and isotope dilution approaches [58]. The developed calibration method is applicable to the multi-element quantification of biological samples including single cells and tissue samples by LA-ICPMS analysis [36,81,82]. The gelatin micro-droplet standards are the first ones that are commercially available for bioimaging by LA-ICPMS [83].

1.7. Solution-based quantification/online addition of standards

Alternatively, solid-liquid calibration is also utilized for quantification purposes in LA-ICPMS. Dual flow systems enable simultaneous introduction of the laser ablated material and a nebulized aqueous standard solution. This method entitles mixing of the carrier gas flow coming from the ablation cell with an aerosol generated by nebulization of an aqueous standard solution. Both standards with natural isotopic composition as well as isotopically enriched standards have been used for such experiments. Alternating addition of standard and blank solutions to the sample stream allows for quantification of the analyte concentration in the sample. The method requires correction for the differences in ablation efficiency as well as desolvation of the wet aerosol prior to its mixing with the sample aerosol, when aiming to maintain the advantages of 'dry plasma' conditions. The main advantage of this calibration method is that it enables quantification based on aqueous elemental standards, which are usually readily available in ICP-MS laboratories. However, it cannot account for possible variations in ablation efficiency or altered transport efficiencies [84].

Various solution-based calibration methods for quantitative analysis of biological samples have been developed over the years. In one study, a dual flow of the carrier and nebulizer gas was used to transport the aerosol of the nebulized aqueous standard and that of the ablated brain tissue sample into the ICP source [85]. Aerosols were introduced separately in the injector tube inside a special ICP torch and then mixed in the inductively coupled plasma as shown in Fig. 5. The nebulizer produces wet aerosols affecting the sensitivity and linearity of the calibration curves. The introduction of water in the plasma by nebulization of aqueous standards increases the formation of polyatomic ions, which can interfere with the signal of the analyte isotopes. The effect of water on the calibration curves is different for different isotopes, and variations in the ratio of the slopes of the calibration curves can be observed. The loss of analytes during the nebulization step may also affect the calibration curves. Thus, calibration in dry plasma utilizing matrix-matched standards, i.e. homogenous brain laboratory standards, was also performed. The ratios of the calibration curves slopes obtained

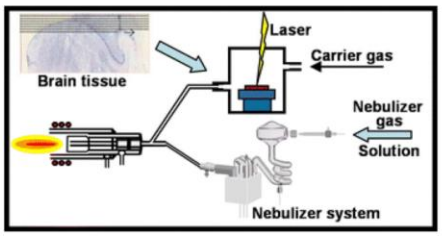

Fig. 5. Schematic of the solution-based calibration approach for the analysis of mouse brain by LA-ICPMS. The laser ablation and the gas nebulizer are coupled separately to the ICP-MS. The aerosols from the nebulizer and LA are simultaneously introduced into the injection tube. The Figure was adapted from Ref. [85] with permission from the publishers.

with the aqueous standards and solid standards approach were applied to correct for the differences of sensitivity among LA-ICPMS and ICP-MS analysis. Generally, it is believed that the sensitivity is lower in the case of LA-ICPMS analysis compared to solution-based ICP-MS analysis. However, this is only the sensitivity of the method *per se*, not taking into account the dilution steps in the process of sample preparation (e.g. during sample digestion). Therefore, sensitivities would need to be evaluated for every sample/nuclide individually. After correcting for differences in sensitivity between ICP-MS and LA-ICPMS analysis, the concentrations of metals in mouse brains determined by calibration with aqueous standards were in agreement with those obtained by calibration with solid standards [85]. Similarly, a method for quantitative analysis was developed using a desolvating nebulizer system (DNS) coupled with LA and on-line internal standardization [86]. The results showed that DNS-ICP-MS signals were much stronger than LA-ICPMS signals for various elements. To correct for the differences in sensitivities, internal standard elements were used to obtain calibration curves. The method was applied to both standard reference materials and biological tissues, and the results were in good agreement with certified values [86].

The solution-based quantification approach was also applied to quantify elements on (external contamination) and in hair samples by LA-ICPMS. In one study, a dual argon flow of the carrier gas and nebulizer gas was used and external calibration was employed via defined standard solutions before analysis of a single hair strand [87]. Again, due to the differences in elemental sensitivities of LA-ICPMS and ICP-MS analysis, correction factors had to be applied. The correction factors were calculated using hair with known analyte concentrations (as measured by ICP-MS). Different essential and toxic metals and iodine were monitored in human and mouse hair, with good linear correlation coefficients of the calibration and limits of detection [87]. In another approach, essential and toxic elements in single hair strands were determined using solution-based calibration in LA-ICPMS with a double focusing sector field mass spectrometer. The method was compared to quadrupole-based ICP-MS (ICP-QMS) and different solution-based quantification strategies such as standard addition, and isotope dilution were employed for the quantification of uranium. A standard addition technique was developed for uranium determination in powdered hair by coupling the laser ablation chamber to an ultrasonic nebulizer. The results showed good agreement between the ablated and digested hair samples for essential and toxic elements, and the technique can be used to compare different components in hair from normal and exposed populations. The method has the potential for isotopic forensics investigation and monitoring after exposure accidents as well as a routine research tool for the assessment of a 'normal' and exposed population [88].

While solution-based calibration in LA-ICPMS can compensate for matrix-related differences and enables quantification based on aqueous standards, it requires correction for differences in ablation efficiencies and in elemental sensitivities between ICP-MS and LA-ICPMS analysis. This is accomplished either by calculating the correction ratio based on calibration curves' slopes obtained via solution standard and solid standard calibrations or by inclusion of an internal standard.

1.8. Isotope dilution approaches for LA-ICPMS analysis

Ideally, quantification procedures that are universally applicable and not laboratory dependent would be favorable for bioimaging applications by LA-ICPMS to facilitate the inter-laboratory comparability of the obtained results. The implementation of isotope dilution mass spectrometry (IDMS) protocols into LA-ICPMS workflows provides an accurate single-point calibration method that is traceable to SI units [89,90]. Isotope dilution analysis (IDA) relies on the principle that a change in the isotopic composition of the analyte of interest is induced by adding a well-defined amount of an isotopically-enriched spike to the sample. The analyte concentration of the sample is determined with high accuracy and precision by measuring the isotopic composition/ratios of the sample, the spike and the mixture/blend (containing the sample and the spike). IDA provides the advantage that the results do not depend on matrix effects and instrument instabilities over the course of an LA-ICPMS experiment due to the measurement of isotope ratios. As disadvantages, IDA requires dedicated isotopically-enriched spike solutions that can be expensive, IDA cannot be applied to monoisotopic elements and the sample preparation can be laborious in comparison to external calibration, which reduces the sample throughput. Moreover, the exact mass/volume of the spike solution added to the sample or the mass flow needs to be known/calculated. The main requirement for isotope dilution analysis is the isotope equilibration between the spike and the sample to ensure that the nuclide of the spike behaves similar to the nuclide of the analyte in the sample. For imaging applications of isotope dilution approaches, this can be a challenging task as a homogenous distribution of the spike is required on the target tissue/cell, while the integrity of the biological sample needs to be preserved. The approximate concentration of the target analyte in the sample has to be already known before adding the spike, as IDA requires an adequate spike/sample ratio (over- or underspiking needs to be avoided) to yield acceptable results without high uncertainties. In the field of bioimaging, IDA in combination with LA-ICPMS has the great potential to validate calibration strategies that provide higher throughput (e.g. matrix-matched external calibration with internal standardization), as would be required for routine medical applications.

The potential of IDA for the accurate quantification of metal-binding proteins by gel electrophoresis (GE) in combination with LA-ICPMS detection was demonstrated in several studies [91,92]. For the absolute quantification of transferrin, species-specific isotope dilution was performed based on the use of an isotopically enriched ^{57}Fe-transferrin complex to quantify natural transferrin in human serum samples. The developed ID method was compared to external calibration and validated using a serum reference material [93]. In one study, isotopically enriched ^{64}Cu, ^{68}Zn-superoxide dismutase (SOD) was prepared to quantify natural SOD in spiked liver extracts using polyacrylamide gel electrophoresis (PAGE) in combination with LA-ICPMS detection [94]. Species-unspecific isotope dilution was applied to quantify transferrin and albumin in human serum by non-denaturing (native) GE and LA-ICPMS detection of the sulphur signal. Spike addition was achieved by immersing the protein strips with a ^{34}S-enriched spike solution after gel electrophoresis and the method was validated using a serum reference material [95].

Different strategies for the addition of the isotopically-enriched spike solution have been described for LA-ICPMS bioimaging experiments. It has to be taken into account that in some of the described approaches, the condition of isotopic equilibration between the spike and the sample is not entirely fulfilled. As a consequence, IDA is no longer an absolute or fully traceable quantification method. This is for example the case, when the isotope equilibrium is obtained in the ion source only (e.g. by addition of the spike as solution post-ablation). One approach was based on a solid-spiking procedure, where powders were spiked with isotopically-enriched standards, dried, homogenized and pressed into the form of a pellet [96]. This ID method was applied to analyze coal samples, soils and sediments by LA-ICPMS [97–99]. The isotope dilution procedures were validated using commercially available solid reference materials and it was shown that the accuracy and uncertainty of the results could be improved in comparison to external calibration. As disadvantage, the sample preparation process for the production of pressed pellets is time-consuming and laborious. Moreover, due to the steps of homogenization, mixing and pressing, it is evident that the solid ID-LA-ICPMS approach is not suitable for biological samples (tissue sections and cells) as the integrity and cell arrangement/spatial information would get lost. For bioimaging applications of isotope dilution in combination with LA-ICPMS, the addition of the spike aerosol can be achieved online after the ablation cell through a micro-nebulizer and spray chamber. This method was applied to study the quantitative accumulation of platinum in rat kidneys after cisplatin perfusion using

quadrupole- and TOF-based LA-ICPMS detection [100,101]. The same approach was used to evaluate the quantitative uptake of platinum in a multicellular tumor spheroid model upon treatment with cisplatin. Validation of the ID method was accomplished by external calibration using gelatin-based standards and confocal fluorescence microscopy imaging of the spheroids [102]. One study reported on online double IDA for the quantification of Fe in homogenized sheep brain as model sample by LA-ICPMS [103]. The isotopically enriched ^{57}Fe spike solution was introduced post-ablation using a total consumption nebulizer. An estimation of the measurement uncertainty was performed, demonstrating that the mass of spike, the measured ratio of the standard blend and the mass of the calibrant were the factors with the greatest contribution to the overall uncertainty. In addition, external calibration with internal standardization was performed as comparison. For this calibration approach, the main contributing factors for the measurement uncertainty were the uncertainty in the linear least square regression and the signal variation [103].For the addition of the spike solution post-ablation, it has to be taken into account that variations occurring during processes in the laser ablation cell are not accounted for. Alternatively, the use of IDMS for imaging approaches requires a homogeneous distribution of the isotopically-enriched spike onto the sample surface for spatial analysis. One strategy was based on the automatic deposition of the spike solution on the sample surface by the use of a commercial inkjet printer. The quantitative uptake of cisplatin, carboplatin and oxaliplatin in mice kidney was studied via this strategy and compared to external calibration [104]. For single-cell analysis, an ID-LA-ICPMS protocol was developed based on a micro-array of single cells and the precise deposition of a known picolitre droplet of an enriched isotope solution onto each cell in the array with a commercial inkjet printer [105]. Single cells containing the analyte and dispensed droplets containing the spike were simultaneously ablated. The method was applied to evaluate the quantitative uptake of silver nanoparticles into macrophages at the single-cell level, as a proof-of-concept [105]. In another LA-ICPMS study, a micro-spotting device was used to deposit pL-volume droplets (containing a platinum-enriched spike solution) onto tissue sections of mice that were treated with a platinum-based drug. The absolute platinum quantity was obtained for μm-sized regions of interest in tissue samples, as defined by the extension of the deposited pL-volume droplet. Isotope dilution analysis was performed to quantify platinum in regions of interest in tumor tissue, mouse liver and spleen and the results were compared to external calibration using gelatin micro-droplet standards [58]. One study used a strategy, where isotopically enriched spike solutions were pipetted onto tissue sections (encircled with a silicon grease pen to create a barrier for the spike droplet) [106]. Isotope exchange/equilibration parameters were optimized and the ID approach was compared to external calibration by homogenous in-house prepared standards. The method was applied to the quantitative LA-ICPMS imaging of Fe, Cu and Zn in mouse brain of Alzheimer's Disease and correlative micro-XRF analysis was performed [106]. A recent ID-LA-ICPMS study used an electrospray-based coating device (ECD) to evenly distribute a known amount of the isotopically-enriched spike solution (^{65}Cu and ^{67}Zn) on mouse brain sections [107]. The mass of the spiked isotopes and the tissue sections on the slides was calculated by weighing them on an analytical balance. As proof-of-principle, the quantitative ID method was applied to quantify Cu and Zn in Alzheimer's disease mouse brain sections and validated by acid digestion and solution-based ICP-MS analysis [107].

1.9. Semiquantification approaches for LA-ICPMS imaging

The wider use of AI in all scientific areas will definitely leave its mark also in analytical chemistry, although the advancement in this field are so far limited, but has been already discussed in the recent review by Pan et al. [24] With more and more laboratories having access to ICP-TOFMS systems and the mantra of 'measure all nuclides all the time', the requirement to 'quantify all nuclides all the time' is a direct consequence. The advances made in the quantification with the use of gelatin standards have made it easier, however, it is practically impossible to fabricate calibration standards that include all the elements. Metarapi et al. have produced different sets of gelatin-based micro--droplet standards cumulatively including 72 elements; single elements standards were kept in acidic media and were not always compatible [108]. From these standards, a library of response factors was constructed and was later used in semiquantitative calibrations. The method was evaluated in two steps, (i) bootstrapping with gelatin standards and (ii) using real murine tissue thin slices. In the first step, a certain number of the elements (out of 48 elements) was chosen to serve as standards for the semiquantitative approach. The other elements were predicted by semiquantitative calibration; this was repeated (*in silico*) for a million times. The difference (the 48 elements had defined known concentrations) was plotted against the number of elements, and it was established that for the suitable accuracy, between 10 and 15 elements should be used (Fig. 6). In the second part, a similar exercise was done on real tissue sections, but only a handful of times were tested. The developed semi-quantification approach was based on 10 elements as calibration standards and provided the determination of 136 nuclides of 63 elements, with errors below 25 %, and for half of the nuclides, below 10 %. Also, a web application was developed and is free to use with all the needed instructions available in the paper electronic supporting information. Until this study, the term 'semiquantitative approach' was used mainly in the cases, where non-matrix matched standards were used; a concept that should not be mistaken with the described approach [108].

1.10. Internal standardization strategies

Internal standards are frequently used to correct for measurement deviations caused by matrix effects, elemental fractionation and instrumental drift in quantitative LA-ICPMS analysis. Ideally, an internal standard (IS) also accounts for variations in the mass ablated and transported to the ICP-MS. An effective IS for LA-ICPMS analysis should therefore match the following criteria, (i) a similar behavior to the analyte during the ablation process, transport and in the ICP, (ii) a homogenous distribution in the sample and the standard, and (iii) a similar atomic mass and/or first ionization potential as the analyte [109], with the proximity of the atomic mass being the most important factor. In literature, different strategies and elements/isotopes have been proposed for internal standardization in bioimaging experiments by LA-ICPMS. Signal normalization in LA-ICPMS analysis makes use of elements that are either intrinsically present in the biological sample or of non-intrinsic elements that are introduced by different approaches (e.g., by placing a thin layer containing the IS beneath or on top of the sample).

1.11. Carbon

The potential of carbon (^{13}C) as 'universal' internal standard for elemental mapping of biological samples by LA-ICPMS was long time under discussion in literature. Due to the presence of carbon and its (apparent) homogeneity in biological matrices, its suitability as internal standard to correct for potential signal drift and variations in the ablated mass of biological samples was extensively evaluated. An excellent overview on the topic regarding the factors affecting internal standard selection for quantitative elemental bioimaging of soft tissues by LA-ICPMS, was written by Austin et al. and it gives the conditions to be met, for ^{13}C to be used as an internal standard, despite of its drawbacks [109]. Importantly, Guenther et al. observed that carbon showed a matrix-dependent partitioning into carbon-containing gaseous species and carbon containing particles [110]. Trace element analytes were exclusively transported as the particulate phase. The matrix-dependent formation of gaseous carbon species can lead to inaccuracies of the target analyte and the IS in the ablation cell and tubing. The formation of the gaseous phase leads to broader or double peaks and thus to a

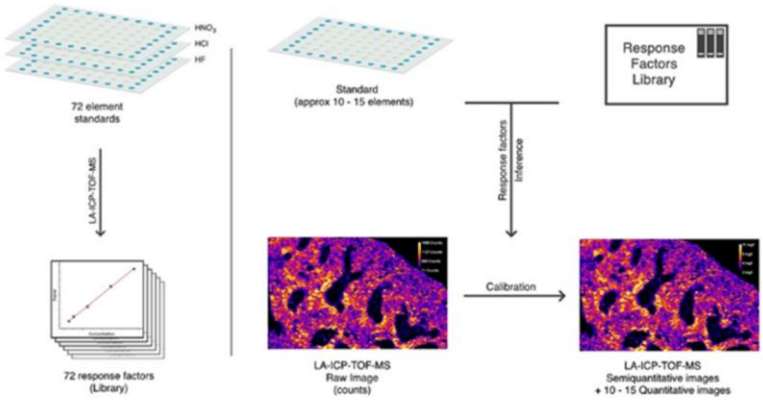

Fig. 6. Workflow for semi-quantitative analysis by LA-ICP-TOFMS. Calibration standards are based on multi-element gelatin micro-droplets [108].

distortion of the results. Further studies have shown that during laser ablation of gelatin (representative of biological samples) with higher laser fluence, an element-specific (C, As, Zn, Se, etc.) gaseous phase is formed, leading to double peaks that cause smearing effects and affect the accuracy of quantification [16,17]. Moreover, ^{13}C shows a background signal in the ICP-MS without ablation due to its presence in the atmosphere and possible impurities from the argon gas. Carbon may not be uniformly distributed in biological samples due to differences in tissue water content. Also, the atomic mass and/or first ionization potential varies significantly to many analytes.

Plant tissues have proven to be specifically difficult to analyze by LA-ICPMS, because of their relatively large size, varied structure and problems with ensuring the flatness and consequently, the focus over the entire sample area [111]. Therefore, ^{13}C has been used as an IS in several LA-ICPMS studies of plants to compensate for the effects of referencing on a loss of laser focus, overlapping layers of leaf tissue and cell damage within the imaged leaf tissue. One LA-ICPMS study assessed C, Mg, P, Ca, and Rb as potential candidates for internal standardization to study the Zn and Cd distribution in leaves of the hyperaccumulator *Arabidopsis helleri* [112]. Signal normalization with ^{13}C was used alongside calibration with cellulose-matrix matched standards to study five different tree species sampled in the area of Daejeon, Korea, and their accumulation rates of metal pollutants in their rings by LA-ICPMS. In order to determine the average concentration of metals in each annual ring, the surfaces of wood cores were analyzed using line scan mode. The results showed that the hardness and properties of the wood varied depending on the tree species and age. To correct for baseline shift of ICP-MS and differences in matrix ablation efficiencies, as well as changes in wood density during the ablation process, ^{13}C was used as an internal standard [113]. Quantitative LA-ICPMS analysis was used to map Ag, Mn and Cu in soybean leaves cultivated in the absence or in the presence of silver nanoparticles in comparison to silver nitrate [114]. The study evaluated suitability of the isotopes ^{12}C and ^{13}C in comparison to ^{28}Si and ^{31}P as IS. Based on the highest precision obtained and the highest homogeneity in the sample surface (verified through the LA images), ^{13}C was found to be the best internal standard [114]. Another LA-ICPMS study performed quantitative mapping of metallic pollutants in sweet basil. The experiment involved the cultivation of sweet basil in a nutrient solution spiked with 100 and 1000 ng mL^{-1} of Cs, followed by determination of the Cs distribution in the leaves using lab-synthesized standard pellets and ^{13}C as an internal standard. This work compared elemental images of the control leaf with the same matrix to the images of the leaf being analyzed, as the element analytes were transported solely as particulate phase from the carbon-containing gaseous species and carbon-containing particles during laser ablation [115]. Interestingly, one study used ^{13}C internal standard for the investigation of the As content in Andean mummy hair, while hairs are made of sulphur rich protein α-keratin and sulphur would therefore be a more appropriate choice [116].

1.12. Other intrinsic elements

Other elements than carbon that are usually present in the biological samples (e.g. phosphorus, sulphur and calcium) can be prone to segmentation to specific compartments and thus inappropriate to be used as IS. The suitability of the isotope ^{34}S as IS was evaluated in different LA-ICPMS biological studies. Sulphur was used as internal standard in an LA-ICPMS study for human hair and nail investigations, where a method was developed to analyze Mn, Cu, Zn, Sr, Y, Pb and U for human biomonitoring [117]. A similar LA-ICPMS study used sulphur as internal standard in the analysis of human hair and nails to determine the element concentrations and isotope ratios of 8 elements. Some isotope ratio changes reflect actual changes in diet, physiology, living area while other changes were attributed to the weathering and external contamination [118]. Leopard seal whiskers were used as a tool for trace element biomonitoring (Hg, Pb, Cd, and Se) and higher Hg burden was observed in comparison to previous studies [119]. A common element that is used an internal standard in LA-ICPMS studies on bone and teeth is ^{43}Ca, as it is homogenously distributed and does not suffer from the same problems as carbon [120–122]. With regard to phosphorus, it was shown that it can be used to compensate for differences in cell thickness and density in a multicellular tumor spheroid model. This approach together with single-cell resolution enabled to detect the quantitative platinum uptake in the different cell compartments of the spheroid model upon treatment with oxaliplatin [123].

1.13. Non-intrinsic elements

There are different strategies described for the use of non-intrinsic element for signal normalization approaches in LA-ICPMS studies. One study reported on the direct elemental analysis of whole blood samples by LA-ICPMS by taking advantage of the possibility to add an element of choice to the blood sample before ablation in a cryogenic cell. Rhodium was selected as internal standard and a low LOD and good accuracy and precision were obtained [124]. For section-based biological samples, another approach for internal standardization without the use of

intrinsic elements was based on adding a thin polymer or metal layer containing internal standard elements beneath the sample. Spin-coating of a PMMA layer doped with yttrium and ruthenium as IS elements onto glass slides provided a thin film, where the sample was placed on top [29]. Co-ablation of the tissue sample and the internal standard layer required careful optimization of the laser fluence to enable selective and quantitative/full ablation of both layers down to the substrate. The IS (Y and Ru) from the polymer layer were compared to ^{13}C in terms of precision and accuracy (quantified values were compared to results obtained by SN-ICPMS analysis). The use of ^{13}C as IS improved precision most likely due to higher background counts, whereas the quantification was less accurate as compared to Y and Ru as IS elements. Signal normalization to Y and Ru resulted in less precision but improved the accuracy of quantification by LA-ICPMS [29]. In one study, a gelatin-layer that was doped with thulium as IS was placed between the glass support and the tissue. Matrix-matched standards were prepared from rat kidney tissue spiked with uranium as target analyte to quantify U concentrations in renal tissue of rats [125].

Alternatively, the internal standard can be deposited on top of the biological sample section. This methodology can be based on sputtering techniques for the homogenous deposition of an IS layer on the tissue surface. LA-ICPMS studies used this strategy by employing gold as internal standard element in the thin films [126,127]. Gold poses several advantages as IS as its first ionization potential is comparable with elements such as zinc or copper. There are no background signals of gold in biological tissue and the mass of ^{197}Au is unlikely to be influenced by any spectral interference. It could be shown that gold standardization compensated instrumental drifts, matrix related ablation differences and day-to-day signal changes [126,127]. Automated deposition of an internal standard layer on top of the sample/tissue surface can be also achieved by the use of an inkjet printer [128–130]. The ink was spiked with the internal standard element (e.g. In and Ir) and printed onto the samples. It was shown that the homogenous distribution of the IS was further improved by coating the samples by gelatin. This approach proved to be effective to overcome day-to-day variations and instrumental drifts [131].

One internal standardization approach introduces the internal standard into the sample by different (labeling) strategies. One study developed a method based on iodination of fibroblast cells and tissue sections. Iodine was employed as an elemental dye with localization in the cell nuclei and lower iodination of the surrounding cytoplasm [132]. The use of iodine as an internal standard to correct for tissue inhomogeneities in LA-ICPMS was investigated for the simultaneous detection of two tumor markers in breast cancer tissue. Additionally, lanthanide background resulting from glass ablation was corrected for by Eu standardization.

One internal standardization strategy for quantitative LA-ICPMS bioimaging used an iridium-based intercalator that is commonly employed in imaging mass cytometry [133]. The Ir-based intercalator binds to the DNA of cells and therefore, it allows visualizing single cells in tissues based on their nuclei and to perform single-cell segmentation. In this study, its potential as internal standard was evaluated as it offers the advantage that it does not only correct for drift and matrix effects but also for differences in the ablated mass. As disadvantage, the metal intercalator binds to DNA, which is confined in the cell nucleus and might not be present to the same extent in all cell types. Therefore, a spatial resolution was employed in the study that was greater than the size of a single cell [133].

1.14. Ablated volume normalized calibration

In LA-ICPMS analysis, quantification usually relies on matrix-matched standards to solve elemental fractionation problems, where internal standardization is commonly used to correct for instrumental drift, and for non-dissectible samples, differences in ablated mass are corrected for. However, it is difficult to ensure a homogeneous distribution of the internal standard and a uniform laser light absorptivity is challenging in practice. Therefore, a new approach has been developed employing an ablation volume normalization method, in which the ablated volume is used to correct for ablation differences. The approach is based on measuring the volume after ablation with profilometry followed by normalization of the LA-ICPMS signal to the ablated volume. The first LA-ICPMS study regarding volume-corrected signals focused on differences in ablation rates within and between samples and standards by normalizing elemental maps based on the ablation volume per pixel measured by optical profilometry [134]. This approach moves from mass-to-mass concentrations to mass-to-volume concentrations and improves the accuracy of 2D LA-ICPMS mapping, as demonstrated using a decorative glass with different elemental concentrations. In a subsequent study, a variety of materials were investigated, including glasses, carbonates, gelatins, plants and zircon materials. Both, "hard" and "soft" materials were considered, serving as calibration standard and sample. A cross-calibration was performed by analyzing each material against each other in bulk analysis mode using a non-matrix-matched calibration by ablation volume normalization for validation of the method. The obtained concentrations in the different materials consistently matched the certified values regardless of the standard material used for calibration, highlighting the effectiveness of transferring calibration standards to materials with clearly defined elemental compositions. In particular, gelatin and glass showed good compatibility and versatility for calibration purposes [135]. One important aspect regarding the use of mass fractions (ppm, ppb etc.) and concentrations (g mL^{-1}, µg $µL^{-1}$ etc.) was also addressed in this study. Converting units from concentrations (actually the amount measured in the volume, either determined by a measurement procedure or with the sample preparation procedure, *e.g.* by preparation of thin sections of desired thickness) to mass fractions requires knowledge on the density of the sample. Considering the complexity of biological specimen, the density will normally not be homogenous across all of the sample and therefore, quantitative LA-ICPMS results should be presented as concentrations.

1.15. Applications of quantification procedures by LA-ICPMS

1.15.1. Quantification in immuno-mass spectrometry imaging by LA-ICPMS

LA-ICPMS is also employed for immuno-mass spectrometry imaging (iMSI), where the spatial expression of biomolecules is targeted in tissue sections following immunostaining procedures. A typical workflow including sample preparation and immuno-labelling for iMSI using LA-ICPMS analysis is shown in Fig. 7A [136]. Various elemental labeling strategies for antibodies have been developed for the application of multiplex immunoassays in combination with LA-ICPMS detection [136–138]. Metal tags include single lanthanide complexes such as DOTA, polymeric tags containing several lanthanides (e.g., MaxPar® metal-conjugated reagents), metal-coded affinity tags (MeCATs), nanoparticles, fluorescent Au or Ag nanoclusters (NCs) and quantum dots [139–144].

In imaging mass cytometry, high-resolution LA-ICP-TOFMS (using a CyTOF instrument) is employed to perform multi-parametric characterization of cell populations in tissue samples [145]. Whereas IMC is used purely in a qualitative way e.g., for cell phenotyping, several approaches were developed in the context of iMSI by LA-ICPMS for the quantification of analytes/biomolecules after metal-labeling strategies. One of the challenges associated with accurate quantification is a non-controllable antibody labeling chemistry. The binding efficiency of multiplexed staining can be affected by a number of factors including epitope blocking and other forms of steric hindrance [136]. To control the labeling degree, one study developed a novel antibody labeling technique that resulted in one label per antibody [146]. The labeling method was based on the use of small antibody-binding C2 domains that were modified with conventional MeCATs. Via this strategy, it was

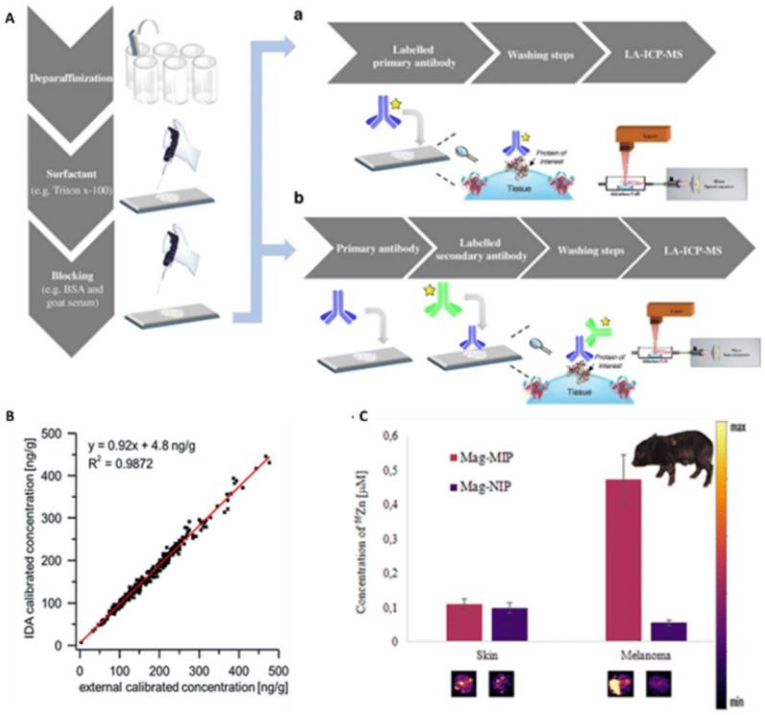

Fig. 7. (A) Workflow for immuno-mass spectrometry bioimaging with LA-ICPMS [136]. (B) Correlation of the Yb concentration determined by on-line isotope dilution analysis (IDA) and external calibration for quantification of enriched metal labels used in immuno-mass spectrometry imaging [148]. (C) Comparison of ^{66}Zn levels in healthy and melanoma skin of minipigs determined by molecularly imprinted polymers (MIPs)-LA-ICPMS [149]. The Figures were adapted from the references [136,148,149], with permission of the publishers.

possible to quantify the amount of introduced lanthanide ions into the sample and the molar amount of the antibody that was bound to the target protein. An LA-ICPMS-based western blot immunoassay was used to evaluate the applicability of six C2-tagged antibodies. Quantification of the labelled antibody–antigen complexes was achieved by the use of house-made calibration membranes [146]. One LA-ICPMS study investigated the effects of multiplexing on reproducible binding using metal-conjugated antibodies for different muscle proteins in murine quadriceps sections [147]. The average concentrations of the lanthanide analytes were determined in a series of sections upon individual and multiplexed immunostaining with the respective metal-conjugated antibodies. This reproducibility study revealed no significant differences between the individual and multiplexed application of the antibodies [147].

LA-ICPMS imaging in combination with gelatin-based mold standards was used to study the quantitative localization of dystrophin in muscle sections [150]. For this purpose, Gd-labelled anti-dystrophin antibodies were employed, where Gd was quantified as a proxy for the relative expression of dystrophin. The method was validated in murine and human skeletal muscle sections following k-means clustering segmentation and applied to patients suffering from Duchenne muscular dystrophy [150]. Online IDA was used to quantify elemental labels routinely used in imaging mass cytometry [148]. In this case, the protocol utilized enriched isotopes for the respective metal-tagged antibodies, which allowed quantification by IDA using LA-ICPMS imaging. The sample aerosol (containing the enriched isotope from the sample) was mixed with a wet aerosol from an aqueous standard containing the analyte (usually a lanthanide) with a natural isotopic abundance. The method was applied to quantify Yb-labelled anti-tyrosine hydroxylase in cryo-section of mouse brain. The mass flow parameters were calculated by ablation of a ^{172}Yb-spiked matrix-matched standard. IDA was compared with external calibration using gelatin standards and proved to be more robust for quantification as the isotope ratios were not influenced by signal drifts or plasma fluctuations (Fig. 7B) [148]. One LA-ICPMS study used molecularly imprinted polymers (MIPs) to target metallothionein, *i.e.* a metal-containing protein (Zn and Cd) [149]. Iron oxide magnetic particles were exploited as carrier of the polymeric layer and due to the agglomeration of the particles in the presence of an external magnet, the MIPs were capable of isolating metallothionein from a tissue sample. As proof-of-principle, the prepared particles were employed for the quantification of metallothionein in melanoma and healthy skin of melanoma-bearing minipigs. Significantly higher amounts of Zn were found in tumor tissue than in healthy skin (Fig. 7C) [149].

Nanoparticles are also commonly used as labels for quantitative determination of biomolecules by LA-ICPMS imaging. One study addressed the quantitative imaging of amyloid beta (Aβ) peptide in the brain, which is important for Alzheimer's disease (AD) research and

drug development [151]. The Aβ antibody was labelled with AuNPs to produce AuNPs-anti-Aβ conjugates that could bind to Aβ in brain sections. Quantitative imaging of Aβ was achieved by measuring Au concentrations using homogenised matrix-matched brain sections standards as external calibrants. The stoichiometric ratios between the metal conjugates and Aβ were optimized, and the efficiency of the immuno-reaction after labelling was investigated. By considering the molar relationship between AuNPs and Anti-Aβ, as well as the ratio of Anti-Aβ to Aβ, Aβ was quantitatively mapped in the brain by LA-ICPMS. The method accurately indicated the location and concentration of Aβ aggregation and was consistent with traditional immunohistochemical staining. The use of AuNPs improved the sensitivity and intuitiveness of the method due to the increased signal from Aβ [151]. In another study, a method for quantitative bioimaging of specific proteins in biological tissues using antibody-conjugated gold nanoclusters (AuNCs) and LA-ICPMS detection was described [152]. The distribution of metallothioneins (MT1/2 protein isoforms) in human retina tissue sections was successfully determined as proof-of-concept. AuNCs were conjugated to the selected antibody and provided high amplification for detection of MT1/2 distribution in the neurosensory retina layers. Elemental images of ^{197}Au were quantified using gelatin matrix-matched standards and converted to quantitative 2D images of MT1/2 concentration. The results obtained with LA-ICPMS were validated by comparison with measurements performed with a commercial ELISA kit. The developed strategy can be extended to other antibodies and metal markers and opens new possibilities for quantitative imaging of proteins in various biological tissues [152].

A recent LA-ICPMS study introduced matrix-matched standards that mimic the matrix of cultured cells by using the same cell line of the sample to create laboratory standards [153]. For this purpose, single-cell laboratory standards based on cells supplemented with Au nanoclusters (NCs) were developed. The cell standards were characterized by ICP-MS and LA-ICPMS analysis. A single biomarker strategy using Au NCs as specific antibody labels was employed for the analysis of selected proteins in individual cells by LA-ICPMS. Quantitative data for the proteins in the cells using the proposed matrix-matched calibration and LA-ICPMS analysis were successfully corroborated with commercial ELISA kits [153].

1.15.2. Quantification strategies for nanoparticle analysis with LA-ICPMS

The increasing use of nanoparticles (NPs) in various fields, e.g., biology, medicine, consumer products, energy production, etc., raises safety concerns, especially with regard to their effects on human health through inhalation and dermal exposure. NPs have different uptake mechanisms than dissolved species, which warrants thorough investigations. As a result, the number of studies on NPs and the development of dedicated measurement methods have greatly increased. The advent of nanotechnology has transformed the field of single-molecule analysis, enabling the detection of nanoparticles with remarkable sensitivity and resolution. LA-ICPMS is an effective technique for monitoring and quantifying nanoparticles in biological tissues. It offers high spatial resolution, allowing precise determination of the spatial distribution of nanoparticles in a sample, and serves as a valuable technique for monitoring NP-labelled antibodies. Several calibration strategies have been explored for the analysis/imaging of nanoparticles and the indirect detection of biomolecules using labelled nanoclusters in tissues, cells and other biological samples by LA-ICPMS. However, a reliable and accurate quantification of NPs by LA-ICPMS is challenging due to the lack of suitable standards and uncertainties associated with matrix effects. Most LA-ICPMS studies on NPs rely on standards that are prepared from elemental standard solutions. They offer the advantage that they are comparably easy to produce and to characterize (in most laboratories they have been already developed and exist based on in-house procedures), and that they can cover a reasonable mass range. However, it is still inconclusive whether the ablation behaviour of elemental standards, their transport to the ICP-MS and atomization and ionization in the ICP is consistent with those of NPs. Standards prepared from NP suspensions require thorough characterization with regard to NP stability and number of particles, they usually only cover a mass range with a NP number $> 10^3$ and NP agglomeration can occur, which impacts the NP number within the standard. Concepts for quantification of NPs by LA-ICPMS are based on the use of frozen and spiked brain tissue, spiked organic materials (e.g., gelatin or agarose), or dried residues on substrates, each strategy having its own capabilities and limitations depending on the type of sample, matrix, and target element or nanoparticle.

In recent years, single particle-inductively coupled plasma mass spectrometry (SP-ICPMS) has transformed the field of nanometallomics [154]. The method allows for differentiation between dissolved and particulate metal signals and enables quantification of the number and size of nanoparticles. However, SP-ICPMS is limited to the analysis of NPs in solution. To address this issue, one study demonstrated the use of solid samples by LA-ICPMS for localized NP analysis in biomaterials. LA-SP-ICPMS conditions, such as laser fluence, beam size, and dwell time were optimized to minimize NP degradation, peak overlap, and interference from dissolved gold and silver nanoparticles in a series of studies (Fig. 8A) [73,155,156]. A data processing algorithm was developed to extract the NP number concentration and size from the measurements. As a proof-of-concept, a cross-section of a sunflower root sample exposed to gold NPs was successfully imaged under the optimized LA-SP-ICPMS conditions, demonstrating the potential for localized NP characterization [73]. In addition, it was observed that the use of a low laser fluence (< 1 J cm^{-2}) is critical to avoid NP degradation and to ensure reliable results. The degradation of gold NPs (AuNPs) during laser ablation was studied and guidelines were provided for selecting the optimal laser fluence for NP analysis in gelatin, a matrix that mimics biological tissue. AuNPs with known sizes and narrow size distribution were used to monitor the measured NP size at different laser fluences. Optical profilometry was used to accurately measure the amount of material ablated at different laser fluences and provide a more accurate estimate of NP degradation [155]. In another study, advanced data processing and visualization techniques in LA-SP-ICPMS were used to image sunflower roots exposed to ionic silver (Ag^+). Detailed multiplexed images were obtained showing the uptake and transformation of Ag^+ into silver nanoparticles (AgNPs) within the root cross sections. The size of the biosynthesized AgNPs was found to be influenced by the reducing power of specific root compartments. Various visualization strategies were used to show the spatial distribution of Ag^+ and AgNPs, focusing on the number and size of individual AgNPs in selected root regions. Statistical analysis of AgNP distribution was also performed [156].

A 'single-cell isotope dilution analysis' (SCIDA) approach was developed to analyze metal NPs in single cells using LA-ICPMS (Fig. 8B) [105]. The principles of SCIDA were demonstrated using macrophage cells as a model to study the uptake of Ag NPs at the single-cell level. A microfluidic technique was used to place single cells in an array, and each cell was dispensed with a precise picoliter drop of an enriched isotope solution using a commercial inkjet printer. Accurate quantification of Ag NPs in single cells was achieved by isotope dilution LA-ICPMS analysis. The average Ag mass of 1100 single cells closely matched the average of the cell population analyzed by solution-based ICP-MS. The detection limit for Ag NPs in single cells was 0.2 fg Ag per cell [105]. Another method to quantify Au NPs in single cells was based on matrix-matched calibration standards from dried residues of picoliter droplets generated by an inkjet printer [77]. The distribution of the gold mass in single cells exposed to NIST Au NPs showed a lognormal distribution. The average measurement agreed well with the measurement from an aqua regia digested Au NP solution. The limit of quantification was determined to be 1.7 fg Au [77].

LA-ICPMS was used to gain insight into the spatial distribution and penetration behavior of NPs in complex three-dimensional tissue models. In one study, collagen-rich microstructures were produced in

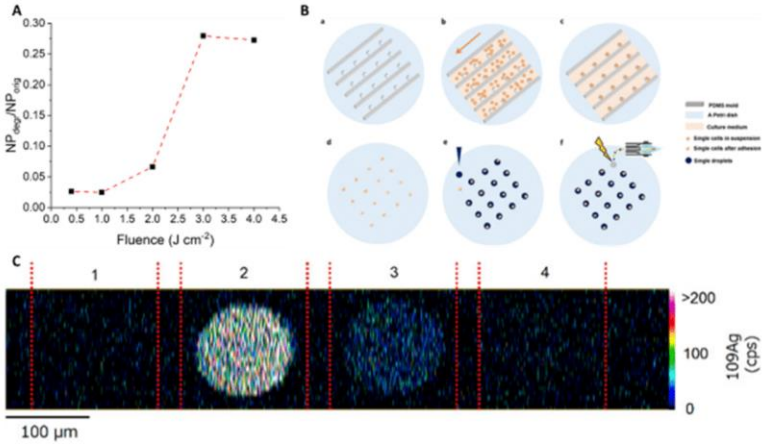

Fig. 8. (A) Influence of the laser fluence on the degradation of gold nanoparticles in gelatin using LA-ICPMS analysis [155]. (B) A schematic diagram of single-cell isotope dilution analysis with LA–ICPMS for the quantification of nanoparticles in single cells [105]. (C) Image of Ag NP calibration spots representing 50 (1), 3500 (2), 350 (3) and 35 (4) fg of Ag NPs [80]. The Figures were adapted from the following references [80,105,155], with permission of the publishers.

multicellular fibroblast spheroids (MCSs) to serve as a three-dimensional tissue analog for studying Ag NPs penetration [157]. LA-ICPMS imaging of the thin sections showed the distribution of Ag NPs along with other elements (Ag, P, Cu, Zn, and Br), indicating the localization of the particles. The distribution correlated with the presence of specific elements and was predominantly located in the outer edge of the spheroid model corresponding to proliferating cells [157]. In a subsequent study, the interactions of Ag NPs and the distributions of intrinsic minerals and biologically relevant elements were studied within thin sections of the MCS, using LA-ICP-(TOF)MS analysis [80]. Matrix-matched calibration standards were designed and printed using a non-contact piezo-driven array spotter with an Ag NP suspension and multi-element standards (Fig. 8C). The method allowed the detection of Ag, Mg, P, K, Mn, Fe, Co, Cu, and Zn in the femtogram range, which is sufficient for the determination of intrinsic minerals in thin MCS sections. After a 48h incubation period, Ag NPs were found to be concentrated in the outer rim of the MCS and undetectable in the core. Quantitative measurement of the total mass of Ag NPs in a thin section using LA-ICP-TOFMS imaging was consistent with results obtained by ICP sector field mass spectrometry in liquid mode after acid-assisted digestion. This approach demonstrates the potential of LA-ICP-TOFMS for spatially resolved nanoparticle imaging and elemental analysis in complex biological samples such as MCS [80].

Moreover, one strategy was developed that combines the concept of bioprinting for the preparation of gelatin-based multi-element standards and LA-ICP-TOFMS analysis [63]. Lanthanide up-conversion nanoparticles were incorporated into a gelatin matrix to produce the bioprinted calibration standards. The bioprinting approach showed higher throughput, better repeatability, and better elemental signal homogeneity compared to manual cryo-sectioning of standards. Bioprinting reduced inter-batch variability and analysis time because multiple standards were printed simultaneously. The bioprinted calibration standards remained stable for two months with proper storage [63]. The suitability of gelatin-printed calibration standards were additionally validated for the absolute quantitation of nanoparticles in Surface-Enhanced Raman Scattering (SERS) by developing a new 2D quantitation model [68]. SC-ICPMS was used to characterize the absolute concentration of the SERS nanotags. Gelatin-based calibration standards containing gold nanoparticles and a Raman reporter were prepared using a novel printing approach. The standards were further characterized using LA-ICP-TOFMS to assess the distribution and response of the nanotags. The LA-ICP-TOFMS analysis demonstrated the homogeneous distribution of nanotags and a linear relationship between the gold concentration and the response [68].

One recent study described a new approach for the preparation of quantitative standards for NPs that is based on particulate standards [158]. AuNP standards were prepared via micro-nano fabrication on an ITO (indium tin oxide) glass substrate. The fabrication process included coating a PMMA layer on the substrate followed by E-beam lithography to create an array of holes and a set of coordinate grids. Three different AuNPs (one synthesized and two commercial AuNPs) were used to prepare the calibration standards. The suspension of each AuNP was spread and dried on the fabricated PMMA layer. After the removal of PMMA, only the AuNPs located in the holes and the lines of the coordinate system were left on the ITO slide. The method allowed the preparation of AuNP standards with high accuracy and precision, covering a wide mass range. The approach highlights the importance of using particulate rather than ion standards for accurate quantification of NP, as Au ions and AuNPs exhibit different signal transduction efficiencies during LA-ICPMS analysis. However, the method has not yet been applied specifically to biological samples [158].

2. Conclusions and outlook

Initially, the development of elemental calibration standards for bioimaging applications by LA-ICPMS was based on manual fabrication and elaborate multi-step procedures, that required skilled personnel, in most cases, the handling of biological material and microtome cutting. The latter one can induce possible thickness inaccuracies of the standards that are biasing the results. Nowadays, state-of-the-art quantification is more and more relying on reliable, automated and most importantly, reproducible and operator-independent processes that are based on spin-coating, inkjet printers and robotic micro-droplet dispensing systems. Automation of the standard production by these processes can drastically increase the throughput to generate calibration standards. This makes these approaches interesting for mass production of standards and potential commercialization. With regard to the matrix of the standards, there is an increasing tendency observable towards the

fabrication of calibration standards that are based on materials (e.g., polymers and gelatin) with properties and characteristics that are easy to control, modify, and fine-tune for a specific application. These more 'universal' biological matrices can mimic the biological sample and can overcome some of the problems associated with tissue-type standards, such as handling of biological material and the background abundance of endogenous elements within the standards, potentially affecting the calibration range and limits of detection. There is still a requirement for certified materials such as NIST 61X glasses that are specific for bioimaging applications by LA-ICPMS.

In comparison to the described progress in the development of matrix-matched standards for elemental quantification in tissues and cells, the quantification of nanoparticles is understandably still in its initial stages, regarding only recent interest in the field. The standardization of the NP size usually relies on a single-point calibration and therefore, multi-point calibration standards are required for the development of the field. Similarly, the quantification of metal-conjugated antibodies is in its beginning, but the more often the methodology is used, the more reliable matrix-matched standards will emerge.

With the upcoming of ICP-TOFMS technology, all nuclides are always measured all the time and therefore, highly multiplexed standards and/or semiquantitative approaches are required to be able to quantify all nuclides of interest.

CRediT authorship contribution statement

Kristina Mervič: Conceptualization, Formal analysis, Investigation, Writing – original draft, Writing – review & editing. **Martin Šala:** Conceptualization, Formal analysis, Investigation, Project administration, Supervision, Writing – original draft, Writing – review & editing, Funding acquisition. **Sarah Theiner:** Conceptualization, Formal analysis, Funding acquisition, Investigation, Project administration, Supervision, Writing – original draft, Writing – review & editing.

Declaration of competing interest

There are no conflicts of interest to declare.

Data availability

No data was used for the research described in the article.

Acknowledgments

Sarah Theiner acknowledges the financial support from the City of Vienna Fund for Innovative Interdisciplinary Cancer Research (Project No. 21206). Kristina Mervič and Martin Šala acknowledge the financial support from the Slovenian Research And Innovation Agency ARIS research core funding no. P1-0034. K.M. thanks the Slovenian Research And Innovation Agency ARIS for funding her PhD research.

References

[1] A.L. Gray, Solid sample introduction by laser ablation for inductively coupled plasma source mass spectrometry, Analyst 110 (5) (1985) 551–556.
[2] S.F. Durrant, N.I. Ward, Laser ablation-inductively coupled plasma-mass spectrometry (LA-ICP-MS) for the multielemental analysis of biological materials: a feasibility study, Food Chem. 49 (3) (1994) 317–323.
[3] S. Wang, R. Brown, D.J. Gray, Application of laser ablation-ICPMS to the spatially resolved micro-analysis of biological tissue, Appl. Spectrosc. 48 (11) (1994) 1321–1325.
[4] D. Pozebon, G.L. Scheffler, V.L. Dressler, Recent applications of laser ablation inductively coupled plasma mass spectrometry (LA-ICP-MS) for biological sample analysis: a follow-up review, J. Anal. At. Spectrom. 32 (5) (2017) 890–919.
[5] T.J. Stewart, Across the spectrum: integrating multidimensional metal analytics for in situ metallomic imaging, Metallomics 11 (1) (2019) 29–49.
[6] P.A. Doble, R.G. de Vega, D.P. Bishop, D.J. Hare, D. Clases, Laser ablation–inductively coupled plasma–mass spectrometry imaging in biology, Chem. Rev. 121 (19) (2021) 11769–11822.
[7] S.J.M. Van Malderen, A.J. Managh, B.L. Sharp, F. Vanhaecke, Recent developments in the design of rapid response cells for laser ablation-inductively coupled plasma-mass spectrometry and their impact on bioimaging applications, J. Anal. At. Spectrom. 31 (2) (2016) 423–439.
[8] A. Gundlach-Graham, D. Günther, Toward faster and higher resolution LA–ICPMS imaging: on the co-evolution of LA cell design and ICPMS instrumentation, Anal. Bioanal. Chem. 408 (11) (2016) 2687–2695.
[9] T. Van Acker, S.J.M. Van Malderen, T. Van Helden, C. Stremtan, M. Šala, J.T. van Elteren, F. Vanhaecke, Analytical figures of merit of a low-dispersion aerosol transport system for high-throughput LA-ICP-MS analysis, J. Anal. At. Spectrom. 36 (6) (2021) 1201–1209.
[10] C. Neff, P. Becker, D. Günther, Parallel flow ablation cell for short signal duration in LA-ICP-TOFMS element imaging, J. Anal. At. Spectrom. 37 (3) (2022) 677–683.
[11] H.A.O. Wang, D. Grolimund, C. Giesen, C.N. Borca, J.R.H. Shaw-Stewart, B. Bodenmiller, D. Günther, Fast chemical imaging at high spatial resolution by laser ablation inductively coupled plasma mass spectrometry, Anal. Chem. 85 (21) (2013) 10107–10116.
[12] M. Šala, V.S. Šelih, C.C. Stremtan, J. Teun van Elteren, Analytical performance of a high-repetition rate laser head (500 Hz) for HR LA-ICP-QMS imaging, J. Anal. At. Spectrom. 35 (9) (2020) 1827–1831.
[13] J.T. van Elteren, V.S. Šelih, M. Šala, Insights into the selection of 2D LA-ICP-MS (multi)elemental mapping conditions, J. Anal. At. Spectrom. 34 (9) (2019) 1919–1931.
[14] J.T. van Elteren, M. Šala, D. Metarapi, Comparison of single pulse, multiple dosage, and 2D oversampling/deconvolution LA-ICPMS strategies for mapping of (ultra)low-concentration samples, Talanta 235 (2021) 122785.
[15] C. Neff, P. Keresztes Schmidt, P.S. Garofalo, G. Schwarz, D. Günther, Capabilities of automated LA-ICP-TOFMS imaging of geological samples, J. Anal. At. Spectrom. 35 (10) (2020) 2255–2266.
[16] A. Jerše, K. Mervič, J.T. van Elteren, V.S. Šelih, M. Šala, Quantification anomalies in single pulse LA-ICP-MS analysis associated with laser fluence and beam size, Analyst 147 (23) (2022) 5293–5299.
[17] T. Van Helden, K. Mervič, I. Nemet, J.T. van Elteren, F. Vanhaecke, S. Ronćević, M. Šala, T. Van Acker, Evaluation of two-phase sample transport upon ablation of gelatin as a proxy for soft biological matrices using nanosecond laser ablation – inductively coupled plasma – mass spectrometry, Anal. Chim. Acta 1287 (2024) 342089.
[18] S.E. Jackson, Calibration strategies for elemental analysis by LA-ICP-MS, in: P. Sylvester (Ed.), Laser Ablation–ICP–MS in the Earth Sciences - Current Practices and Outstanding Issues, vol. 40, 2008.
[19] H.P. Longerich, D. Günther, S.E. Jackson, Elemental fractionation in laser ablation inductively coupled plasma mass spectrometry, Fresen. J. Anal. Chem. 355 (5) (1996) 538–542.
[20] S. Zhang, M. He, Z. Yin, E. Zhu, W. Hang, B. Huang, Elemental fractionation and matrix effects in laser sampling based spectrometry, J. Anal. At. Spectrom. 31 (2) (2016) 358–382.
[21] I. Konz, B. Fernández, M.L. Fernández, R. Pereiro, A. Sanz-Medel, Laser ablation ICP-MS for quantitative biomedical applications, Anal. Bioanal. Chem. 403 (8) (2012) 2113–2125.
[22] A. Limbeck, P. Galler, M. Bonta, G. Bauer, W. Nischkauer, F. Vanhaecke, Recent advances in quantitative LA-ICP-MS analysis: challenges and solutions in the life sciences and environmental chemistry, Anal. Bioanal. Chem. 407 (22) (2015) 6593–6617.
[23] D. Hare, C. Austin, P. Doble, Quantification strategies for elemental imaging of biological samples using laser ablation-inductively coupled plasma-mass spectrometry, Analyst 137 (7) (2012) 1527–1537.
[24] H. Pan, L. Feng, Y. Lu, Y. Han, J. Xiong, H. Li, Calibration strategies for laser ablation ICP-MS in biological studies: a review, TrAC, Trends Anal. Chem. 156 (2022) 116710.
[25] J.S. Becker, M.V. Zoriy, M. Dehnhardt, C. Pickhardt, K. Zilles, Copper, zinc, phosphorus and sulfur distribution in thin section of rat brain tissues measured by laser ablation inductively coupled plasma mass spectrometry: possibility for small-size tumor analysis, J. Anal. At. Spectrom. 20 (9) (2005) 912–917.
[26] D.J. Hare, J. Lear, D. Bishop, A. Beavis, P.A. Doble, Protocol for production of matrix-matched brain tissue standards for imaging by laser ablation-inductively coupled plasma-mass spectrometry, Anal. Methods 5 (8) (2013) 1915–1921.
[27] A.E. Egger, S. Theiner, C. Kornauth, P. Heffeter, W. Berger, B.K. Keppler, C. G. Hartinger, Quantitative bioimaging by LA-ICP-MS: a methodological study on the distribution of Pt and Ru in viscera originating from cisplatin- and KP1339-treated mice, Metallomics 6 (9) (2014) 1616–1625.
[28] J.A.T. Pugh, A.G. Cox, C.W. McLeod, J. Bunch, B. Whitby, B. Gordon, T. Kalber, E. White, A novel calibration strategy for analysis and imaging of biological thin sections by laser ablation inductively coupled plasma mass spectrometry, J. Anal. At. Spectrom. 26 (8) (2011) 1667–1673.
[29] C. Austin, D. Hare, T. Rawling, A.M. McDonagh, P. Doble, Quantification method for elemental bio-imaging by LA-ICP-MS using metal spiked PMMA films, J. Anal. At. Spectrom. 25 (5) (2010) 722–725.
[30] O. Reifschneider, C.A. Wehe, I. Raj, J. Ehmcke, G. Ciarimboli, M. Sperling, U. Karst, Quantitative bioimaging of platinum in polymer embedded mouse organs using laser ablation ICP-MS, Metallomics 5 (10) (2013) 1440–1447.
[31] M. Bonta, H. Lohninger, V. Laszlo, B. Hegedus, A. Limbeck, Quantitative LA-ICP-MS imaging of platinum in chemotherapy treated human malignant pleural mesothelioma samples using printed patterns as standard, J. Anal. At. Spectrom. 29 (11) (2014) 2159–2167.

[32] S.J.M. Van Malderen, E. Vergucht, M. De Rijcke, C. Janssen, L. Vincze, F. Vanhaecke, Quantitative determination and subcellular imaging of Cu in single cells via laser ablation-ICP-mass spectrometry using high-density microarray gelatin standards, Anal. Chem. 88 (11) (2016) 5783–5789.

[33] M.T. Westerhausen, T.E. Lockwood, R. Gonzalez de Vega, A. Röhnelt, D.P. Bishop, N. Cole, P.A. Doble, D. Clases, Low background mould-prepared gelatine standards for reproducible quantification in elemental bio-imaging, Analyst 144 (23) (2019) 6881–6888.

[34] D. Gholap, J. Verhulst, W. Ceelen, F. Vanhaecke, Use of pneumatic nebulization and laser ablation–inductively coupled plasma–mass spectrometry to study the distribution and bioavailability of an intraperitoneally administered Pt-containing chemotherapeutic drug, Anal. Bioanal. Chem. 402 (6) (2012) 2121–2129.

[35] T. Van Acker, T. Buckle, S.J.M. Van Malderen, D.M. van Willigen, V. van Unen, F. W.B. van Leeuwen, F. Vanhaecke, High-resolution imaging and single-cell analysis via laser ablation-inductively coupled plasma-mass spectrometry for the determination of membranous receptor expression levels in breast cancer cell lines using receptor-specific hybrid tracers, Anal. Chim. Acta 1074 (2019) 43–53.

[36] A. Schweikert, S. Theiner, D. Wernitznig, A. Schoeberl, M. Schaier, S. Neumayer, B.K. Keppler, G. Koellensperger, Micro-droplet-based calibration for quantitative elemental bioimaging by LA-ICPMS, Anal. Bioanal. Chem. 414 (2022) 485–495.

[37] M. Costas-Rodríguez, T. Van Acker, A.A.M.B. Hastuti, L. Devisscher, S. Van Campenhout, H. Van Vlierberghe, F. Vanhaecke, Laser ablation-inductively coupled plasma-mass spectrometry for quantitative mapping of the copper distribution in liver tissue sections from mice with liver disease induced by common bile duct ligation, J. Anal. At. Spectrom. 32 (9) (2017) 1805–1812.

[38] K.-A. Dorph-Petersen, J.R. Nyengaard, H.J.G. Gundersen, Tissue shrinkage and unbiased stereological estimation of particle number and size, J. Microsc. 204 (3) (2001) 232–246.

[39] K. Jurowski, M. Szewczyk, W. Piekoszewski, M. Herman, B. Szewczyk, G. Nowak, S. Walas, N. Miliszkiewicz, A. Tobiasz, J. Dobrowolska-Iwanek, A standard sample preparation and calibration procedure for imaging zinc and magnesium in rats' brain tissue by laser ablation-inductively coupled plasma-time of flight-mass spectrometry, J. Anal. At. Spectrom. 29 (8) (2014) 1425–1431.

[40] K. Billimoria, D.N. Douglas, G. Huelga-Suarez, J.F. Collingwood, H. Goenaga-Infante, Investigating the effect of species-specific calibration on the quantitative imaging of iron at mg kg−1 and selenium at μg kg−1 in tissue using laser ablation with ICP-QQQ-MS, J. Anal. At. Spectrom. 36 (5) (2021) 1047–1054.

[41] H. Sela, Z. Karpas, H. Cohen, Y. Zakon, Y. Zeiri, Preparation of stable standards of biological tissues for laser ablation analysis, Int. J. Mass Spectrom. 307 (1) (2011) 142–148.

[42] J. O'Reilly, D. Douglas, J. Braybrook, P.W. So, E. Vergucht, J. Garrevoet, B. Vekemans, L. Vincze, H. Goenaga-Infante, A novel calibration strategy for the quantitative imaging of iron in biological tissues by LA-ICP-MS using matrix-matched standards and internal standardisation, J. Anal. At. Spectrom. 29 (8) (2014) 1378–1384.

[43] O. Reifschneider, K.S. Wentker, K. Strobel, R. Schmidt, M. Masthoff, M. Sperling, C. Faber, U. Karst, Elemental bioimaging of thulium in mouse tissues by laser ablation-ICPMS as a complementary method to heteronuclear proton magnetic resonance imaging for cell tracking experiments, Anal. Chem. 87 (8) (2015) 4225–4230.

[44] C.R. VanderSchee, D. Frier, D. Kuter, K.K. Mann, B.P. Jackson, D.S. Bohle, Quantification of local zinc and tungsten deposits in bone with LA-ICP-MS using novel hydroxyapatite–collagen calibration standards, J. Anal. At. Spectrom. 36 (11) (2021) 2431–2438.

[45] M.T. Westerhausen, M. Bernard, G. Choi, C. Jeffries-Stokes, R. Chandrajith, R. Banati, D.P. Bishop, Preparation of matrix-matched standards for the analysis of teeth via laser ablation-inductively coupled plasma-mass spectrometry, Anal. Methods 15 (6) (2023) 797–806.

[46] M.L. Praamsma, P.J. Parsons, Calibration strategies for quantifying the Mn content of tooth and bone samples by LA-ICP-MS, Accred Qual. Assur. 21 (6) (2016) 385–393.

[47] A. Hanć, A. Olszewska, D. Baralkiewicz, Quantitative analysis of elements migration in human teeth with and without filling using LA-ICP-MS, Micochem. J. 110 (2013) 61–69.

[48] D.L.R. Novo, T. Van Acker, J. Belza, F. Vanhaecke, M.F. Mesko, Laser ablation-ICP-mass spectrometry for determination of the concentrations and spatial distributions of bromine and iodine in human hair, J. Anal. At. Spectrom. 37 (4) (2022) 775–782.

[49] R. Luo, X. Su, W. Xu, S. Zhang, X. Zhuo, D. Ma, Determination of arsenic and lead in single hair strands by laser ablation inductively coupled plasma mass spectrometry, Sci. Rep. 7 (1) (2017) 3426.

[50] S. Byrne, D. Amarasiriwardena, B. Bandak, L. Bartkus, J. Kane, J. Jones, J. Yañez, B. Arriaza, L. Cornejo, Were Chinchorros exposed to arsenic? Arsenic determination in Chinchorro mummies' hair by laser ablation inductively coupled plasma-mass spectrometry (LA-ICP-MS), Microchem. J. 94 (1) (2010) 28–35.

[51] U. Kumtabtim, A. Matusch, S. Ulhoa Dani, A. Siripinyanond, J. Sabine Becker, Biomonitoring for arsenic, toxic and essential metals in single hair strands by laser ablation inductively coupled plasma mass spectrometry, Int. J. Mass Spectrom. 307 (1) (2011) 185–191.

[52] D. Pozebon, V.L. Dressler, A. Matusch, J.S. Becker, Monitoring of platinum in a single hair by laser ablation inductively coupled plasma mass spectrometry (LA-ICP-MS) after cisplatin treatment for cancer, Int. J. Mass Spectrom. 272 (1) (2008) 57–62.

[53] P. Cheajesadagul, W. Wananukul, A. Siripinyanond, J. Shiowatana, Metal doped keratin film standard for LA-ICP-MS determination of lead in hair samples, J. Anal. At. Spectrom. 26 (3) (2011) 493–498.

[54] C. Arnaudguilhem, M. Larroque, O. Sgarbura, D. Michau, F. Quenet, S. Carrère, B. Bouyssière, S. Mounicou, Toward a comprehensive study for multielemental quantitative LA-ICP MS bioimaging in soft tissues, Talanta 222 (2021) 121537.

[55] C. Köppen, O. Reifschneider, I. Castanheira, M. Sperling, U. Karst, G. Ciarimboli, Quantitative imaging of platinum based on laser ablation-inductively coupled plasma-mass spectrometry to investigate toxic side effects of cisplatin, Metallomics 7 (12) (2015) 1595–1603.

[56] B. Crone, L. Schlatt, R.A. Nadar, N.W.M. van Dijk, N. Margiotta, M. Sperling, S. Leeuwenburgh, U. Karst, Quantitative imaging of platinum-based antitumor complexes in bone tissue samples using LA-ICP-MS, J. Trace Elem. Med. Biol. 54 (2019) 98–102.

[57] T. Gao, T. Ren, Y. Zhou, P. Song, S. Wang, The production of polymer reference materials for microanalysis with high homogeneity by a 3D printing method, J. Anal. At. Spectrom. 38 (4) (2023) 893–901.

[58] A. Schweikert, S. Theiner, M. Šala, P. Vician, W. Berger, B.K. Keppler, G. Koellensperger, Quantification in elemental bioimaging - evaluation of different calibration strategies enabled by micro-droplets, Anal. Chim. Acta 1223 (2022) 340200.

[59] R. Niehaus, M. Sperling, U. Karst, Study on aerosol characteristics and fractionation effects of organic standard materials for bioimaging by means of LA-ICP-MS, J. Anal. At. Spectrom. 30 (10) (2015) 2056–2065.

[60] O. Hachmöller, M. Aichler, K. Schwamborn, L. Lutz, M. Werner, M. Sperling, A. Walch, U. Karst, Element bioimaging of liver needle biopsy specimens from patients with Wilson's disease by laser ablation-inductively coupled plasma-mass spectrometry, J. Trace Elem. Med. Biol. 35 (2016) 97–102.

[61] M. Cruz-Alonso, B. Fernandez, A. Navarro, S. Junceda, A. Astudillo, R. Pereiro, Laser ablation ICP-MS for simultaneous quantitative imaging of iron and ferroportin in hippocampus of human brain tissues with Alzheimer's disease, Talanta 197 (2019) 413–421.

[62] J. Liu, L. Zheng, X. Wei, B. Wang, H. Chen, M. Chen, M. Wang, W. Feng, J. Wang, Quantitative imaging of trace elements in brain sections of Alzheimer's disease mice with laser ablation inductively coupled plasma-mass spectrometry, Microchem. J. 172 (2022) 106912.

[63] K. Billimoria, Y.A.D. Fernandez, E. Andresen, I. Sorzabal-Bellido, G. Huelga-Suarez, D. Bartczak, C. Ortiz de Solórzano, U. Resch-Genger, H.G. Infante, The potential of bioprinting for preparation of nanoparticle-based calibration standards for LA-ICP-ToF-MS quantitative imaging, Metallomics 14 (12) (2022).

[64] T. Van Acker, S.J.M. Van Malderen, M. Van Heerden, J.E. McDuffie, F. Cuyckens, F. Vanhaecke, High-resolution laser ablation-inductively coupled plasma-mass spectrometry imaging of cisplatin-induced nephrotoxic side effects, Anal. Chim. Acta 945 (2016) 23–30.

[65] S. Fingerhut, A.-C. Niehoff, M. Sperling, A. Jeibmann, W. Paulus, T. Niederstadt, T. Allkemper, W. Heindel, M. Holling, U. Karst, Spatially resolved quantification of gadolinium deposited in the brain of a patient treated with gadolinium-based contrast agents, J. Trace Elem. Med. Biol. 45 (2018) 125–130.

[66] S. Strekopytov, K. Billimoria, H. Goenaga-Infante, A systematic study of high resolution multielemental quantitative bioimaging of animal tissue using LA-ICP-TOFMS, J. Anal. At. Spectrom. 38 (3) (2023) 704–715.

[67] M. Šala, V.S. Šelih, J.T. van Elteren, Gelatin gels as multi-element calibration standards in LA-ICP-MS bioimaging: fabrication of homogeneous standards and microhomogeneity testing, Analyst 142 (18) (2017) 3356–3359.

[68] A.A. Leventi, K. Billimoria, D. Bartczak, S. Laing, H. Goenaga-Infante, K. Faulds, D. Graham, New model for quantifying the nanoparticle concentration using SERS supported by multimodal mass spectrometry, Anal. Chem. 95 (5) (2023) 2757–2764.

[69] R.D. Deegan, O. Bakajin, T.F. Dupont, G. Huber, S.R. Nagel, T.A. Witten, Capillary flow as the cause of ring stains from dried liquid drops, Nature 389 (6653) (1997) 827–829.

[70] T. Kajiya, D. Kaneko, M. Doi, Dynamical visualization of "coffee stain phenomenon" in droplets of polymer solution via fluorescent microscopy, Langmuir 24 (21) (2008) 12369–12374.

[71] K. Kysenius, B. Paul, J.B. Hilton, J.R. Liddell, D.J. Hare, P.J. Crouch, A versatile quantitative microdroplet elemental imaging method optimised for integration in biochemical workflows for low-volume samples, Anal. Bioanal. Chem. 411 (3) (2019) 603–616.

[72] C. Carlier, B. Laforce, S.J.M. Van Malderen, F. Gremonprez, R. Tucoulou, J. Villanova, O. De Wever, L. Vincze, F. Vanhaecke, W. Ceelen, Nanoscopic tumor tissue distribution of platinum after intraperitoneal administration in a xenograft model of ovarian cancer, J. Pharm. Biomed. Anal. 131 (2016) 256–262.

[73] D. Metarapi, M. Šala, K. Vogel-Mikuš, V.S. Šelih, J.T. van Elteren, Nanoparticle analysis in biomaterials using laser Ablation–Single Particle–Inductively coupled plasma mass spectrometry, Anal. Chem. 91 (9) (2019) 6200–6205.

[74] T. Van Acker, E. Bolea-Fernandez, E. De Vlieghere, J. Gao, O. De Wever, F. Vanhaecke, Laser ablation-tandem ICP-mass spectrometry (LA-ICP-MS/MS) imaging of iron oxide nanoparticles in Ca-rich gelatin microspheres, J. Anal. At. Spectrom. 34 (9) (2019) 1846–1855.

[75] F. Kuczelinis, J.H. Petersen, P. Weis, N.H. Bings, Calibration of LA-ICP-MS via standard addition using dried picoliter droplets, J. Anal. At. Spectrom. 35 (2020) 1922–1931.

[76] J. Zhai, Y. Wang, C. Xu, L. Zheng, M. Wang, W. Feng, L. Gao, L. Zhao, R. Liu, F. Gao, Y. Zhao, Z. Chai, X. Gao, Facile approach to observe and quantify the αIIbβ3 integrin on a single-cell, Anal. Chem. 87 (5) (2015) 2546–2549.

[77] M. Wang, L.-N. Zheng, B. Wang, H.-Q. Chen, Y.-L. Zhao, Z.-F. Chai, H.J. Reid, B. L. Sharp, W.-Y. Feng, Quantitative analysis of gold nanoparticles in single cells by laser ablation inductively coupled plasma-mass spectrometry, Anal. Chem. 86 (20) (2014) 10252–10256.
[78] K. Löhr, H. Traub, A.J. Wanka, U. Panne, N. Jakubowski, Quantification of metals in single cells by LA-ICP-MS: comparison of single spot analysis and imaging, J. Anal. At. Spectrom. 33 (9) (2018) 1579–1587.
[79] K. Löhr, O. Borovinskaya, G. Tourniaire, U. Panne, N. Jakubowski, Arraying of single cells for quantitative high throughput laser ablation ICP-TOF-MS, Anal. Chem. 91 (18) (2019) 11520–11528.
[80] A. Arakawa, N. Jakubowski, G. Koellensperger, S. Theiner, A. Schweikert, S. Flemig, D. Iwahata, H. Traub, T. Hirata, Quantitative imaging of silver nanoparticles and essential elements in thin sections of fibroblast multicellular spheroids by high resolution laser ablation inductively coupled plasma time-of-flight mass spectrometry, Anal. Chem. 91 (15) (2019) 10197–10203.
[81] A. Schoeberl, M. Gutmann, S. Theiner, M. Schaier, A. Schweikert, W. Berger, G. Koellensperger, Cisplatin uptake in macrophage subtypes at the single-cell level by LA-ICP-TOFMS imaging, Anal. Chem. 93 (49) (2021) 16456–16465.
[82] M. Schaier, S. Theiner, D. Baier, G. Braun, W. Berger, G. Koellensperger, Multiparametric tissue characterization utilizing the cellular metallome and immuno-mass spectrometry imaging, JACS Au 3 (2) (2023) 419–428.
[83] https://metallomic.com/(accessed 8/August/2023).
[84] C. O' Connor, B.L. Sharp, P. Evans, On-line additions of aqueous standards for calibration of laser ablation inductively coupled plasma mass spectrometry: theory and comparison of wet and dry plasma conditions, J. Anal. At. Spectrom. 21 (6) (2006) 556–565.
[85] D. Pozebon, V.L. Dressler, M.F. Mesko, A. Matusch, J.S. Becker, Bioimaging of metals in thin mouse brain section by laser ablation inductively coupled plasma mass spectrometry: novel online quantification strategy using aqueous standards, J. Anal. At. Spectrom. 25 (11) (2010) 1739–1744.
[86] G. Zhang, Q. Li, Y. Zhu, Z. Wang, Solution-based calibration strategy for laser ablation–inductively coupled plasma–mass spectrometry using desolvating nebulizer system, Spectrochim. Acta, Part B 145 (2018) 51–57.
[87] V.L. Dressler, D. Pozebon, M.F. Mesko, A. Matusch, U. Kumtabtim, B. Wu, J. Sabine Becker, Biomonitoring of essential and toxic metals in single hair using on-line solution-based calibration in laser ablation inductively coupled plasma mass spectrometry, Talanta 82 (5) (2010) 1770–1777.
[88] H. Sela, Z. Karpas, M. Zoriy, C. Pickhardt, J.S. Becker, Biomonitoring of hair samples by laser ablation inductively coupled plasma mass spectrometry (LA-ICP-MS), Int. J. Mass Spectrom. 261 (2) (2007) 199–207.
[89] P. Rodríguez-González, J.M. Marchante-Gayón, J.I. García Alonso, A. Sanz-Medel, Isotope dilution analysis for elemental speciation: a tutorial review, Spectrochim. Acta, Part B 60 (2) (2005) 151–207.
[90] K.G. Heumann, Isotope-dilution ICP–MS for trace element determination and speciation: from a reference method to a routine method? Anal. Bioanal. Chem. 378 (2) (2004) 318–329.
[91] A. Sussulini, J.S. Becker, Combination of PAGE and LA-ICP-MS as an analytical workflow in metallomics: state of the art, new quantification strategies, advantages and limitations, Metallomics 3 (12) (2011) 1271–1279.
[92] J. Chen, R. Wang, M. Ma, L. Gao, B. Zhao, M. Xu, Laser ablation–inductively coupled plasma–mass spectrometry (LA-ICP-MS)–based strategies applied for the analysis of metal-binding protein in biological samples: an update on recent advances, Anal. Bioanal. Chem. 414 (24) (2022) 7023–7033.
[93] I. Konz, B. Fernández, M.L. Fernández, R. Pereiro, A. Sanz-Medel, Absolute quantification of human serum transferrin by species-specific isotope dilution laser ablation ICP-MS, Anal. Chem. 83 (13) (2011) 5353–5360.
[94] C.L. Deitrich, S. Braukmann, A. Raab, C. Munro, B. Pioselli, E.M. Krupp, J. E. Thomas-Oates, J. Feldmann, Absolute quantification of superoxide dismutase (SOD) using species-specific isotope dilution analysis, Anal. Bioanal. Chem. 397 (8) (2010) 3515–3524.
[95] L. Feng, D. Zhang, J. Wang, D. Shen, H. Li, A novel quantification strategy of transferrin and albumin in human serum by species-unspecific isotope dilution laser ablation inductively coupled plasma mass spectrometry (ICP-MS), Anal. Chim. Acta 884 (2015) 19–25.
[96] M. Tibi, K.G. Heumann, Isotope dilution mass spectrometry as a calibration method for the analysis of trace elements in powder samples by LA-ICP-MS, J. Anal. At. Spectrom. 18 (9) (2003) 1076–1081.
[97] J. Terán-Baamonde, A. Carlosena, R.M. Soto-Ferreiro, J.M. Andrade, A. Cantarero-Roldán, S. Muniategui-Lorenzo, A solid-spiking matrix matched calibration strategy for simultaneous determination of cadmium and chromium in sediments by isotope dilution laser ablation inductively coupled plasma mass spectrometry, J. Anal. At. Spectrom. 35 (3) (2020) 580–591.
[98] B. Fernández, F. Claverie, C. Pécheyran, O.F.X. Donard, Solid-spiking isotope dilution laser ablation ICP-MS for the direct and simultaneous determination of trace elements in soils and sediments, J. Anal. At. Spectrom. 23 (3) (2008) 367–377.
[99] S.F. Boulyga, J. Heilmann, T. Prohaska, K.G. Heumann, Development of an accurate, sensitive, and robust isotope dilution laser ablation ICP-MS method for simultaneous multi-element analysis (chlorine, sulfur, and heavy metals) in coal samples, Anal. Bioanal. Chem. 389 (3) (2007) 697–706.
[100] O.B. Bauer, C. Köppen, M. Sperling, H.-J. Schurek, G. Ciarimboli, U. Karst, Quantitative bioimaging of platinum via online isotope dilution-laser ablation-inductively coupled plasma mass spectrometry, Anal. Chem. 90 (11) (2018) 7033–7039.
[101] O.B. Bauer, O. Hachmöller, O. Borovinskaya, M. Sperling, H.-J. Schurek, G. Ciarimboli, U. Karst, LA-ICP-TOF-MS for rapid, all-elemental and quantitative bioimaging, isotopic analysis and the investigation of plasma processes, J. Anal. At. Spectrom. 34 (4) (2019) 694–701.
[102] S. Marković, K. Uršič, M. Cemazar, G. Sersa, B. Starešinič, R. Milačič, J. Ščančar, High spatial resolution imaging of cisplatin and Texas Red cisplatin in tumour spheroids using laser ablation isotope dilution inductively coupled plasma mass spectrometry and confocal fluorescence microscopy, Anal. Chim. Acta 1162 (2021) 338424.
[103] D.N. Douglas, J. O'Reilly, C. O'Connor, B.L. Sharp, H. Goenaga-Infante, Quantitation of the Fe spatial distribution in biological tissue by online double isotope dilution analysis with LA-ICP-MS: a strategy for estimating measurement uncertainty, J. Anal. At. Spectrom. 31 (1) (2016) 270–279.
[104] I. Moraleja, M.L. Mena, A. Lázaro, B. Neumann, A. Tejedor, N. Jakubowski, M. M. Gómez-Gómez, D. Esteban-Fernández, An approach for quantification of platinum distribution in tissues by LA-ICP-MS imaging using isotope dilution analysis, Talanta 178 (2018) 166–171.
[105] L.-N. Zheng, L.-X. Feng, J.-W. Shi, H.-Q. Chen, B. Wang, M. Wang, H.-F. Wang, W.-Y. Feng, Single-cell isotope dilution analysis with LA–ICP–MS: a new approach for quantification of nanoparticles in single cells, Anal. Chem. 92 (21) (2020) 14339–14345.
[106] L. Feng, J. Wang, H. Li, X. Luo, J. Li, A novel absolute quantitative imaging strategy of iron, copper and zinc in brain tissues by Isotope Dilution Laser Ablation ICP-MS, Anal. Chim. Acta 984 (2017) 66–75.
[107] J. Liu, L. Zheng, Q. Li, L. Feng, B. Wang, M. Chen, M. Wang, J. Wang, W. Feng, Isotope dilution LA-ICP-MS for quantitative imaging of trace elements in mouse brain sections, Anal. Chim. Acta 1273 (2023) 341524.
[108] D. Metarapi, A. Schweikert, A. Jerše, M. Schaier, J.T. van Elteren, G. Koellensperger, S. Theiner, M. Šala, Semiquantitative analysis for high-speed mapping applications of biological samples using LA-ICP-TOFMS, Anal. Chem. 95 (19) (2023) 7804–7812.
[109] C. Austin, F. Fryer, J. Lear, D. Bishop, D. Hare, T. Rawling, L. Kirkup, A. McDonagh, P. Doble, Factors affecting internal standard selection for quantitative elemental bio-imaging of soft tissues by LA-ICP-MS, J. Anal. At. Spectrom. 26 (7) (2011) 1494–1501.
[110] D.A. Frick, D. Günther, Fundamental studies on the ablation behaviour of carbon in LA-ICP-MS with respect to the suitability as internal standard, J. Anal. At. Spectrom. 27 (8) (2012) 1294–1303.
[111] P.d.S. Moreau, M.A.Z. Arruda, Direct analysis of tree rings using laser ablation-ICP-MS and quantitative evaluation of Zn and Cu using filter paper as a solid support for calibration, J. Anal. At. Spectrom. 37 (4) (2022) 795–804.
[112] M. von Bremen-Kühne, H. Ahmadi, M. Sperling, U. Krämer, U. Karst, Elemental bioimaging of Zn and Cd in leaves of hyperaccumulator Arabidopsis halleri using laser ablation-inductively coupled plasma-mass spectrometry and referencing strategies, Chemosphere 305 (2022) 135267.
[113] J.Y. Kim, J. Park, J. Choi, J. Kim, Determination of metal concentration in road-side trees from an industrial area using laser ablation inductively coupled plasma mass spectrometry, Minerals 10 (2) (2020) 175.
[114] K. Chacón-Madrid, M.A. Zezzi Arruda, Internal standard evaluation for bioimaging soybean leaves through laser ablation inductively coupled plasma mass spectrometry: a plant nanotechnology approach, J. Anal. At. Spectrom. 33 (10) (2018) 1720–1728.
[115] J.A. Ko, N. Furuta, H.B. Lim, Quantitative mapping of elements in basil leaves (Ocimum basilicum) based on cesium concentration and growth period using laser ablation ICP-MS, Chemosphere 190 (2018) 368–374.
[116] D. Amarasiriwardena, M. Ahmed, B. Arriaza, Environmental arsenic exposure by ancient Andeans: measurement of as in mummy hair using LA-ICP-MS, J. Archaeol. Sci. Rep. 48 (2023) 103883.
[117] Y.-N. Chan, J.T.-S. Lum, K.S.-Y. Leung, Development of a comprehensive method for hair and nail analysis using laser ablation-inductively coupled plasma-mass spectrometry, Micochem. J. 188 (2023) 108503.
[118] K. Rodiouchkina, I. Rodushkin, S. Goderis, F. Vanhaecke, Longitudinal isotope ratio variations in human hair and nails, Sci. Total Environ. 808 (2022) 152059.
[119] P. Charapata, C.T. Clark, N. Miller, S.S. Kienle, D.P. Costa, M.E. Goebel, H. Gunn, E.S. Sperou, S.B. Kanatous, D.E. Crocker, R. Borras-Chavez, S.J. Trumble, Whiskers provide time-series of toxic and essential trace elements, Se:Hg molar ratios, and stable isotope values of an apex Antarctic predator, the leopard seal, Sci. Total Environ. 854 (2023) 158651.
[120] M. Arora, A. Reichenberg, C. Willfors, C. Austin, C. Gennings, S. Berggren, P. Lichtenstein, H. Anckarsäter, K. Tammimies, S. Bölte, Fetal and postnatal metal dysregulation in autism, Nat. Commun. 8 (1) (2017) 15493.
[121] A.L. Wright, E.T. Earley, C. Austin, M. Arora, Equine odontoclastic tooth resorption and hypercementosis (EOTRH): microspatial distribution of trace elements in hypercementosis-affected and unaffected hard dental tissues, Sci. Rep. 13 (1) (2023) 5048.
[122] A.-F. Maurer, P. Barrulas, A. Person, J. Mirão, C. Barrocas Dias, O. Boudouma, L. Segalen, Testing LA-ICP-MS analysis of archaeological bones with different diagenetic histories for paleodiet prospect, Palaeogeogr. Palaeoclimatol. Palaeoecol. 534 (2019) 109287.
[123] S. Theiner, S.J.M. Van Malderen, T. Van Acker, A. Legin, B.K. Keppler, F. Vanhaecke, G. Koellensperger, Fast high-resolution laser ablation-inductively coupled plasma mass spectrometry imaging of the distribution of platinum-based anticancer compounds in multicellular tumor spheroids, Anal. Chem. 89 (23) (2017) 12641–12645.
[124] F. Li, X. Lei, H. Li, H. Cui, W. Guo, L. Jin, S. Hu, Direct multi-elemental analysis of whole blood samples by LA-ICP-MS employing a cryogenic ablation cell, J. Anal. At. Spectrom. 38 (1) (2023) 90–96.

[125] N. Grijalba, A. Legrand, V. Holler, C. Bouvier-Capely, A novel calibration strategy based on internal standard–spiked gelatine for quantitative bio-imaging by LA-ICP-MS: application to renal localization and quantification of uranium, Anal. Bioanal. Chem. 412 (13) (2020) 3113–3122.

[126] I. Konz, B. Fernández, M.L. Fernández, R. Pereiro, H. González, L. Álvarez, M. Coca-Prados, A. Sanz-Medel, Gold internal standard correction for elemental imaging of soft tissue sections by LA-ICP-MS: element distribution in eye microstructures, Anal. Bioanal. Chem. 405 (10) (2013) 3091–3096.

[127] M. Bonta, H. Lohninger, M. Marchetti-Deschmann, A. Limbeck, Application of gold thin-films for internal standardization in LA-ICP-MS imaging experiments, Analyst 139 (6) (2014) 1521–1531.

[128] S. Hoesl, B. Neumann, S. Techritz, M. Linscheid, F. Theuring, C. Scheler, N. Jakubowski, L. Mueller, Development of a calibration and standardization procedure for LA-ICP-MS using a conventional ink-jet printer for quantification of proteins in electro- and Western-blot assays, J. Anal. At. Spectrom. 29 (7) (2014) 1282–1291.

[129] S. Hoesl, B. Neumann, S. Techritz, G. Sauter, R. Simon, H. Schlüter, M. W. Linscheid, F. Theuring, N. Jakubowski, L. Mueller, Internal standardization of LA-ICP-MS immuno imaging via printing of universal metal spiked inks onto tissue sections, J. Anal. At. Spectrom. 31 (3) (2016) 801–808.

[130] I. Moraleja, D. Esteban-Fernández, A. Lázaro, B. Humanes, B. Neumann, A. Tejedor, M.L. Mena, N. Jakubowski, M.M. Gómez-Gómez, Printing metal-spiked inks for LA-ICP-MS bioimaging internal standardization: comparison of the different nephrotoxic behavior of cisplatin, carboplatin, and oxaliplatin, Anal. Bioanal. Chem. 408 (9) (2016) 2309–2318.

[131] B. Neumann, S. Hösl, K. Schwab, F. Theuring, N. Jakubowski, Multiplex LA-ICP-MS bio-imaging of brain tissue of a parkinsonian mouse model stained with metal-coded affinity-tagged antibodies and coated with indium-spiked commercial inks as internal standards, J. Neurosci. Methods 334 (2020) 108591.

[132] C. Giesen, L. Waentig, T. Mairinger, D. Drescher, J. Kneipp, P.H. Roos, U. Panne, N. Jakubowski, Iodine as an elemental marker for imaging of single cells and tissue sections by laser ablation inductively coupled plasma mass spectrometry, J. Anal. At. Spectrom. 26 (11) (2011) 2160–2165.

[133] D.A. Frick, C. Giesen, T. Hemmerle, B. Bodenmiller, D. Günther, An internal standardisation strategy for quantitative immunoassay tissue imaging using laser ablation inductively coupled plasma mass spectrometry, J. Anal. At. Spectrom. 30 (1) (2015) 254–259.

[134] K. Mervič, J.T. van Elteren, M. Bele, M. Šala, Utilizing ablation volume for calibration in LA-ICP-MS mapping to address variations in ablation rates within and between matrices, Talanta 269 (2024) 125379.

[135] K. Mervič, M. Šala, V. Šelih, J.T. van Elteren, Non-matrix-matched calibration in bulk multi-element laser ablation – inductively coupled plasma – mass spectrometry analysis of diverse materials, Talanta 271 (2024) 125712.

[136] M. Cruz-Alonso, A. Lores-Padín, E. Valencia, H. González-Iglesias, B. Fernández, R. Pereiro, Quantitative mapping of specific proteins in biological tissues by laser ablation–ICP-MS using exogenous labels: aspects to be considered, Anal. Bioanal. Chem. 411 (3) (2019) 549–558.

[137] S. Theiner, K. Loehr, G. Koellensperger, L. Mueller, N. Jakubowski, Single-cell analysis by use of ICP-MS, J. Anal. At. Spectrom. 35 (9) (2020) 1784–1813.

[138] L. Mueller, A.J. Herrmann, S. Techritz, U. Panne, N. Jakubowski, Quantitative characterization of single cells by use of immunocytochemistry combined with multiplex LA-ICP-MS, Anal. Bioanal. Chem. 409 (14) (2017) 3667–3676.

[139] J. Pisonero, D. Bouzas-Ramos, H. Traub, B. Cappella, C. Álvarez-Llamas, S. Richter, J.C. Mayo, J.M. Costa-Fernandez, N. Bordel, N. Jakubowski, Critical evaluation of fast and highly resolved elemental distribution in single cells using LA-ICP-SFMS, J. Anal. At. Spectrom. 34 (4) (2019) 655–663.

[140] C. Giesen, T. Mairinger, L. Khoury, L. Waentig, N. Jakubowski, U. Panne, Multiplexed immunohistochemical detection of tumor markers in breast cancer tissue using laser ablation inductively coupled plasma mass spectrometry, Anal. Chem. 83 (21) (2011) 8177–8183.

[141] E. Valencia, B. Fernández, M. Cruz-Alonso, M. García, H. González-Iglesias, M. T. Fernández-Abedul, R. Pereiro, Imaging of proteins in biological tissues by fluorescence microscopy and laser ablation-ICP-MS using natural and isotopically enriched silver nanoclusters, J. Anal. At. Spectrom. 35 (2020) 1868–1879.

[142] B. Paul, D.J. Hare, D.P. Bishop, C. Paton, V.T. Nguyen, N. Cole, M.M. Niedwiecki, E. Andreozzi, A. Vais, J.L. Billings, L. Bray, A.I. Bush, G. McColl, B.R. Roberts, P. A. Adlard, D.I. Finkelstein, J. Hellstrom, J.M. Hergt, J.D. Woodhead, P.A. Doble, Visualising mouse neuroanatomy and function by metal distribution using laser ablation-inductively coupled plasma-mass spectrometry imaging, Chem. Sci. 6 (10) (2015) 5383–5393.

[143] L. Waentig, N. Jakubowski, S. Hardt, C. Scheler, P.H. Roos, M.W. Linscheid, Comparison of different chelates for lanthanide labeling of antibodies and application in a Western blot immunoassay combined with detection by laser ablation (LA-)ICP-MS, J. Anal. At. Spectrom. 27 (8) (2012) 1311–1320.

[144] D.P. Bishop, N. Cole, T. Zhang, P.A. Doble, D.J. Hare, A guide to integrating immunohistochemistry and chemical imaging, Chem. Soc. Rev. 47 (11) (2018) 3770–3787.

[145] Q. Chang, O.I. Ornatsky, I. Siddiqui, A. Loboda, V.I. Baranov, D.W. Hedley, Imaging mass cytometry, Cytometry 91 (2) (2017) 160–169.

[146] S. Kanje, A.J. Herrmann, S. Hober, L. Mueller, Next generation of labeling reagents for quantitative and multiplexing immunoassays by the use of LA-ICP-MS, Analyst 141 (23) (2016) 6374–6380.

[147] M.G. Mello, M.T. Westerhausen, P. Singh, P.A. Doble, J. Wanagat, D.P. Bishop, Assessing the reproducibility of labelled antibody binding in quantitative multiplexed immuno-mass spectrometry imaging, Anal. Bioanal. Chem. 413 (21) (2021) 5509–5516.

[148] D. Clases, R. Gonzalez de Vega, P.A. Adlard, P.A. Doble, On-line reverse isotope dilution analysis for spatial quantification of elemental labels used in immunohistochemical assisted imaging mass spectrometry via LA-ICP-MS, J. Anal. At. Spectrom. 34 (2) (2019) 407–412.

[149] K. Veverkova, K. Pavelicova, M. Vlcnovska, M. Vejvodova, V. Horák, V. Kanicky, V. Adam, T. Vaculovic, M. Vaculovicova, Detection of metallothionein as melanoma marker by LA-ICP-MS combined with sample pretreatment by magnetic particles coated with an imprinted polymeric layer, J. Anal. At. Spectrom. 38 (2023) 1618–1625.

[150] D.P. Bishop, M.T. Westerhausen, F. Barthelemy, T. Lockwood, N. Cole, E. M. Gibbs, R.H. Crosbie, S.F. Nelson, M.C. Miceli, P.A. Doble, J. Wanagat, Quantitative immuno-mass spectrometry imaging of skeletal muscle dystrophin, Sci. Rep. 11 (1) (2021) 1128.

[151] X. Gao, H. Pan, Y. Han, L. Feng, J. Xiong, S. Luo, H. Li, Quantitative imaging of amyloid beta peptide (Aβ) in Alzheimer's brain tissue by laser ablation ICP-MS using gold nanoparticles as labels, Anal. Chim. Acta 1148 (2021) 238197.

[152] M. Cruz-Alonso, B. Fernandez, M. García, H. González-Iglesias, R. Pereiro, Quantitative imaging of specific proteins in the human retina by laser ablation ICPMS using bioconjugated metal nanoclusters as labels, Anal. Chem. 90 (20) (2018) 12145–12151.

[153] A. Lores-Padín, B. Fernández, M. García, H. González-Iglesias, R. Pereiro, Real matrix-matched standards for quantitative bioimaging of cytosolic proteins in individual cells using metal nanoclusters as immunoprobes-label: a case study using laser ablation ICP-MS detection, Anal. Chim. Acta 1221 (2022) 340128.

[154] M.D. Montaño, J.W. Olesik, A.G. Barber, K. Challis, J.F. Ranville, Single Particle ICP-MS: advances toward routine analysis of nanomaterials, Anal. Bioanal. Chem. 408 (19) (2016) 5053–5074.

[155] D. Metarapi, J.T. van Elteren, M. Šala, Studying gold nanoparticle degradation during laser ablation–single particle-inductively coupled plasma mass spectrometry analysis, J. Anal. At. Spectrom. 36 (9) (2021) 1879–1883.

[156] D. Metarapi, J.T. van Elteren, M. Šala, K. Vogel-Mikuš, I. Arčon, V.S. Šelih, M. Kolar, S.B. Hočevar, Laser ablation-single-particle-inductively coupled plasma mass spectrometry as a multimodality bioimaging tool in nano-based omics, Environ. Sci.: Nano 8 (3) (2021) 647–656.

[157] A. Arakawa, N. Jakubowski, S. Flemig, G. Koellensperger, M. Rusz, D. Iwahata, H. Traub, T. Hirata, High-resolution laser ablation inductively coupled plasma mass spectrometry used to study transport of metallic nanoparticles through collagen-rich microstructures in fibroblast multicellular spheroids, Anal. Bioanal. Chem. 411 (16) (2019) 3497–3506.

[158] W. Luo, F. Dong, M. Wang, T. Li, Y. Wang, W. Dai, J. Zhang, C. Jiao, Z. Song, J. Shen, Y. Ma, Y. Ding, F. Yang, Z. Zhang, X. He, Particulate standard establishment for absolute quantification of nanoparticles by LA-ICP-MS, Anal. Chem. 95 (15) (2023) 6391–6398.

3.3 Manuscript 3: Non-Matrix-Matched Calibration in Bulk Multi-Element Laser Ablation – Inductively Coupled Plasma – Mass Spectrometry Analysis of Diverse Materials

Published: Mervič K., Šelih V. S., Šala M., van Elteren J.T., (2024). Talanta, 271, 117574, doi: 10.1016/j.talanta.2024.125712.

Despite significant advances in LA-ICP-MS analysis, achieving accurate calibration is still difficult due to matrix effects, unless the sample and calibration standards have similar matrix composition. Differences in matrix properties such as reflectivity, absorptivity, thermal conductivity, *etc.* lead to differences in ablation (*i.e.* mass of ablated volume) and elemental fractionation and interfere with the calibration process. Although matrix matching is preferable, there is often a lack of suitable certified standard materials, especially for biological and environmental samples. Gelatin gels have proven to be promising matrix-matched standards for biological samples as they behave similarly during laser ablation, are easy to prepare and have a flexible concentration range. However, the search for suitable standards for other sample types, especially in geology, is challenging.

This study focuses on non-matrix-matched calibration using ablation volume normalization, which compensates for the differences in ablation rates between sample and standard. Different materials that can serve as both sample and standard by cross-calibration were investigated. The LA-ICP-MS experiments were carried out with ten different standard materials with different matrix properties. These ranged from gelatin gel produced in-house to three types of glass standards (three NIST SRM 61X series glass standards, a Corning Museum of Glass (CMG) standard and a modern synthetic glass DLH-8) as well as two carbonate materials, a zircon and a NIST SRM 1547 plant standard pressed into a pallet. A set of major, minor and trace elements were measured in all samples using the same operating parameters, with the exception of laser fluence, which was optimized for each sample for the reasons explained in Articles 1 and 2. The ablation volume after laser ablation analysis was measured using a 3D profilometer, and the signal data from the LA-ICP-MS were normalized to their respective volumes for each sample. The standards were then cross-calibrated, with each serving as both sample and calibration standard. Primarily, a single-point calibration was used, although a multi-point calibration was also performed were available. The calibration yielded mass-to-volume concentrations, so density was measured to allow conversion to mass-to-mass concentrations and comparison with available certified values, mostly from the GeoReM database. The quantified concentrations consistently matched the certified values for all materials, highlighting the effectiveness of transferring calibration standards between materials with clearly defined elemental compositions. Of particular note, gelatin and glass proved to be particularly suitable, especially gelatin because of its adaptability, which allows for a wide range of elements and concentrations. The differences in the determination of element concentrations were mostly below 10 %, with the exception of cases with very low concentrations.

In contrast to conventional LA-ICP-MS calibration, which relies on matrix-matched standards, our quantification method introduces a more robust calibration approach that remains effective even when such standards are not available or do not exist. This groundbreaking advance has the potential to improve the accuracy and precision of elemental analysis by LA-ICP-MS in various research fields.

Talanta 271 (2024) 125712

Contents lists available at ScienceDirect

Talanta

journal homepage: www.elsevier.com/locate/talanta

Non-matrix-matched calibration in bulk multi-element laser ablation – Inductively coupled plasma – Mass spectrometry analysis of diverse materials

Kristina Mervič [a,b], Vid S. Šelih [a], Martin Šala [a,*], Johannes T. van Elteren [a,**]

[a] Department of Analytical Chemistry, National Institute of Chemistry, Hajdrihova 19, 1000, Ljubljana, Slovenia
[b] Jožef Stefan International Postgraduate School, Jamova Cesta 39, SI-1000, Ljubljana, Slovenia

ARTICLE INFO

Handling editor: J. Wang

ABSTRACT

Laser ablation inductively coupled plasma - mass spectrometry (LA-ICP-MS) is a frequently used microanalytical technique in elemental analysis of solid samples. In most instances the use of matrix-matched calibration standards is necessary for the accurate determination of elemental concentrations. However, the main drawback of this approach is the limited availability of certified reference materials. Here, we present a novel conceptual framework in LA-ICP-MS quantification without the use of matrix-matched calibration standards but instead employment of an ablation volume-normalization method (via measurement of post-ablation line scan volumes by optical profilometry) in combination with a matrix-adapted fluence (slightly above the ablation threshold). This method was validated by cross-matrix quantification of reference materials typically investigated by LA-ICP-MS, including geological and biological materials. This allows for more accurate and precise multi-element quantification, and enables quantification of previously unquantifiable elements/materials.

1. Introduction

Laser ablation inductively coupled plasma mass spectrometry (LA-ICP-MS) is a surface microanalytical technique that provides spatially resolved information on the distribution of major, minor, and trace elements. It enables direct analysis of solid materials with high detection performance and lateral resolution in the order of micrometers for large sample areas. Because of the qualitative and quantitative capabilities of the technique, the minimal sample preparation requirements, and major cell/instrumentation improvements and data processing developments, LA-ICP-MS is now used in a wide variety of fields (geology, archaeology, mineralogy, materials studies, forensics, environmental research, medicine, and biology) [1–9].

In recent years, development of fast washout cells enabled rapid analysis by shortening the single pulse response down to 1 ms or even below [10], and thus much faster mapping compared to conventional systems where a typical single pulse response was approximately 500 ms, depending on the instrument, resulting in either mapping of larger areas or the application of smaller spot sizes without increasing experiment time. In addition, rapid aerosol transport allows for much higher sample throughput, resulting in higher signals and consequently improving the signal-to-noise ratio, i.e., achieving better sensitivity [11–13]. In recent years, significant improvements in instrument hardware, combined with a better understanding of the effects of operating conditions on image quality, have made LA-ICP-MS mapping not only faster, but also much more powerful. Advancements in laser ablation parameter optimization to avoid mapping artefacts such as smearing, noise, blurring, and aliasing, are yielding high quality 2D LA-ICP-MS (multi)element maps [14–16]. The use of recently introduced ICP-time-of-flight (TOF)-MS instruments has pushed the technique even further. Compared to the commonly used sequential quadrupole mass analyzers, ICP-TOFMS provides quasi-simultaneous analysis of the entire elemental mass spectrum. Several applications of ICP-TOF-MS have been described, from thin biological tissue samples to meteorites. The combination of laser ablation with ICP-TOF-MS has proven to be a powerful tool for comprehensive sample characterization, allowing simultaneous detection of ions over the entire elemental m/z range with very low sample consumption [12,17–20].

Despite the tremendous progress made in LA-ICP-MS analysis, primarily leading to faster surface element mapping, calibration still proves

* Corresponding author.
** Corresponding author.
E-mail addresses: martin.sala@ki.si (M. Šala), elteren@ki.si (J.T. van Elteren).

https://doi.org/10.1016/j.talanta.2024.125712
Received 13 November 2023; Received in revised form 11 January 2024; Accepted 22 January 2024
Available online 1 February 2024

Table 1
Specification of the standard materials used in this non-matrix-matched LA-ICP-MS calibration study.

Standard	Material type	Nominal concentration	Density	
In-house prepared gelatin standards [16]	10 % (m/V) porcine-skin gelatin, type A, bloom strength 300	~10–250 μg g^{-1}	1.35 g cm^{-3}[a]	Sigma-Aldrich, St. Louis, MO, USA
NIST SRM 614	Silicate glass	~5 μg g^{-1}	2.57 g cm^{-3}[a]	National Institute for Standards and Technology, Gaithersburg, MD, USA
NIST SRM 612	Silicate glass	~50 μg g^{-1}	2.52 g cm^{-3}[a]	
NIST SRM 610	Silicate glass	~500 μg g^{-1}	2.52 g cm^{-3}[a]	
Corning Museum of Glass (CMG-B)	Silicate glass synthetic glass replicating ancient compositions	/	2.60 g cm^{-3}[a]	Corning Museum of Glass, Corning, NY, USA
GSJ CRM JCp-1 Coral (*Porites* sp.)	Carbonate material	/	2.0 g cm^{-3}[b]	myStandards GmbH, Kiel, Germany
GSJ CRM JCt-1 Giant Clam (*Tridacna gigas*)	Carbonate material	/	2.0 g cm^{-3}[b]	
NIST SRM 1547 Peach leaves	Botanical material	/	1.65 g cm^{-3}[a]	National Institute for Standards and Technology, Gaithersburg, MD, USA
Plešovice	Zircon mineral		4.60 g cm^{-3}[c]	
DLH-8	Silicate glass	~150 μg g^{-1}	2.65 g cm^{-3}[a]	P&H Developments Ltd.

[a] Measured with a gas pycnometer.
[b] Calculated based on their composition via approximation of their structure and main component.
[c] Gathered from a known source [34].

to be a challenging matter due to matrix effects, unless there is a harmonization of the matrix composition between the sample and the calibration standard(s). Differences in the properties of the matrices analyzed, e.g., absorptivity, reflectivity, thermal conductivity, etc., may lead to differences in ablation rate (mass or volume of material ablated), particle size distribution, particle transport in the interface and their vaporization, atomization and ionization in the ICP [21,22]. This can lead to elemental fractionation, wherein the signals detected for different elements do not accurately reflect the composition of the ablated matrix. Consequently, this can significantly disrupt the calibration process [23,24].

As in most instances matrix-matching is the preferred choice to avoid calibration issues, in practice suitable certified standard materials are not always available, especially for biological, environmental, and medical samples. To this end, several in-house produced standard materials have been developed that closely resemble certain samples [25,26]. One of these are gelatin gels, which have proven to be excellent multielement matrix-matched standards for biological samples due to their very similar matrix behavior upon laser ablation [27–29], ease of preparation and the possibility of adjusting the concentration range [30,31]. However, finding suitable standards is a problem for other types of samples than proteinaceous samples, especially in geology, where LA-ICP-MS is widely used. In order to have suitable matrix-matched standards, there would have to be a homogeneous standard for each mineral species, which is a practical impossibility. Alternatively, nano-particulate pressed powder pellets are made either from naturally occurring minerals or pre-existing CRMs for LA-ICP-MS analysis [32]. Nonetheless, micro-standards are powdered, compressed materials that might not have the same ablation properties as the mineral samples.

This work will focus on a procedure based on non-matrix-matched calibration via ablation volume-normalization, where the LA-ICP-MS signals are normalized to the ablated volume (or mass when matrix densities are known or measurable), thereby correcting for potential ablation rate differences between sample and calibration standard. A variety of materials (several glasses, carbonates, gelatin, as well as plant and zircon material) was studied, including "hard" and "soft" materials, to act as both sample and calibration standard via cross-calibrating each material against every other material in bulk analysis mode.

2. Experimental section

2.1. Materials and standards

LA-ICP-MS experiments were performed using ten different standard materials with widely varying matrix properties, either custom-prepared or commercially available (Table 1): i) an in-house prepared gelatin gel [30], often used as the "standard of choice" for calibration of biological material as their matrix is very similar to that of biological samples [29,31], containing nine elements (As, Be, Co, Cr, Fe, Mn, Ni, Pb and Sr) in the concentration range 10–250 μg g^{-1}; ii) three frequently used multielement National Institute of Standards (NIST) glass standards with nominal concentrations of ca. 500 μg g^{-1} (NIST 610), ca. 50 μg g^{-1} (NIST 612), and ca. 5 μg g^{-1} (NIST 614); iii) a Corning Museum of Glass (CMG) standard mimicking historic compositions (CMG-B); iv) a modern synthetic glass from P&H Developments Ltd. (DLH-8); v) two carbonate materials (myStandards GmbH)) originating from coral (JCp-1, *Porites* sp., Geological Survey of Japan, GSJ) and giant clam (JCt-1, *Tridacna gigas*, Geological Survey of Japan, GSJ), and commonly used in geochronology; vi) a zircon often used as a quality control in geological studies (Plešovice) [33]; and vii) a plant material from ground peach leaves (NIST 1547) subjected to pressed powder pelletizing yielding a ca. 3 mm thick pellet.

Certified values for the commercial standard materials (NIST and GSJ) are available from their Certificate of Analysis (COA), mostly giving average element concentrations with an expanded uncertainty, which were recalculated to averages with a standard deviation. For the non-certified materials or elements, average element concentrations and their variability were determined by unweighted averaging of the element concentrations obtained from the GeoReM database (http://georem.mpch-mainz.gwdg.de) as weighted averaging was impossible due to the non-consistent nature of the reported associated uncertainties.

Reported densities of the materials in Table 1 were either known or measured (see section 2.2). The ten materials were used as both calibration standards and samples in cross-matrix quantification experiments, mostly based on one-point calibration. However, also multi-point calibration was performed using the NIST 61X SRM glasses for several certified element concentrations, and the gelatin gels with custom-selected element concentrations.

2.2. Instrumentation and measurement

Experiments were performed with an Analyte G2 193 nm ArF* excimer laser ablation system (Teledyne Photon Machines Inc., Bozeman, MT) equipped with a standard two-volume ablation cell (HelEx II). The LA system was connected to a quadrupole ICP-MS instrument (Agilent 7900x, Agilent Technologies, Santa Clara, CA, USA) via the Aerosol Rapid Introduction System (ARIS) coupled to the LA Adaptor Assembly glass expansion unit (Glass Expansion Inc., Pocasset, MA), a long-pulse module with a total aerosol particle washout time of approximately 100 ms. The LA-ICP-MS multi-element analysis

Table 2
Operational LA-ICP-MS conditions used for multielement mapping of the 10 different samples (standard materials).[a]

LA (Analyte G2, ARIS, and glass expansion unit)	
Wavelength (nm)	193
Laser fluence (J cm^{-2})	−0.5 (gelatin) −1.0 (NIST SRM 1547 Peach leaves) −3.6 (NIST SRM 610/612/614, CMG-B, DLH-8, Plešovice, JCt-1, JCp-1)
Repetition rate (Hz)	100
Scanning mode	Line scanning
Dosage (shots per pixel)	10
Washout time (ms)	ca. 100
Beam size (μm)	10
Mask shape	Square
He carrier flow rate (L min^{-1}) cup|cell	0.3|0.3
ICP-MS (Agilent 7900x)	
R_f power (W)	1500
Plasma gas flow rate (L min^{-1})	15
Auxiliary gas flow rate (L min^{-1})	0.9
Ar makeup flow rate (L min^{-1})	0.8
Data acquisition	Time-resolved
Dwell time (ms)	8.5 (^{9}Be,^{52}Cr) 9.0 (^{54}Co,^{55}Mn,^{56}Fe,^{60}Ni,^{75}As,^{88}Sr,^{208}Pb)
Acquistion time (ms)	100
Nuclides measured	^{9}Be,^{52}Cr,^{54}Co,^{55}Mn,^{56}Fe,^{60}Ni,^{75}As,^{88}Sr,^{208}Pb

[a] To mitigate the signal drift effects, sensitivity, and reproducibility on different days or measurement rounds, the advancements in optimizing parameters for the best image quality in LA-ICP-MS, were implemented.A 3D optical interference microscope (Zegage PRO HR, Zygo Corporation, Middlefield, CT) was used to determine the ablation volumes of the ablated line scans in samples and standards. The 3D information was recorded using a 50 × magnification objective lens with a lateral resolution of 0.173 μm and a surface topography repeatability of ≤3.5 nm. Since all the samples and standards involved were flat and smooth, it was not necessary to measure the initial pre-ablation surface morphology.

conditions for different (standard) materials in line scan mode are listed in Table 2. In contrast to matrix-matched calibration where a fixed fluence is used, in this work fluences were selected just above the matrix-dependent ablation threshold where the highest signal-to-noise ratio is observed [35], and the most accurate concentration values are obtained. Each LA-ICP-MS analysis was based on five replicate line scans on both the sample and standard, followed by subtraction of the elemental gas blank, and processing of the data according to section 3.2.

As calibration via ablation-volume normalization results in mass/volume concentrations (μg cm^{-3}), to convert to mass/mass concentrations (μg g^{-1}), densities of materials (g cm^{-3}) should be available. Densities of NIST 610, NIST 612, NIST 614, CMG-B, NIST 1547 pellet, DLH-8, and gelatin gels were measured using a helium gas pycnometer (1345 AccuPyc II, Micromeritics, Norcross, GA). The density of the materials GSJ JCp-1, and GSJ CRM JCt-1 were calculated based on their composition via approximation of their structure and main components, whereas for the Plešovice material the density was available from known sources [34].

2.3. Data processing software

ImageJ (National Institute of Health, USA), OriginLab (OriginPro 2018, OriginLab Corporation, Northampton, MA, USA) and RStudio (R version 4.1.0, 2021, The R Foundation for Statistical Computing) software packages were used for data processing of element data. The surface topography data were processed using Mx™ software (v. 8.0.0.23, Zygo Corporation, Middlefield, CT), followed by conversion to csv files in MatLab R2020a (MathWorks).

3. Results and discussion

3.1. Matrix-dependent material removal upon LA

Depending on the properties of the matrix and its coupling with the laser beam, the amount of material ablated per laser spot differs significantly for different materials, under the same laser pulse energy. This is illustrated in Fig. 1, where it can be seen that the amount of material ablated with the same laser fluence can vary by as much as 5.4 times (for the gelatin: NIST 610 crater volume ratio), which is why using different material types for standard and sample will not give accurate results if the ablated volume is not considered. This underscores the potential inaccuracy of results when employing diverse material types for the standard and sample, unless the ablated volume is accounted for or matrix compatibility is ensured.

3.2. Non-matrix-matched calibration via ablation volume-normalization

To perform non-matrix-matched calibration via ablation volume-normalization, line scan volumes in samples and calibration standards were measured by optical interference profilometry. Even though this method solely addresses discrepancies in ablation rates within matrices, and does not account for variations in particle size distribution, the transport of particles to the ICP, and their ionization within the plasma, we will demonstrate that significant quantification improvements can be made compared to direct calibration without matrix matching when no matrix-matched calibration standards are available. Fig. 2 shows a flowchart of the volume-normalization method for multi-point calibration although this can also be used for one-point calibration. This approach has already been used successfully for calibration in LA-ICP-MS mapping to account for variations in ablation rates between and within samples of the same matrix origin in samples that are not entirely homogenous – composite [36].

LA-ICP-MS analysis of elements in the calibration standards (Cx, with x the calibration standard number) and the sample (S) yields the gas blank-subtracted intensities A_{Cx} and A_S (in cps); associated ablation craters have volumes V_{Cx} and V_S (in μm^{-3}). By definition the element concentration $conc_{(S,m/V)}$ in the sample produced by this calibration

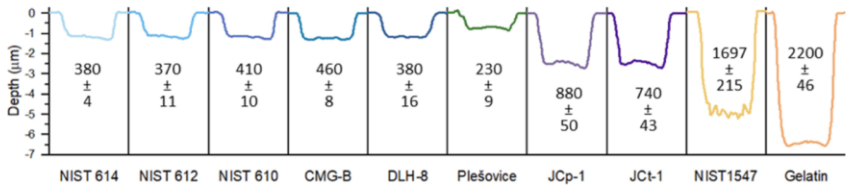

Fig. 1. Cross-sectional ablation crater profiles in diverse materials applying 10 cumulative laser shots per crater with a beam size of 20 μm (square mask) at a fluence of 3.6 J cm^{-2}; for each material the average crater volume and standard deviation (μm^3) is given (N = 10).

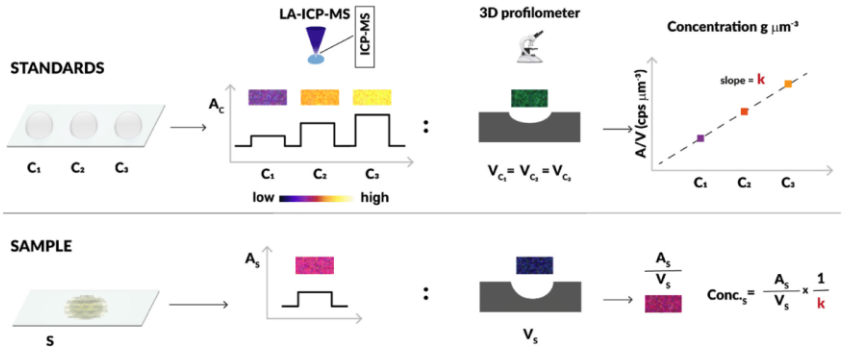

Fig. 2. Flowchart of the ablation volume-normalization method where sample S is subjected to multi-point calibration with calibration standards Cx (C1, C2 and C3).

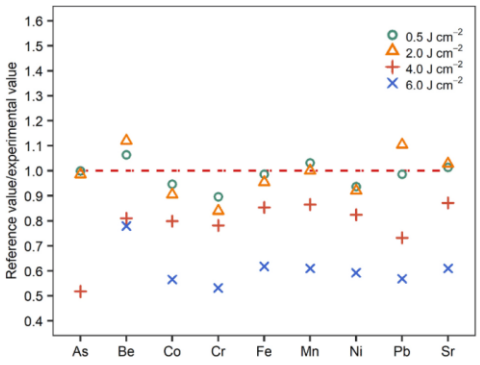

Fig. 3. Accuracy of the ablation-volume normalization method for LA-ICP-MS analysis of NIST 610 glass treated as a sample using custom-prepared multielement gelatin calibration standards. The NIST 610 glass was ablated at a fluence of 3.6 J cm^{-2} whereas the gelatin standard underwent ablation at fluences of 0.5, 2.0, 4.0 and 6.0 J cm^{-2} (further operational details can be found in Table 2). The red dashed line refers to a correct concentration determination, i.e., the concentrations measured are in agreement with the certified concentration for NIST610.

approach is in mass/volume units (µg cm^{-3}), calculated via

$$conc_{(S,m/V)}=(A_S/V_S)/k \quad (1)$$

where $k=(A_{Cx}/V_{Cx})/conc_{(Cx,\ m/V)}$is the slope of the calibration graph (linear regression, forced through zero) shown in Fig. 2. This implies that the calibration standard concentrations $conc_{(Cx,m/V)} = conc_{(Cx,m/m)}\cdot D_{Cx}$ (in µg cm^{-3}) require knowledge of the densities D_{Cx} (in µg g^{-1}). When the density D_S (in g cm^{-3}) of the sample is also available, the mass/mass concentration of the sample follows from $conc_{(S,m/m)} = conc_{(S,m/V)}/D_S$ (in µg g^{-1}).

3.3. Influence of laser fluence on calibration by ablation volume-normalization

Because laser fluence impacts not only the quantity of ablated material but also the particle size distribution within the laser ablation plume, which in turn could influence particle transfer and ionization dynamics within the ICP [35,37], it is evident that optimal laser fluences exist for ablating 'hard' and 'soft' materials. We conducted a series of ablation volume-normalization experiments whereby custom-prepared multielement gelatin standards (10–250 µg g^{-1}) at a range of laser fluences (0.5, 2.0, 4.0, and 6.0 J cm^{-2}) were used to analyse NIST 610 at a fixed laser fluence of 3.6 J cm^{-2}.

Nine experimental concentration values obtained by treating NIST 610 glass as a sample were compared with reference concentration values (Fig. 3). Concentrations obtained from the calibration with the lowest fluence (0.5 J cm^{-2}) most closely matched the reference values, with deviations less than 10 %. Higher fluence values, particularly those of 4.0 and 6.0 J cm^{-2}, produced results that showed notable deviations from the reference values, i.e., 20 % for 4.0 J cm^{-2} and >40 % for 6.0 J cm^{-2}. This underlines the critical role of fluence in the selection of appropriate calibration parameters, especially for "soft" materials. Therefore, it is crucial to use the most suitable fluence for each material (see Table 2 in the experimental section), i.e., slightly above the ablation threshold and associated with the highest signal-to-noise ratios [35].

3.4. Cross-matrix quantification via the ablation volume-normalization method in one-point calibration mode

Given the growing range of laser ablation applications, the requirement of matrix-matched calibration has become a challenge due to the limited availability of suitable reference materials. As a result, this scenario has fostered the development of various calibration methods over time, mostly with the goal of identifying suitable matrices tailored to specific samples [27]. The ablation volume-normalization method put forward here may change the calibration paradigm if accurate and precise quantification results can be obtained using a non-matrix matched calibration approach.

Validation of the ablation volume-normalization method, as outlined in Fig. 2, was carried out through cross-matrix calibration. This involved quantifying nine elements across ten distinct matrices via one-point calibration (see Table 2 for details, including an optimal ablation fluence for each of the matrices with known or measurable density), where each material was measured against every other material in bulk analysis mode, and using them both as sample and calibration standard. Heat maps in Fig. 4 display the absolute relative bias (=100 × |experimental value – recommended value|/recommended value, in %) with and without ablation-volume normalization in the cross-calibration of the nine elements (more detailed heat maps can be found in Figure S1). The heat maps indicate that the majority of the calibration standards lack certain elements, with the exception of Sr and Mn, which further emphasizes the challenge posed by matrix-matched calibration. Moreover,

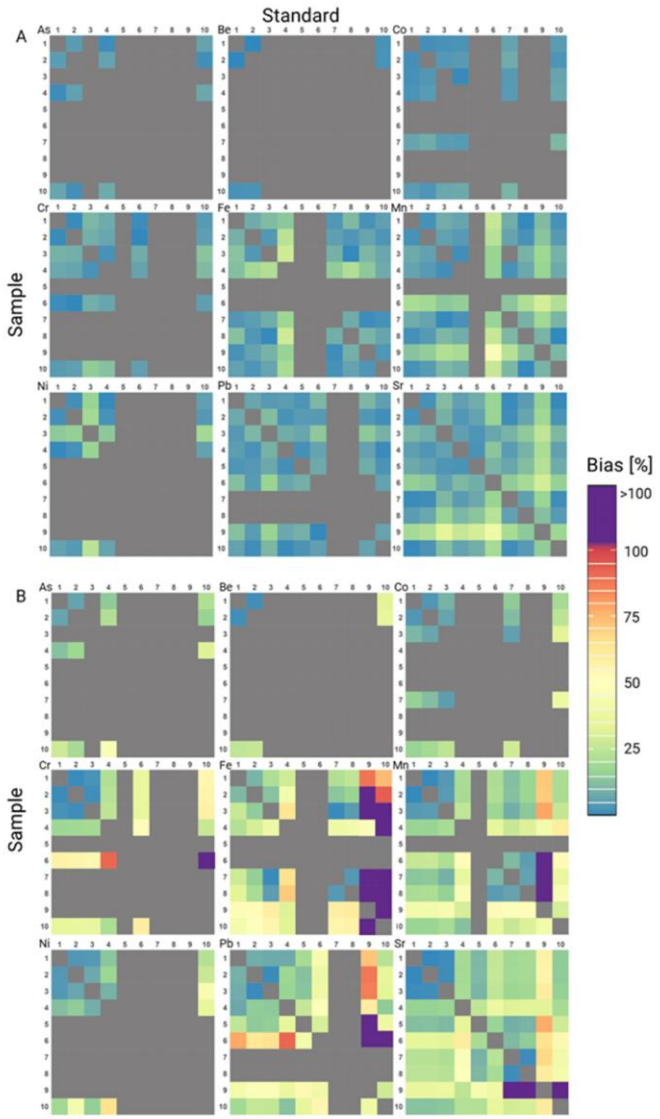

Fig. 4. Heat maps showing the average measurement bias by cross-calibrating nine elements (As, Be, Co, Cr, Fe, M, Ni, Pb and Sr), with (A) and without (B) ablation volume-normalization. Pixels in the maps are defined by one-point calibration standards in the columns and samples in the rows, where 1 = NIST 610, 2 = NIST 612, 3 = NIST 614, 4 = CMG-B, 5 = DLH8, 6 = Plešovice, 7 = JCp-1, 8 = JCt-1, 9 = NIST 1547, and 10 = Gelatin gel.

the superiority of data acquired through ablation-volume normalization is clearly evident compared to data obtained without employing this method.

In addition to the overall enhancement in concentration determination accuracy, Fig. 4 reveals several other important details. Fig. 4A shows that the bias in the majority of the measured concentrations with ablation volume-normalization is less than 15 %. For the less well-defined standards Plešovice and NIST 1547, a higher bias is observed in Fig. 4A for most materials. For Plešovice this is due to a lack of microscale homogeneity [33], further compounded by the potential

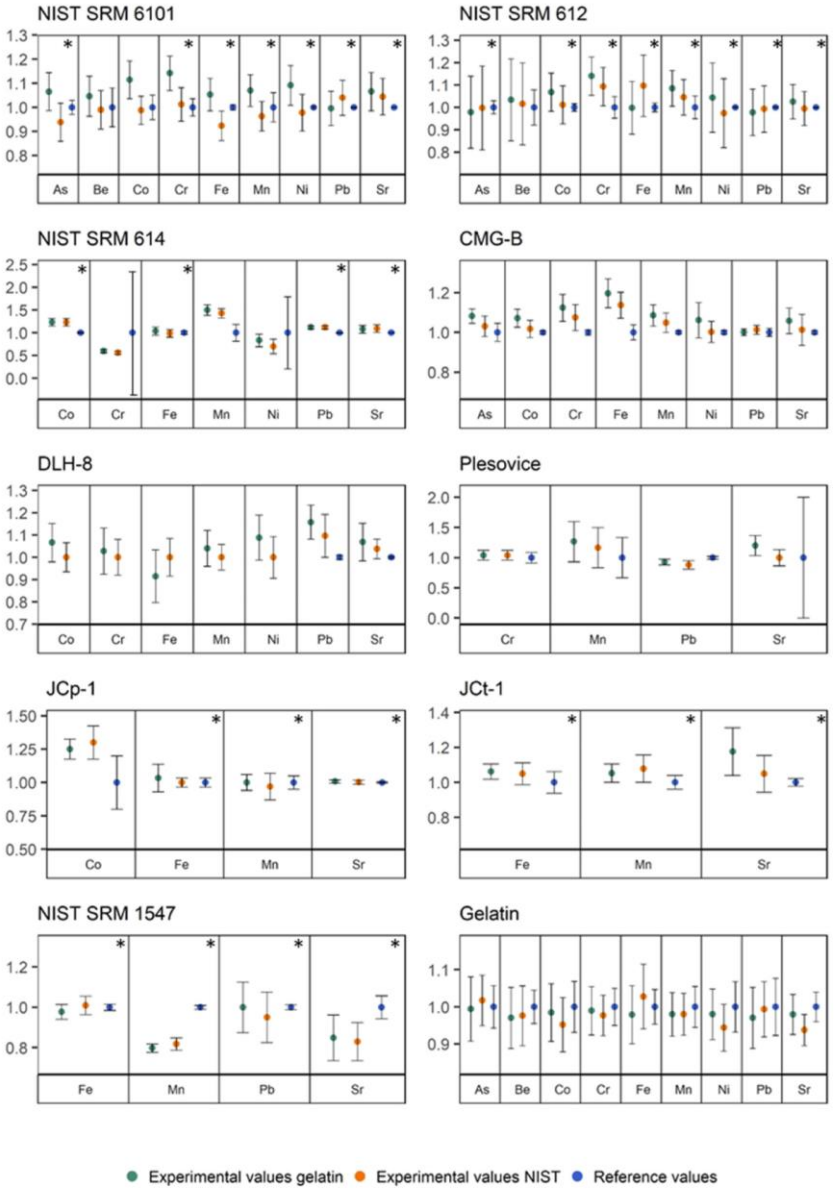

Fig. 5. Validation of accuracy and precision of the ablation volume-normalization method in multi-point calibration mode by comparing the concentrations obtained with the reference concentrations of up to nine elements in ten CRMs. The results are displayed as concentrations normalized to the reference concentrations, where unity values in the figure are directly linked to the reference concentrations. The error bars are representative for the standard deviations in the experimental data for the NIST 61X (5, 50 and 500 μg g^{-1}) and gelatin standards (10–250 μg g^{-1}) and the reference data, either the certified reference values in the COA (indicated with an asterisk) or the calculated values from reported concentrations in the GeoRem database (for the missing elements).

inaccuracy of the reported density [34] used in the calculations, whereas for NIST 1547 pelletizing issues associated with the hydraulic pressure might be the culprit. As expected, quantification data without ablation volume-normalization in Fig. 4B show a much higher bias, and only were matrices of standard and sample exactly match, e.g., for the NIST 61X glasses or the two carbonate materials - JCt, JCp lower bias values can be observed. The latter confirms the LA-ICP-MS prerequisite, that for the accurate quantitative work a matrix matched standard is obligatory in the conventional way, whereas in the proposed approach a well-defined (certified) standard can be used for quantification of any other material. However, even when using a matrix-matched standard, care must be taken if the sample is not homogeneous, as differences may occur during the ablation of the same sample, hence making an accurate quantification impossible without volume normalization [36].

3.5. Accuracy and precision of the ablation volume-normalization method in multi-point calibration mode

The versatility of the proposed method gains further significance when one can locate commercial or custom-prepared multielement standards across various concentration levels. This enables the execution of multi-point calibration, and thus establishment of a slope (see Fig. 2), instead of one-point calibration used in Fig. 4. Candidates for such calibration standards are i) the NIST 61X standards, having similar main matrix compositions (comparable concentrations of SiO_2, Na_2O, Al_2O_3, and CaO, which make up more than 96 % of the matrices), but variable minor and trace element concentrations, and ii) the custom-prepared gelatin standards with the flexibility to span the necessary concentration range for any element required, particularly in the context of biomedical mapping where standard references are typically unavailable.

In Fig. 5 (Table S1 gives the actual concentrations associated with this figure) it is visually demonstrated that in the absence of matrix-matched standards, the ablation volume-normalization method can generate accurate and precise data using the NIST 61X standards (5, 50 and 500 μg g^{-1}) or the custom-prepared gelatin standards (10–250 μg g^{-1}) using multi-point calibration for measurement of up to nine elements in ten standard reference matrices. Even though only a portion (ca. 47 %) of the nine elements selected are certified in all reference materials (elements with an asterisk in Fig. 5), the missing data were "filled in" by unweighted averaging of the element concentrations reported in the GeoReM database for the individual elements [38,39]. The error bars are representative for the standard deviations in i) the experimental data for the NIST 61X and gelatin standards (N = 5), and ii) the reference data, either the certified reference values (after recalculation from expanded uncertainties in the COA), or the calculated values from reported concentrations in the GeoRem database (for the missing elements). From Fig. 5 we can see that in all cases the experimental uncertainties obtained with the ablation volume-normalization method are closely matching the uncertainties of the reference data.

While the gelatin standards are very easy to work with (*i.e.* good crater shapes, low energy, easy to focus …), allow the addition of any element in a wide concentration range, the NIST 61X glass standards are readily available, certified, widely used and easy to work with. Despite extrapolating the concentrations of certain elements in specific samples from the calibration curve's range, these findings remained consistent with the certified values of the CRMs. This agreement was due to the broad linear range of ICP-MS and the adoption of a calibration curve, which alleviated the potential adverse impact of a single measurement error on the calibration slope. This situation could arise when employing a one-point calibration, a common practice in LA-ICP-MS measurements, primarily because suitable matrix-matched standards are often unavailable, especially in the diverse range necessary to construct a comprehensive calibration curve.

4. Conclusions

The utilization of commonly accessible certified reference materials (CRMs), such as NIST 61X glasses, is generally limited to samples sharing a similar matrix composition. This limitation hinders their applicability in accurately quantifying elements if e.g. biological samples, which lack widely accepted CRMs and instead resort to custom-prepared standards. In this investigation, we present a calibration technique for LA-ICP-MS that eliminates the necessity for matrix-matching. This pioneering method holds great potential across various fields and offers a simplified quantification solution for scenarios where traditional certified reference materials are unavailable.

Our approach, involving ablation-volume normalization, underwent thorough assessment across diverse material types including glass (NIST SRM 610, NIST SRM 612, NIST SRM 614, CMG-B, DLH-8), carbonates (JCp-1, JCt-1), plant specimens (NIST SRM 1547), zircons (Plešovice), and proteinaceous substances (gelatin). The quantified concentrations for all materials consistently matched certified values, effectively showcasing the transferability of calibration standards among materials with well-defined elemental compositions. Notably, gelatin and glass demonstrated remarkable suitability. Discrepancies in elemental concentration determinations mostly remained below 10 %, except in cases of exceedingly low concentrations.

In stark contrast to the conventional LA-ICP-MS calibration dependent on matrix-matched standards, our innovative methodology introduces a more robust calibration procedure that remains effective even when such standards are unavailable. This groundbreaking advancement holds the potential to enhance the accuracy and precision of elemental analysis through LA-ICP-MS, spanning a wide array of research applications.

CRediT authorship contribution statement

Kristina Mervič: Data curation, Formal analysis, Software, Validation, Visualization, Writing – original draft, Writing – review & editing. **Vid S. Šelih:** Conceptualization, Writing – review & editing. **Martin Šala:** Conceptualization, Funding acquisition, Investigation, Methodology, Resources, Supervision, Validation, Writing – original draft, Writing – review & editing. **Johannes T. van Elteren:** Conceptualization, Methodology, Validation, Writing – review & editing.

Declaration of competing interest

The authors declare that they have no known competing financial interests or personal relationships that could have appeared to influence the work reported in this paper.

Data availability

Data will be made available on request.

Acknowledgment

The authors acknowledge the financial support from the Slovenian Research Agency ARRS research core funding no. P1-0034. K.M. thanks the Slovenian Research Agency ARRS for funding her PhD research.

Appendix A. Supplementary data

Supplementary data to this article can be found online at https://doi.org/10.1016/j.talanta.2024.125712.

References

[1] D. Chew, K. Drost, J.H. Marsh, J.A. Petrus, LA-ICP-MS imaging in the geosciences and its applications to geochronology, Chem. Geol. 559 (2021) 119917.

[2] J. Almirall, A. Akmeemana, K. Lambert, P. Jiang, E. Bakowska, R. Corzo, C. M. Lopez, E.C. Pollock, K. Prasch, T. Trejos, P. Weis, W. Wiarda, H. Xie, P. Zoon, Determination of seventeen major and trace elements in new float glass standards for use in forensic comparisons using laser ablation inductively coupled plasma mass spectrometry, Spectrochim. Acta, Part B 179 (2021) 106119.

[3] Q. Li, Z. Wang, J. Mo, G. Zhang, Y. Chen, C. Huang, Imaging gold nanoparticles in mouse liver by laser ablation inductively coupled plasma mass spectrometry, Sci. Rep. 7 (1) (2017) 2965.

[4] R. Luo, X. Su, W. Xu, S. Zhang, X. Zhuo, D. Ma, Determination of arsenic and lead in single hair strands by laser ablation inductively coupled plasma mass spectrometry, Sci. Rep. 7 (1) (2017) 3426.

[5] H.R. Ali, H.W. Jackson, V.R.T. Zanotelli, E. Danenberg, J.R. Fischer, H. Bardwell, E. Provenzano, C.I.G.C. Team, O.M. Rueda, S.F. Chin, S. Aparicio, C. Caldas, B. Bodenmiller, Imaging mass cytometry and multiplatform genomics define the phenogenomic landscape of breast cancer, Nat. Cancer. 1 (2) (2020) 163–175.

[6] P.A. Doble, R.G. de Vega, D.P. Bishop, D.J. Hare, D. Clases, Laser ablation-inductively coupled plasma-mass spectrometry imaging in biology, Chem. Rev. (2021) 11769–11822.

[7] T. Ubide, B.S. Kamber, Volcanic crystals as time capsules of eruption history, Nat. Commun. 9 (1) (2018) 326.

[8] C. Giesen, H.A.O. Wang, D. Schapiro, N. Zivanovic, A. Jacobs, B. Hattendorf, P. J. Schüffler, D. Grolimund, J.M. Buhmann, S. Brandt, Z. Varga, P.J. Wild, D. Günther, B. Bodenmiller, Highly multiplexed imaging of tumor tissues with subcellular resolution by mass cytometry, Nat. Methods 11 (4) (2014) 417–422.

[9] T. Van Acker, S. Theiner, E. Bolea-Fernandez, F. Vanhaecke, G. Koellensperger, Inductively coupled plasma mass spectrometry, Nat. Rev. Methods Primers 3 (1) (2023) 53.

[10] T. Van Acker, S.J.M. Van Malderen, T. Van Helden, C. Stremtan, M. Šala, J.T. van Elteren, F. Vanhaecke, Analytical figures of merit of a low-dispersion aerosol transport system for high-throughput LA-ICP-MS analysis, J. Anal. Atom. Spectrom. 36 (6) (2021) 1201–1209.

[11] S.J.M. Van Malderen, J.T. van Elteren, F. Vanhaecke, Development of a fast laser ablation-inductively coupled plasma-mass spectrometry cell for sub-μm scanning of layered materials, J. Anal. Atom. Spectrom. 30 (1) (2015) 119–125.

[12] A. Gundlach-Graham, M. Burger, S. Allner, G. Schwarz, H.A. Wang, L. Gyr, D. Grolimund, B. Hattendorf, D. Gunther, High-speed, high-resolution, multielemental laser ablation-inductively coupled plasma-time-of-flight mass spectrometry imaging: part I. Instrumentation and two-dimensional imaging of geological samples, Anal. Chem. 87 (16) (2015) 8250–8258.

[13] G. Craig, A.J. Managh, C. Stremtan, N.S. Lloyd, M.S.A. Horstwood, Doubling sensitivity in multicollector ICPMS using high-efficiency, rapid response laser ablation technology, Anal. Chem. 90 (19) (2018) 11564–11571.

[14] J.T. van Elteren, V.S. Šelih, M. Šala, Insights into the selection of 2D LA-ICP-MS (multi)elemental mapping conditions, J. Anal. Atom. Spectrom. 34 (9) (2019) 1919–1931.

[15] J.T. van Elteren, D. Metarapi, M. Šala, V.S. Šelih, C.C. Stremtan, Fine-tuning of LA-ICP-QMS conditions for elemental mapping, J. Anal. Atom. Spectrom. 35 (11) (2020) 2494–2497.

[16] M. Šala, V.S. Šelih, C.C. Stremtan, T. Tămaș, J.T. van Elteren, Implications of laser shot dosage on image quality in LA-ICP-QMS imaging, J. Anal. Atom. Spectrom. 36 (1) (2021) 75–79.

[17] O.B. Bauer, O. Hachmöller, O. Borovinskaya, M. Sperling, H.-J. Schurek, G. Ciarimboli, U. Karst, LA-ICP-TOF-MS for rapid, all-elemental and quantitative bioimaging, isotopic analysis and the investigation of plasma processes, J. Anal. Atom. Spectrom. 34 (4) (2019) 694–701.

[18] M. Burger, G. Schwarz, A. Gundlach-Graham, D. Käser, B. Hattendorf, D. Günther, Capabilities of laser ablation inductively coupled plasma time-of-flight mass spectrometry, J. Anal. Atom. Spectrom. 32 (10) (2017) 1946–1959.

[19] M. Vázquez Peláez, J.M. Costa-Fernández, A. Sanz-Medel, Critical comparison between quadrupole and time-of-flight inductively coupled plasma mass spectrometers for isotope ratio measurements in elemental speciation, J. Anal. Atom. Spectrom. 17 (8) (2002) 950–957.

[20] M. Balcerzak, An overview of analytical applications of time of flight-mass spectrometric (TOF-MS) analyzers and an inductively coupled plasma-TOF-MS technique, Anal. Sci. 19 (7) (2003) 979–989.

[21] D. Günther, C.A. Heinrich, Comparison of the ablation behaviour of 266 nm Nd: YAG and 193 nm ArF excimer lasers for LA-ICP-MS analysis, J. Anal. Atom. Spectrom. 14 (9) (1999) 1369–1374.

[22] I. Kroslakova, D. Günther, Elemental fractionation in laser ablation-inductively coupled plasma-mass spectrometry: evidence for mass load induced matrix effects in the ICP during ablation of a silicate glass, J. Anal. Atom. Spectrom. 22 (1) (2007) 51–62.

[23] H.P. Longerich, D. Günther, S.E. Jackson, Elemental fractionation in laser ablation inductively coupled plasma mass spectrometry, Fresenius' J. Anal. Chem. 355 (5) (1996) 538–542.

[24] M. Guillong, D. Günther, Effect of particle size distribution on ICP-induced elemental fractionation in laser ablation-inductively coupled plasma-mass spectrometry, J. Anal. Atom. Spectrom. 17 (8) (2002) 831–837.

[25] H. Pan, L. Feng, Y. Lu, Y. Han, J. Xiong, H. Li, Calibration strategies for laser ablation ICP-MS in biological studies: a review, TrAC, Trends Anal. Chem. 156 (2022) 116710.

[26] M. Martínez, M. Baudelet, Calibration strategies for elemental analysis of biological samples by LA-ICP-MS and LIBS – a review, Anal. Bioanal. Chem. 412 (1) (2020) 27–36.

[27] A. Limbeck, P. Galler, M. Bonta, G. Bauer, W. Nischkauer, F. Vanhaecke, Recent advances in quantitative LA-ICP-MS analysis: challenges and solutions in the life sciences and environmental chemistry, Anal. Bioanal. Chem. 407 (22) (2015) 6593–6617.

[28] J. Cizdziel, K. Bu, P. Nowinski, Determination of elements in situ in green leaves by laser ablation ICP-MS using pressed reference materials for calibration, Anal. Methods 4 (2) (2012) 564–569.

[29] A. Schweikert, S. Theiner, M. Šala, P. Vician, W. Berger, B.K. Keppler, G. Koellensperger, Quantification in bioimaging by LA-ICPMS - evaluation of isotope dilution and standard addition enabled by micro-droplets, Anal. Chim. Acta 1223 (2022) 340200.

[30] M. Šala, V.S. Šelih, J.T. van Elteren, Gelatin gels as multi-element calibration standards in LA-ICP-MS bioimaging: fabrication of homogeneous standards and microhomogeneity testing, Analyst 142 (18) (2017) 3356–3359.

[31] A. Schweikert, S. Theiner, D. Wernitznig, A. Schoeberl, M. Schaier, S. Neumayer, B. K. Keppler, G. Koellensperger, Micro-droplet-based calibration for quantitative elemental bioimaging by LA-ICPMS, Anal. Bioanal. Chem. 414 (1) (2022) 485–495.

[32] **Calibration standards for microanalysis.** https://www.my-standards.com/, **2023. (Accessed 4 April 2023).**

[33] J. Sláma, J. Košler, D.J. Condon, J.L. Crowley, A. Gerdes, J.M. Hanchar, M.S. A. Horstwood, G.A. Morris, L. Nasdala, N. Norberg, U. Schaltegger, B. Schoene, M. N. Tubrett, M.J. Whitehouse, Plešovice zircon — a new natural reference material for U–Pb and Hf isotopic microanalysis, Chem. Geol. 249 (1) (2008) 1–35.

[34] **Zircon Mineral Data.** http://webmineral.com/data/Zircon.shtml#.Y7UsK9XMKUk. **(Accessed 29.September 2023).**

[35] A. Jerše, K. Mervič, J.T. van Elteren, V.S. Šelih, M. Šala, Quantification anomalies in single pulse LA-ICP-MS analysis associated with laser fluence and beam size, Analyst 147 (23) (2022) 5293–5299.

[36] K. Mervič, J.T. van Elteren, M. Bele, M. Šala, Utilizing ablation volume for calibration in LA-ICP-MS mapping to address variations in ablation rates within and between matrices, Talanta (2023) 125379.

[37] S. Zhang, M. He, Z. Yin, E. Zhu, W. Hang, B. Huang, Elemental fractionation and matrix effects in laser sampling based spectrometry, J. Anal. Atom. Spectrom. 31 (2) (2016) 358–382.

[38] K. Jochum, U. Nohl, K. Herwig, E. Lammel, B. Stoll, A. Hofmann, GeoReM: a new geochemical database for reference materials and isotopic standards, Geostand. Geoanal. Res. 29 (2007) 333–338.

[39] **GeoReM - Database on geochemical and environmental reference materials.** http://georem.mpch-mainz.gwdg.de/. **(Accessed 29.September. 2023).**

3.4 Manuscript 4: Utilizing Ablation Volume for Calibration in LA-ICP-MS Mapping to Address Variations in Ablation Rates Within and Between Matrices

Published: Mervič K., van Elteren J.T., Bele M., Šala M., (2024). Talanta, 269, 125379, doi: 10.1016/j.talanta.2023.125379.

The evolution of laser ablation cells with rapid aerosol washout in 2D LA-ICP-MS elemental mapping has significantly enhanced spatial resolution and mapping speed. However, as with LA-ICP-MS bulk analysis, quantification of 2D elemental mapping remains a complex process that mainly relies on matrix-matched external standards and internal standardization. The problems lie in elemental fractionation – non-stoichiometric effects that occur during vaporization, particle transport, atomization and ionization in the plasma, as well as differences in ablated mass due to matrix-dependent ablation rates caused by differences in reflectivity, absorptivity and thermal conductivity. To avoid these problems, most calibration approaches rely on matrix-matched standards, but their availability is limited, as explained in Manuscript 2. Therefore, many customized standards such as gelatin, 3D-printed polymer reference materials, pressed tablets, *etc.* have been developed for calibration purposes to mimic the sample matrix as closely as possible and overcome the problem of lack of suitable standards. In addition, internal standardization methods that correct for instrumental drift and fluctuation, but also account for matrix effects and differences in ablation rates within a sample, are often unpredictable and depend on the nature of the sample under investigation. Some of the commonly used approaches to correct for matrix effects are the use of homogeneously distributed elements in the sample, total consumption of thin samples and standards, aspiration of a standard solution during laser sampling, application of a "film" standard on/under a biosample in combination with the total consumption of the assembly, and labeling of tissue components with a metallo-intercalator. However, suitable internal standards are limited and total consumption approach only applies to thin biosamples, so a more general approach is required to aid quantification in different matrices.

In this manuscript, the ablated volume per pixel measurement is used to correct for mass differences between samples and standards within and between different matrices, resulting in mass per volume concentrations. As a proof-of-concept, ablation volume-based calibration was employed for LA-ICP-MS quantification of highly variable elemental concentrations in decorative glass (Murrina). Normalization of the elemental maps using pixel-associated ablation volumes corrected for differences in ablation rate within the Murrina and between the Murrina and the standards. This approach was validated using LA-ICP-MS with sum normalization calibration and scanning electron microscopy with energy dispersive X-ray spectroscopy (SEM-EDXS). In addition, geological thin section analysis underlined the importance of volume normalization in correcting for ablation rate variations.

Talanta 269 (2024) 125379

Contents lists available at ScienceDirect

Talanta

journal homepage: www.elsevier.com/locate/talanta

Utilizing ablation volume for calibration in LA-ICP-MS mapping to address variations in ablation rates within and between matrices

Kristina Mervič [a], Johannes T. van Elteren [a,**], Marjan Bele [b], Martin Šala [a,*]

[a] Department of Analytical Chemistry, National Institute of Chemistry, Hajdrihova 19, Ljubljana, 1000, Slovenia
[b] Department of Materials Chemistry, National Institute of Chemistry, Hajdrihova 19, Ljubljana 1000, Slovenia

ARTICLE INFO

Keywords:
Laser ablation
Optical profilometry
LA-ICP-MS
Mapping
SEM-EDX

ABSTRACT

Quantification in 2D LA-ICP-MS mapping generally requires matrix-matched standards to minimize issues related to elemental fractionation. In addition, internal standardization is commonly applied to correct for instrumental drift and fluctuation, whereas also differences in ablated mass can be rectified for samples that cannot be sectioned and subjected to total ablation. However, it is crucial that the internal standard element is homogeneously distributed in the sample and that the laser light absorptivity is uniform over the surface. As in practice these requirements are often not met, this work will focus on correction of ablation rate differences within/between samples and standards by normalizing the element maps using the associated ablation volume per pixel as measured by optical profilometry. Due to the volume correction approach the element concentrations are no longer defined as mass per mass concentrations (in μg g^{-1}) but by mass per volume concentrations (in μg cm^{-3}), which can be interconverted in case matrix densities are known. The findings show that ablation volume-aided calibration yields more accurate element concentrations in 2D LA-ICP-MS maps for a decorative glass with highly varying elemental concentrations (murrina). This research presents a warning that if there are variations in ablation rates between samples and standards within and across matrices, even when their sensitivities are the same, generic LA-ICP-MS calibration protocols may not accurately depict the actual element concentrations.

1. Introduction

The development of LA cells with fast washout of aerosol particles in 2D LA-ICP-MS elemental mapping has led to major improvements in mapping speed and spatial resolution [1,2]. However, quantification of elements remains challenging due to elemental fractionation issues (non-stoichiometric effects during vaporization, transport of ablated particles, atomization, and ionization in the plasma), causing the signal measured not to be entirely representative of the composition of the sample. Furthermore, differences in mass ablated due to matrix-dependent ablation rates caused by differences in absorptivity, reflectivity, and thermal conductivity complicate the quantification process [3,4]. Several approaches have been reported to counteract these quantification problems, but so far, the most dependable solution is to matrix-match external standards and samples and the use of suitable internal standards.

Even though the availability of matrix-matched external standards is limited, especially for biological samples, they are often custom-prepared via pressing of tablets from certified biomaterial standards or from nano-particulate powders after wet-milling of refractory materials [5–7]. Internal standardization methods that correct for instrumental drift and fluctuation, but also deal with matrix effects and differences in intra-sample ablation rates, are often unpredictable and depend on the type of sample under study [8]. Approaches in use rely on i) total consumption of thin biosamples and standards [9–11], ii) application of a "film" standard on/under a biosample combined with total consumption of the assembly [12,13], iii) (in-cell or in-torch) aspiration of a standard solution during laser sampling [14–16], iv) the use of homogeneously distributed elements in the sample [17,18], and v) labelling of tissue components with a metallo-intercalator [19,20].

Total consumption approaches can correct for differences in ablation rate, but only for precisely sectioned "thin" biosamples (and standards), whereas homogeneously distributed elements or labelling approaches can also correct for ablation differences in "thick" biosamples. However, suitable elements that can act as an internal standard are rare, and for aiding the quantification process of all kinds of matrices, also inorganic

* Corresponding author.
** Corresponding author.
E-mail addresses: elteren@ki.si (J.T. van Elteren), martin.sala@ki.si (M. Šala).

https://doi.org/10.1016/j.talanta.2023.125379
Received 6 October 2023; Received in revised form 20 October 2023; Accepted 31 October 2023
Available online 3 November 2023

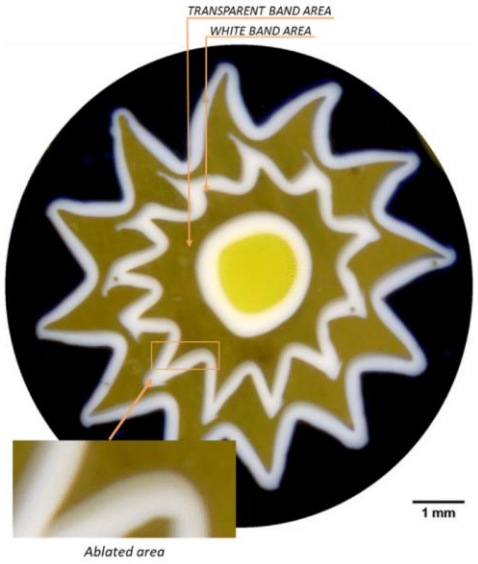

Fig. 1. Murrina used for ablation volume-aided calibration in multielement LA-ICP-MS mapping; the insert gives the actual analyzed section.

ones, a more generic approach is needed. We chose to measure the ablated volume per pixel as a means of correction for differences in ablated mass between samples and standards within and across matrices. This ablation approach yields by definition mass per volume concentrations instead of the conventional mass per mass concentrations, unless interconversion via known or measurable (local) densities of the matrices involved is possible.

As a proof-of-concept, ablation volume-aided calibration was applied for LA-ICP-MS quantification of highly variable elemental concentrations in a decorative glass (murrina). Ablation rate differences within the murrina, and between the murrina and the standards, were corrected by normalizing the element maps using the pixel-associated ablation volumes. The approach was validated using LA-ICP-MS with sum normalization calibration [21,22], as well as with scanning electron microscopy with energy dispersive X-ray spectroscopy (SEM-EDXS). To demonstrate that ablation rate variations are not so uncommon, we also analyzed a geological thin section consisting of several mineralogical phases with and without volume normalization.

2. Material and methods

2.1. Samples and standards for the volume-aided calibration approach

In the murrina production process, glass canes (long rods of glass) are formed based on stretching a compact mass of hot glass to great length, implying that it retains its radial pattern in longitudinal direction perfectly, and as such a several millimeters thick slice of the cane (=murrina) has a high depth homogeneity, making it an ideal sample for repeated mapping on the same area. A modern murrina (Murano, Italy) (Fig. 1), embedded in epoxy resin, and polished with silica carbide polishing disks (800 and 2400 grit) and diamond slurry (Diamond suspension, polycrystalline, Reflex LDP, 3 μm, Presi, France), was subjected to LA-ICP-MS multi-element mapping in line scanning mode to quantify the highly variable elemental concentrations. Glass standards used in

Table 1
Operational LA-ICP-MS settings used for multielement mapping of the murrina.

LA (Analyte G2, ARIS, and glass expansion unit)	
Wavelength (nm)	193
Laser fluence (J cm^{-2})	3.6
Repetition rate (Hz)	100
Scanning mode	Line scanning
Dosage (shots per pixel)	10
Washout time (ms)	Ca. 100
Beam size (μm)	5
Mask shape	Square
He flow rate (L min^{-1}) cup|cell	0.3|0.3
ICP-MS (Agilent 7900x)	
R_f power (W)	1500
Plasma gas flow rate (L min^{-1})	15
Auxiliary gas flow rate (L min^{-1})	0.9
Ar makeup flow rate (L min^{-1})	0.8
Data acquisition	Time-resolved
Isotopes measured	^{29}Si,^{23}Na,^{27}Al,^{39}K,^{43}Ca,^{75}As,^{137}Ba and^{208}Pb
Dwell time (ms)	10

the calibration were the NIST SRM glasses 610 and 612, having nominal concentrations of 500 and 50 μg g^{-1}, respectively, for ca. 60 elements. The proposed approach was also used to analyze a well-prepared geological thin section, which contained various mineralogical phases like garnets, cordierite, biotite, and others. This is a typical geological sample frequently analyzed by LA-ICP-MS, and will aid to demonstrate that intra-sample ablation rate variations are rather common and may need extra attention with regard to accurate quantification via volume normalization.

2.2. Instrumentation and measurement protocols

Elemental mapping was performed using a laser ablation system (193 nm ArF*; Analyte G2, Teledyne Photon Machines Inc., Bozeman, MT) equipped with a standard active two-volume ablation cell (HelEx II), including the Aerosol Rapid Introduction System (ARIS, Teledyne CETAC Technologies) coupled with glass expansion unit, a so-called long pulse module having an overall aerosol particle washout time of ca. 100 ms (=FW0.01 M, full width at 1 % of the maximum). The laser ablation system was interfaced with a quadrupole ICP-MS instrument (Agilent 7900*x*, Agilent Technologies, Santa Clara, CA). The LA-ICP-MS mapping conditions for element mapping of the murrina in line scanning mode are given in Table 1. Line scanning was performed with a dosage *D* of 10, implying that signals of 10 laser shots were accumulated in the analysis time *AT* of 100 ms, requiring a repetition rate *RR* of 100 Hz ($D = RR{\cdot}AT$) [23–25]. In essence, 10 overlapping laser shots generated a square pixel equal to the beam size *BS* although the material sampled originates from a slightly larger area ($[2{\bullet}BS{-}BS/D] \times [BS]$). To measure the surface morphology of the murrina surface we used an optical interferometer (Zegage PRO HR, Zygo Corporation, Middlefield, CT). 3D information was recorded using a 50 × magnification lens with a lateral resolution of 0.173 μm, and a surface topography repeatability better than 3.5 nm. Data associated with the surface topography was first processed with the manufacturer's MxTM software (version 8.0.0.23), and then "sur" and "int" files were imported and converted into csv format using MatLab R2020a (MathWorks); missing data corresponding to extremely sloped areas was filled in with adjacent data using the regionfill function in MatLab. The high-resolution topography maps were resampled to match the pixel size of the LA-ICP-MS element maps, followed by registration of the different modality maps, i.e., the element and volume maps. ImageJ, OriginLab, and HDIP (Teledyne Photon Machines Inc., Bozeman, MT) software packages were used for image and data processing.

For the highest precision and accuracy, the ablation volume-aided calibration approach requires pre-knowledge about the density of the standards. To this end, we measured the density of the NIST SRM 610

Table 2
The LA-ICP-MS murrina data generated by the volume-aided calibration approach (Vol) was validated by comparing it with data obtained from LA-ICP-MS with sum normalization calibration (Sum) and SEM-EDXS. The transparent (T) and white (W) areas on the murrina were analyzed separately. The data in the table are reported as averages ±95 % confidence limits (volume concentrations converted to %m/m or μg g^{-1} concentrations), by measuring the signal and volume of multiple areas (10 × 10 pixels) for both the white and transparent parts.

Elem	Area	Vol	Sum	SEM-EDXS
Si %m/m	T	32.7 ± 0.5	31.4 ± 2.1	35.2 ± 0.2
	W	19.2 ± 0.2	20.5 ± 1.7	21.7 ± 0.1
Na	T	13.3 ± 0.5	12.7 ± 0.8	13.5 ± 0.1
%m/m	W	6.0 ± 0.1	5.9 ± 0.5	6.3 ± 0.1
Al %m/m	T	0.40 ± 0.01	0.33 ± 0.02	0.38 ± 0.04
	W	0.57 ± 0.01	0.54 ± 0.04	0.60 ± 0.03
K %m/m	T	2.3 ± 0.1	2.3 ± 0.2	2.1 ± 0.1
	W	1.7 ± 0.1	1.9 ± 0.1	1.9 ± 0.1
Ca %m/m	T	5.2 ± 0.2	5.1 ± 0.4	5.1 ± 0.1
	W	0.9 ± 0.1	0.95 ± 0.2	0.9 ± 0.2
As %m/m	T	0.±0.03	0.33 ± 0.01	0.26 ± 0.04
	W	4.9 ± 0.2	4.7 ± 0.4	4.9 ± 0.1
Pb %m/m	T	nd*	nd*	nd*
	W	31.0 ± 0.4	32 ± 2.3	31.1 ± 0.2
Ba μg g^{-1}	T	27 ± 3.3	30 ± 4.0	nd*
	W	20 ± 3.7	20 ± 2.0	nd*

*, not detectable.

and 612 standards with a gas pycnometer (1345 AccuPyc II, Micromeritics, Norcross, GA). To convert mass per volume concentrations in the murrina sample to mass per mass concentrations, the local densities need to be determined as well. As local densities cannot be determined directly, we inferred them from their local composition using a global model [26] based on concentration data obtained with SEM-EDXS (see Table 2). Calculated densities were as follows: approximately 2.49 g cm^{-3} for the transparent area and 3.20 g cm^{-3} for the white area; these data are in line with the densities of soda-lime-silica glasses and lead glass, respectively [27]. This allows us to validate the results of LA-ICP-MS volume-corrected calibration data with SEM-EDXS and LA-ICP-MS sum normalized calibration data (see Table 2).

2.3. Validation

To validate the volume-corrected calibration approach, complementary techniques were used to measure the concentrations of selected elements (see Table 1) in the white and transparent areas indicated in Fig. 1, using LA-ICP-MS with sum normalization calibration and direct SEM-EDXS analysis. The sum normalization approach is a mathematically formulated technique based on the simultaneous measurement of 54 elements and normalizing them to 100 % m/m based on their corresponding oxide concentrations [21]. Additionally, direct SEM-EDXS analysis was carried out using a FE-SEM Zeiss Supra TM 35 VP Carl Zeiss, Oberkochen, Germany) field emission scanning electron microscope equipped with an energy-dispersive X-ray spectrometer SDD EDX Ultim Max 100 (Oxford Instruments, Oxford, UK). Samples were coated with 6 nm of platinum using a precision etching coating system (PECS), model 682 (Gatan, US). The operating voltage was set to 20 kV.

3. Results and discussion

Generally, external calibration by solid sampling techniques such as LA-ICP-MS requires closely matrix-matched reference materials to account for differences in ablation rate, and the use of suitable internal standards to correct for instrumental drift and fluctuation. As matrix-matching is only possible for samples with "known" characteristics, and the fact that internal standards are usually difficult to pinpoint, we discuss here an ablation volume-aided calibration approach that corrects for temporal variations in ablated mass during elemental mapping for the best possible localized quantification of selected elements in a murrina (Fig. 1). We used a murrina because of reproducible mapping areas and the fact that concentrations can be conveniently validated via the sum normalization approach and SEM-EDXS.

3.1. Volume-corrected calibration

To perform ablation volume-corrected quantification of elements in a sample (*S*) by 2D LA-ICP-MS mapping, we not only measure the signal intensity $A_{S,i}$ (in cps), but also the volume ablated ($V_{S,i}$) (in μm^3) per pixel *i* (see Fig. 2). A number of n calibrants (*C*n) with known mass concentrations $c_{Cn,mass}$ (in μg g^{-1}) and densities D_{Cn} (in g cm^{-3}) are

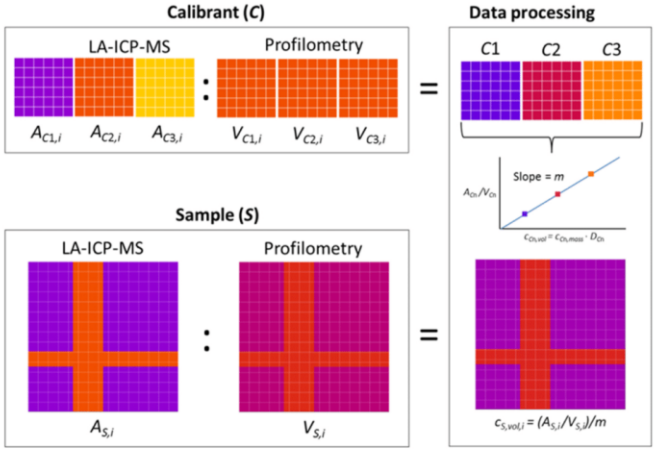

Fig. 2. Principle of the ablation volume-aided calibration approach based on LA-ICP-MS and profilometry measurements, and using calibrants (*C*1, *C*2 and *C*3) with equal densities ($D_{C1} = D_{C2} = D_{C3}$), yielding a sample map with pixels *i* showing mass per volume concentrations $C_{S,vol,i}$.

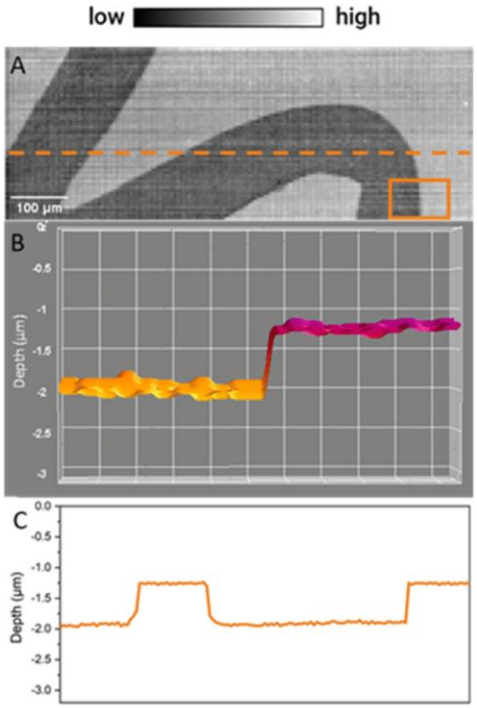

Fig. 3. Surface morphology of the ablated section of the murrina (Fig. 1, insert) measured by optical profilometry and shown as a 2D-greyscale image (A) showcasing the actual depth ablated with 10 shots with further detailing in the orange rectangle (B), and along the orange dashed line (C). The zero-levels correspond to the pristine, unablated murrina surface.

applied for external standardization; when measured similarly as the sample, the average calibrant signal intensities A_{Cn} per pixel (in cps) and the average calibrant volumes ablated V_{Cn} per pixel (in µm^3) yield a calibration graph as presented in Fig. 2. Here the average volume concentrations $c_{Cn,vol}$ of the calibrants (in µg cm^{-3}) are given by $c_{Cn,mass}{\cdot}D_{Cn}$ and the slope of the calibration graph by m (linear regression, forced through zero). The unknown volume concentrations $c_{S,vol,i}$ in pixel i of the sample (in µg cm^{-3}) are given by $(A_{S,i}/V_{S,i})/m$. Most often it is unlikely that $c_{S,vol,i}$ can be converted into $c_{S,mass,i}$ as local densities in the sample need to be known, implying that this approach generally calculates the elemental concentrations in pixels of the sample map as mass per volume concentrations. By recording pixels of calibrants and samples similarly (pixel width = scanning speed SS × acquisition time AT; pixel height = distance between line scans L), their area is uniform, and correction based on ablation volume becomes an ablation depth correction. When a sample has a flat, smooth surface prior to ablation, it suffices to merely measure the post-ablation surface, but when this is not the case both the pre- and post-ablation need to be measured to reliably construct the locally ablated volume [28].

3.2. Surface morphology

Due to the fact that the murrina has a flat and polished surface, it suffices to only measure the post-ablation surface topography. Fig. 3A shows the grayscale post-ablation topography map of an ablated section of the murrina, indicating a significant difference in ablation rate between the white and transparent areas. Fig. 3B and C detail the 3D surface depth in the area framed by the orange rectangle and the line scan depth along the orange dashed line in Fig. 3A, respectively. The ablated section has consistent ablation depths for the white (dark grey in Fig. 3A) and transparent (light grey in Fig. 3A) areas, being 1.98 and 1.25 µm, respectively. A potential reason for better ablation characteristics of the white area is that it contains a significant amount of Pb (31.1 % m/m, SEM-EDXS, Table 2), making it much softer for ablation but also denser than the transparent area which is primarily silica (75.3 % m/m, SiO_2 calculated from SEM-EDXS, Table 2). The post-ablation surface topography was also measured for NIST SRM 610 and NIST SRM 612 (data not shown), which are commonly used as matrix-matched standards for LA-ICP-MS calibration of glass samples. The ablated areas of NIST SRM 610 and NIST SRM 612 have a consistent ablation depth of 1.10 and 1.30 µm, respectively, using the same LA-ICP-MS operational settings as for the murrina sample. An image with isometric projection (Fig. S1) is added for better portrayal of the differences in laser ablation of the measured area in Fig. 3.

3.3. Volume-corrected surface quantification of major, minor and trace elements in the murrina

We selected major, minor and trace elements (Si, Na, Al, Ca, K, As, Pb and Ba) for measurement in selected locations of the murrina (Fig. 1) using optimized LA-ICP-MS conditions (Table 1) to minimize aliasing and elemental fractionation. Fig. 4A and 5A show the not volume-corrected maps (in % m/m) for Si and As obtained by direct two point calibration with the NIST SRM glasses 610 and 612. Fig. 4B and 5B show the volume-corrected maps (converted to % m/m via measured densities) for Si and As based on volume correction using the surface

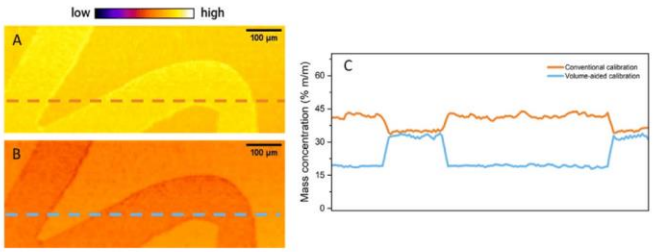

Fig. 4. LA-ICP-MS concentration map of Si in a section of the murrina (Fig. 1, insert) using conventional, not volume-corrected calibration (A) and volume-corrected calibration (B); the not-volume-corrected concentrations and corrected concentrations (in % m/m) along the dashed lines in A and B are shown in C.

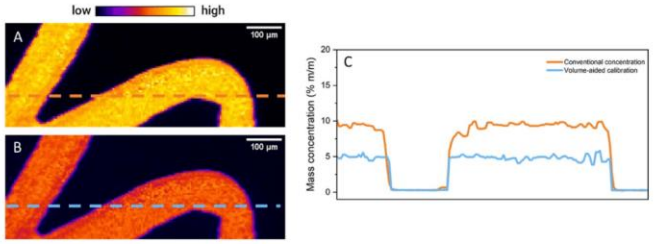

Fig. 5. LA-ICP-MS concentration map of As in a section of the murrina (Fig. 1, insert) using conventional, not volume-corrected calibration (A) and volume-corrected calibration (B); the not-volume-corrected concentrations and corrected concentrations (in % m/m) along the dashed lines in A and B are shown in C.

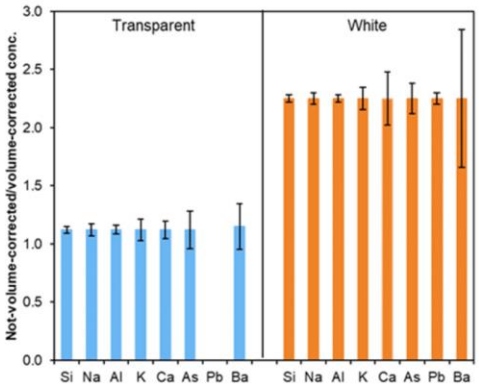

Fig. 6. Comparing the concentrations (with 95 % confidence limits) of eight elements obtained by the volume-corrected calibration approach and the not volume-corrected calibration approach in the transparent and white areas of the murrina.

topography maps in Fig. 3. Fig. 4C and 5C show the concentration profiles along the dashed lines for Si and As.

Respectively, both for the not-volume corrected data (in % m/m) and the volume-corrected data (converted to % m/m via measured densities). For the other six elements the respective maps are given in Figs. S2–S7 (Supporting information). The not volume-corrected Si map shows higher concentrations in the white area than in the transparent area, whereas for the volume-corrected Si maps the results are reversed. This suggests that the higher not volume-corrected Si concentrations in the white area are not due to an actual higher concentration, but are merely the effect of a higher mass ablated per laser shot, and thus a better representation of the actual volume concentration. This corresponds well with the high concentration of lead (31.0 % m/m, Table 2) in the white area, making the glass softer and easier to ablate. Consequently, there is less silicon on the expense of lead, therefore making the not volume-corrected maps questionable with regard to Si content. Similar to Si, in the not volume-corrected map also more As was found in the white area than in the transparent area. However, when normalized on volume, the differences between the two areas in the corrected maps become significantly smaller.

As seen from the surface morphology data (Fig. 3), different ablation rate characteristics are found for different glass areas within the murrina. This significantly affects the elemental concentrations in 2D LA-ICP-MS maps when conventional calibration is performed. We postulate that for precise quantification the volume-correction calibration approach corrects for inter- and intra-sample ablation rate differences, and yields more accurate data when the transport efficiencies and matrix sensitivities are the same.

3.4. Validation of the volume-corrected calibration approach

The volume-aided calibration approach highlighted above was validated by comparing concentrations of all eight elements in the white and transparent areas on the murrina by LA-ICP-MS with sum normalization calibration and SEM-EDXS analysis. After conversion of the volume concentration data via local densities to mass concentrations, validation of the ablation volume-corrected concentrations becomes feasible. Table 2 summarizes the results for all elements. The average concentrations obtained with the volume-aided calibration method are in good agreement with the LA-ICP-MS sum normalization and SEM-EDXS data.

However, from Fig. 6 it can be seen how the not volume-corrected data deviated significantly from the volume-corrected data, especially in the white area. The white area showcased a larger ablated volume (see Fig. 3) and higher densities compared to the transparent area and the NIST SRM glass standards, leading to higher signals due to larger amounts of ablated material entering the ICP-MS, and thus resulting in overestimation of the concentrations.

On the other hand, there is not much difference between the conventional, not volume-corrected data and the volume-corrected data for the transparent area, because the glass of the transparent area shows similar characteristics, i.e., ablation depth and density, as the NIST SRM 610 and 612 standards. This is an additional proof that exact matrix-matched standards are needed for determination of the correct concentrations by LA-ICP-MS, and confirms our hypothesis that for reliable quantification in 2D LA-ICP-MS mapping, volume-corrected elemental maps are the way forward, especially in cases where matrix-matching is problematic. Although the sum normalization approach seems the best and most convenient of all of the approaches, and might be the method of choice aiming for the most accurate results, glass is a rare example where the sum normalization can be used. For a more complex polished geological thin section sample we demonstrate (see Figs. S8 and S9, Supporting information) that considerable ablation rate differences exist within the sample, which may be dealt with by ablation volume normalization, most likely leading to improved quantification data, despite uncertainties in transport efficiencies and relative matrix sensitivities which exist for other calibration approaches as well.

4. Conclusions

Calibration has long been the Achilles' heel in LA-ICP-MS quantification as elemental fractionation, instrumental drift, and fluctuation, as well matrix-dependent ablation rates, all have to be considered in the calibration process. In this work, we have focused on investigating

(local) ablation rate differences in a decorative glass (murrina) and calibration standards upon measurement of major, minor and trace elements, and correcting for them using the ablated volume per pixel. Validation with complementary techniques has shown that conventional, not-volume calibration with supposedly appropriate standards may yield inaccurate quantification data. Furthermore, we have shown that 2D LA-ICP-MS mapping of a more complex geological sample with different phases shows ablation rate differences within the sample which can be mitigated by volume normalization of the individual pixel intensities.

This is especially relevant for "hard" (geological, metallurgical, etc.) samples which cannot be sectioned into very thin cross-sections as in the case of biosamples. Consequently, the resulting concentrations may have to be reported in m/V units (μg cm^{-3}) as intra-sample densities are mostly unknown. Further research is being conducted to demonstrate that this technique indeed delivers superior quantification data for diverse matrices. Summarizing we can say that neglecting the actual volumes ablated may result in potentially inaccurate LA-ICP-MS data when significant variations in ablation rates are found between samples and standards within and across matrices.

Credit author statement

Conceptualization: J.T.v.E. and M.Š., Investigation: K.M. and M.B. Visualization: K.M. Resources: J.T.v.E., M.Š., and M.B., Writing (review and editing): All authors.

Declaration of competing interest

The authors declare that they have no known competing financial interests or personal relationships that could have appeared to influence the work reported in this paper.

Data availability

Data will be made available on request.

Acknowledgements

The authors acknowledge the financial support from the Slovenian Research Agency ARRS (research core funding no. P1-0034 and P2-0393). K.M. thanks the Slovenian Research Agency ARRS for funding her PhD research.

Appendix A. Supplementary data

Supplementary data to this article can be found online at https://doi.org/10.1016/j.talanta.2023.125379.

References

[1] S.J.M. Van Malderen, A.J. Managh, B.L. Sharp, F. Vanhaecke, Recent developments in the design of rapid response cells for laser ablation-inductively coupled plasma-mass spectrometry and their impact on bioimaging applications, J. Anal. At. Spectrom 31 (2) (2016) 423–439, https://doi.org/10.1039/c5ja00430f.

[2] H.A.O. Wang, D. Grolimund, C. Giesen, C.N. Borca, J.R.H. Shaw-Stewart, B. Bodenmiller, D. Günther, Fast chemical imaging at high spatial resolution by laser ablation inductively coupled plasma mass spectrometry, Anal. Chem 85 (21) (2013) 10107–10116, https://doi.org/10.1021/ac400996x.

[3] S. Zhang, M. He, Z. Yin, E. Zhu, W. Hang, B. Huang, Elemental fractionation and matrix effects in laser sampling based spectrometry, J. Anal. At. Spectrom 31 (2) (2016) 358–382, https://doi.org/10.1039/C5JA00273G.

[4] I. Kroslakova, D. Günther, Elemental fractionation in laser ablation-inductively coupled plasma-mass spectrometry: evidence for mass load induced matrix effects in the ICP during ablation of a silicate glass, J. Anal. At. Spectrom 22 (1) (2007) 51–62, https://doi.org/10.1039/B606522H.

[5] A. Limbeck, P. Galler, M. Bonta, G. Bauer, W. Nischkauer, F. Vanhaecke, Recent advances in quantitative LA-ICP-MS analysis: challenges and solutions in the life sciences and environmental chemistry, Anal. Bioanal. Chem. 407 (22) (2015) 6593–6617, https://doi.org/10.1007/s00216-015-8858-0.

[6] P.A. Doble, R.G. de Vega, D.P. Bishop, D.J. Hare, D. Clases, Laser ablation-inductively coupled plasma-mass spectrometry imaging in biology, Chem. Rev (2021), https://doi.org/10.1021/acs.chemrev.0c01219.

[7] D. Garbe-Schönberg, S. Müller, Nano-particulate pressed powder tablets for LA-ICP-MS, J. Anal. At. Spectrom 29 (6) (2014) 990–1000, https://doi.org/10.1039/C4JA00007B.

[8] M. von Bremen-Kühne, H. Ahmadi, M. Sperling, U. Krämer, U. Karst, Elemental bioimaging of Zn and Cd in leaves of hyperaccumulator Arabidopsis halleri using laser ablation-inductively coupled plasma-mass spectrometry and referencing strategies, Chemosphere 305 (2022), 135267, https://doi.org/10.1016/j.chemosphere.2022.135267.

[9] M. Aramendía, L. Rello, S. Bérail, A. Donard, C. Pécheyran, M. Resano, Direct analysis of dried blood spots by femtosecond-laser ablation-inductively coupled plasma-mass spectrometry. Feasibility of split-flow laser ablation for simultaneous trace element and isotopic analysis, J. Anal. At. Spectrom 30 (1) (2015) 296–309, https://doi.org/10.1039/C4JA00313F.

[10] A. Arakawa, N. Jakubowski, G. Koellensperger, S. Theiner, A. Schweikert, S. Flemig, D. Iwahata, H. Traub, T. Hirata, Quantitative imaging of silver nanoparticles and essential elements in thin sections of fibroblast multicellular spheroids by high resolution laser ablation inductively coupled plasma time-of-flight mass spectrometry, Anal. Chem 91 (15) (2019) 10197–10203, https://doi.org/10.1021/acs.analchem.9b02239.

[11] D. Drescher, C. Giesen, H. Traub, U. Panne, J. Kneipp, N. Jakubowski, Quantitative imaging of gold and silver nanoparticles in single eukaryotic cells by laser ablation ICP-ms, Anal. Chem 84 (22) (2012) 9684–9688, https://doi.org/10.1021/ac302639c.

[12] C. Austin, D. Hare, T. Rawling, A.M. McDonagh, P. Doble, Quantification method for elemental bio-imaging by LA-ICP-MS using metal spiked PMMA films, J. Anal. At. Spectrom 25 (5) (2010) 722–725, https://doi.org/10.1039/B911316A.

[13] M. Bonta, H. Lohninger, M. Marchetti-Deschmann, A. Limbeck, Application of gold thin-films for internal standardization in LA-ICP-MS imaging experiments, Analyst 139 (6) (2014) 1521–1531, https://doi.org/10.1039/C3AN01511D.

[14] J.S. Becker, C. Pickhardt, H.-J. Dietze, Determination of trace elements in high-purity platinum by laser ablation inductively coupled plasma mass spectrometry using solution calibration, J. Anal. At. Spectrom 16 (6) (2001) 603–606, https://doi.org/10.1039/B008519G.

[15] V.L. Dressler, D. Pozebon, M.F. Mesko, A. Matusch, U. Kumtabtim, B. Wu, J. Sabine Becker, Biomonitoring of essential and toxic metals in single hair using on-line solution-based calibration in laser ablation inductively coupled plasma mass spectrometry, Talanta 82 (5) (2010) 1770–1777, https://doi.org/10.1016/j.talanta.2010.07.065.

[16] S.F. Boulyga, C. Pickhardt, J.S. Becker, New approach of solution-based calibration in laser ablation inductively coupled plasma mass spectrometry of trace elements in metals and reduction of fractionation effects, At. Spectrosc 25 (2004) 53–63, https://doi.org/10.46770/AS.2004.02.001.

[17] A. Kindness, C.N. Sekaran, J.r. Feldmann, Two-Dimensional mapping of copper and zinc in liver sections by laser ablation–inductively coupled plasma mass spectrometry, Clin. Chem 49 (11) (2003) 1916–1923, https://doi.org/10.1373/clinchem.2003.022046.

[18] J. Koelmel, D. Amarasiriwardena, Imaging of metal bioaccumulation in Hay-scented fern (Dennstaedtia punctilobula) rhizomes growing on contaminated soils by laser ablation ICP-MS, Environ. Pollut. 168 (2012) 62–70, https://doi.org/10.1016/j.envpol.2012.03.035.

[19] D.A. Frick, C. Giesen, T. Hemmerle, B. Bodenmiller, D. Günther, An internal standardisation strategy for quantitative immunoassay tissue imaging using laser ablation inductively coupled plasma mass spectrometry, J. Anal. At. Spectrom 30 (1) (2015) 254–259, https://doi.org/10.1039/C4JA00293H.

[20] S.J.M. Van Malderen, T. Van Acker, B. Laforce, M. De Bruyne, R. de Rycke, T. Asaoka, L. Vincze, F. Vanhaecke, Three-dimensional reconstruction of the distribution of elemental tags in single cells using laser ablation ICP-mass spectrometry via registration approaches, Anal. Bioanal. Chem. 411 (19) (2019) 4849–4859, https://doi.org/10.1007/s00216-019-01677-6.

[21] J.T. van Elteren, N.H. Tennent, V.S. Šelih, Multi-element quantification of ancient/historic glasses by laser ablation inductively coupled plasma mass spectrometry using sum normalization calibration, Anal. Chim. Acta 644 (1–2) (2009) 1–9, https://doi.org/10.1016/j.aca.2009.04.025.

[22] Y. Liu, Z. Hu, S. Gao, D. Günther, J. Xu, C. Gao, H. Chen, In situ analysis of major and trace elements of anhydrous minerals by LA-ICP-MS without applying an internal standard, Chem. Geol. 257 (1–2) (2008) 34–43, https://doi.org/10.1016/j.chemgeo.2008.08.004.

[23] J.T. van Elteren, V.S. Šelih, M. Šala, Insights into the selection of 2D LA-ICP-MS (multi)elemental mapping conditions, J. Anal. At. Spectrom 34 (9) (2019) 1919–1931, https://doi.org/10.1039/c9ja00166b.

[24] M. Šala, V.S. Šelih, C.C. Stremtan, T. Tămaş, J.T. van Elteren, Implications of laser shot dosage on image quality in LA-ICP-QMS imaging, J. Anal. At. Spectrom 36 (1) (2021) 75–79, https://doi.org/10.1039/d0ja00381f.

[25] J.T. van Elteren, V.S. Šelih, M. Šala, S.J.M. Van Malderen, F. Vanhaecke, Imaging artifacts in continuous scanning 2D LA-ICPMS imaging due to nonsynchronization issues, Anal. Chem 90 (4) (2018) 2896–2901, https://doi.org/10.1021/acs.analchem.7b05134.

[26] A. Fluegel, Global model for calculating room-temperature glass density from the composition, J. Anal. At. Spectrom 90 (8) (2007) 2622–2625, https://doi.org/10.1111/j.1551-2916.2007.01751.x.

[27] D.C. Giancoli, Physics: principles with applications, Pearson (2014).

[28] J.T. van Elteren, D. Metarapi, K. Mervič, M. Šala, Exploring the benefits of ablation grid adaptation in 2D/3D laser ablation inductively coupled plasma mass

spectrometry mapping through geometrical modeling, Anal. Chem (2023), https://doi.org/10.1021/acs.analchem.3c00774.

Chapter 4

Conclusions

This dissertation contributes to science by deepening the fundamentals of LA-ICP-MS analysis and developing a new, non-matrix-matched, volume-based calibration approach. This enables quantitative analysis for a larger number of samples as it is not dependent on the availability of matrix-matched standards. While many calibration methods for LA-ICP-MS analysis have been developed over the years, most of them still rely heavily on matrix-matched standards and a homogeneously distributed internal standard to obtain accurate quantitative results. However, finding a suitable matrix-matched standard and an internal standard for signal normalization is an extremely difficult task for many sample types, especially those with more complex matrices or heterogeneous inter-sample composition. Therefore, the main objective of this work was to develop a volume-based calibration approach to improve the quantitative capabilities of LA-ICP-MS. The aim of this thesis was summarized in five hypotheses, which were addressed in the four manuscripts presented.

The first hypothesis states that the different operating parameters of the LA-ICP-MS, especially the energy density (e.g. fluence), have a significant impact on the accuracy and signal-to-noise ratio and thus on the precision of the results obtained. This was addressed in Manuscript 1, where the effects of beam size, energy density and aerosol transport on quantification in single-pulse LA-ICP-MS analysis were investigated by analyzing signal intensity, noise characteristics, ablated volumes, *etc.* The effects were investigated for different matrices (gelatin standards, NIST SRM 612 glass standard), concentrations (10-1000 $\mu g\ g^{-1}$) and different elements (As, Gd, La, Ni, Te and Zn). The work has shown that the use of larger beam sizes and higher energy densities, well above the ablation threshold of the material, can indeed lead to various problems. These include a reduction in the ratio of signal to ablated volume, higher noise and relative standard deviations (RSDs) and the occurrence of double peaks in the single pulse response mode. The results of the current study are consistent with previously published research indicating that higher fluences tend to produce larger particles, while excessively large beam sizes produce an abundance of aerosol particles. This can lead to overloading and therefore reduced transport efficiency from the ablation cell to the inductively coupled plasma (ICP) as well as suboptimal atomization and/or ionization of the elements present in the large particles, resulting in partial signal loss. Therefore, these results confirm the first hypothesis that the selection of optimal parameters for the analyzed sample can significantly improve the accuracy and precision of the results obtained by LA-ICP-MS analysis and is in fact paramount for accurate work.

In this context, **the second hypothesis** assumes that the use of energy densities well above the ablation thresholds of carbon-based matrices leads not only to the formation of larger particles, but also to the formation of a gaseous and a particulate phase for certain

elements causing double peaks. The double peak phenomenon was studied Manuscript 1 and then in further detail in Appendix A.1 in collaboration with the Atomic and Mass Spectrometry Research Group of the Department of Chemistry at Ghent University. The influence of different parameters was assessed by studying single pulse response profiles for a large collection of elements obtained upon ablation of gelatin. During the experiments, bimodal peaks were observed for certain elements, indicating the formation of two distinct phases. This was further investigated using a cryotrap to remove the gas phase and a filter to remove the particle phase. The results support the second hypothesis and confirm that for certain elements (such as C, Zn, As, Se, Cd, Te and I) the use of higher fluences leads to the formation of both a gaseous and a particulate phase, which can be seen as two peaks in the SPR profiles. The double peaks are the result of different transport behavior of the phases. Furthermore, the results indicate that the laser wavelength also has an influence on the formation of the gaseous phase. During ablation with the 213 nm laser, either a similar or a higher amount of gaseous phase was observed compared to the 193 nm laser. In addition, elements that appeared completely in the particulate phase when ablated with a lower wavelength (193 nm) are partially converted to gas when 213 nm is used.

The third hypothesis is aimed at non-matrix matched calibration, which has not been investigated on the basis of the literature review described in Manuscript 2. It assumes that calibration is possible in cases where standards and samples do not have the same matrix properties by taking into account the ablated volume/mass and using the optimal operational parameters. This is discussed in the first part of Manuscript 3, where the effectiveness of the ablation volume normalization technique for LA-ICP-MS analysis was evaluated. As previously mentioned, laser fluence affects both the amount of material ablated and the particle size distribution within the ablated aerosol, which in turn affects particle transfer and ionization dynamics and efficiency in the ICP. To investigate whether the ablated volume normalization approach combined with the use of the correct laser fluence allows for non-matrix-matched calibration, a series of experiments were performed using custom-made multi-element gelatin standards (ranging from 10 to 250 μg g^{-1}) at different laser fluences (0.5, 2.0, 4.0 and 6.0 J cm^{-2}) to analyze NIST 610, which was ablated at a fixed laser fluence of 3.6 J cm^{-2}. Nine experimental element concentration values obtained by treating NIST 610 glass as a sample were compared with reference concentration values. The concentrations obtained from the calibration with the lowest fluence (0.5 J cm^{-2}) agreed well with the reference values and deviated by less than 10 %. However, higher fluence values, in particular 4.0 and 6.0 J cm^{-2}, gave results that deviated significantly from the reference values, with deviations of about 20% for 4.0 J cm^{-2} and over 40% for 6.0 J cm^{-2}. This again underlines the importance of using appropriate fluence and confirms the third hypothesis by successfully calibrating glass samples using gelatin standards as a calibrant. In Manuscript 3, non-matrix-matched calibration for LA-ICP-MS bulk analysis is further investigated by cross-calibrating different materials (*e.g.* glass, zircon, carbonates, plants, proteins, *etc.*) to test **the fourth hypothesis**. The ablation volume normalization approach, which combines LA-ICP-MS and 3D profilometry, is based on normalizing the signal intensity to the ablated volume and thus corrects for differences in ablation between different matrices. The approach was tested by cross-calibrating different material types, including glass (NIST SRM 610, NIST SRM 612, NIST SRM 614, CMG-B, DLH-8), carbonates (JCp-1, JCt-1), plant sample (NIST SRM 1547), zircon (Plešovice) and proteinaceous substances (gelatin). The measured concentrations consistently matched the certified values for all materials, demonstrating the effectiveness of using calibration standards for materials with clearly defined elemental compositions and thus confirming the fourth hypothesis. Gelatin and glass in particular showed remarkable compatibility, which is probably due to the fact that they are the best defined and have good ablation. In addition, multi-point calibration is possible, whereas only single-

point calibration is possible with other standards. This makes gelatin and NIST SRM 61X glasses the most versatile and useful standards. The deviations in elemental concentration measurements remained mostly below 10 %, except in cases with extremely low concentrations.

Finally, the developed ablation-volume normalization approach was applied to quantification in LA-ICP-MS mapping to test the last, **fifth hypothesis**, which assumes that not using a non-matrix-matched volume-aided calibration leads to inaccuracies unless the matrix of the sample and the standard match perfectly. This is evaluated in Manuscript 4, where the differences in the ablation rate of a decorative glass (Murrina) and the calibration standards (NIST SRM 610 and 612) when measuring major, minor and trace elements were investigated and then corrected using the ablated volume per pixel. In general, quantitative 2D laser ablation mapping analysis requires an appropriate matrix-matched standard as well as a homogeneously distributed internal standard to minimize element fractionation issues, correct for instrumental drift, and account for differences in ablated mass. However, as these requirements are often not met, the volume correction calibration approach was tested for the multi-element quantification of decorative glass. The surface morphology data revealed discrepancies in ablation rate characteristics within the Murrina sample and between the decorative glass sample and the CRM glass standards. The white region of Murrina had a larger ablated volume and higher density than its transparent region and the NIST-SRM glass standards, resulting in higher signals due to a greater amount of ablated material being measured by the ICP-MS. This resulted in significantly inaccurate determination of elemental concentrations in 2D LA-ICP-MS maps with conventional calibration compared to the elemental concentrations obtained with the volume-corrected approach. The effectiveness of the volume-based calibration method was further verified by comparing the concentrations of eight elements in different sections of the Murrina using LA-ICP-MS with sum normalization calibration and SEM-EDXS analysis. The eight elements were selected based on the possibility of detecting them by SEM-EDXS analysis. The average concentrations derived from the volume-based calibration method agree well with those of the LA-ICP-MS sum normalization and the SEM-EDXS data, confirming the last hypothesis.

In summary, this dissertation makes a significant contribution to the field of LA-ICP-MS analysis by improving our understanding of the fundamental principles and introducing a novel volume-based calibration approach that does not rely on matrix-matched standards. By bypassing the need for such standards, this innovative method facilitates the quantitative analysis of a wider range of samples and improving the versatility and applicability of LA-ICP-MS in different research contexts. Despite the variety of calibration methods that have been developed over the years, most still rely on matrix-matched standards and internal standardization, which is challenging for many sample types with complex matrices. However, the volume-based calibration approach developed in this work addresses this limitation, as demonstrated by a series of hypotheses tested in several manuscripts. From evaluating the impact of operating parameters on precision, to investigating the formation of double peaks, to validating calibration methods that are not adapted to the matrix, each hypothesis contributed to the refinement and validation of the proposed approach. Overall, the results highlight the potential of the volume-based calibration method to significantly improve the accuracy and reliability of LA-ICP-MS analysis and pave the way for wider adoption and application in various research fields.

Appendices

A.1 Evaluation of Two-Phase Sample Transport upon Ablation of Gelatin as a Proxy for Soft Biological Matrices Using Nanosecond Laser Ablation – Inductively Coupled Plasma – Mass Spectrometry

Published: Van Helden T., Mervič K., Nemet I., van Elteren J.T., Vanhaecke F., Rončević S., Šala M., Van Acker T., (2024). Analytica Chimica Acta, 1287, 342089, doi: 10.1016/j.aca.2023.342089.

Based on the conclusions of Manuscript 1 and additional papers reporting on formation of double peaks upon ablation of carbon-based materials this study aims to improve the understanding of the matter of double peaks. In several recent studies double-peak formation has been observed for certain elements especially when ablating biological samples, however this phenomenon has not been thoroughly examined. The working theory was that some elements form particulate and gaseous phase upon ablation, showcasing as double peaks. This is concerning for two reasons. Firstly, the two phases exhibit different transport characteristics, which can lead to smearing in elemental maps. Additionally, particulate and gaseous phase might be ionized in the ICP differently, and thus affecting the accuracy of quantification.

Generally, upon ablation analytes are primarily transported in particulate form. However, this work demonstrates that during gelatin ablation a notable portion of certain elements is partially transported in a gaseous phase. This occurs even at low laser fluences, but the phenomenon is more pronounced with application of higher laser fluences. Using time-of-flight mass spectrometer, which enables simultaneous detection of the whole mass range, behavior of elements was observed, showcasing that this phenomenon is very element dependent. Therefore, using a 193nm laser the ratio of signal intensity transported in gaseous phase to the signal intensity, ranging from 0 % for sodium to 95 % for carbon. Additionally, the experiments were also conducted with 213 nm to see if the wavelength also affects the formation of gaseous phase. Upon ablation with 213 nm laser all elements exhibit either similar (*e.g.* C, Cd) or increased (*e.g.* Zn, Te) gas formation compared to a 193 nm laser. Furthermore, some elements (*e.g.* Pb) which occur mainly in particulate form with 193 nm laser, also exhibit formation of gas phase with 213 nm laser. This could possibly be due to thermal effects induced by the photon beam. As explained above, at 193 nm only a small part of the energy is converted into heat, whereas at 213 nm significantly more energy is converted into heat.

In this study, the underexamined phenomena of two-phase sample transport during LA-ICP-MS ablation of biological matrices with nm laser is thoroughly investigated. The work demonstrates that certain elements can undergo partial conversion into gaseous phase

under specific conditions, potentially causing smearing effects and lower accuracy of quantitative results. Therefore, when analyzing biological samples, element-specific peak profiles should be assessed in advance and, if necessary, data acquisition should be slowed down and instrument settings adjusted.

A.2 Exploring the Benefits of Ablation Grid Adaptation in 2D/3D Laser Ablation Inductively Coupled Plasma Mass Spectrometry Mapping Through Geometrical Modeling

Published: van Elteren J.T., Metarapi D., Mervič K., Šala M., (2023). Analytical Chemistry, 95(26), 9863–9871, doi: 10.1021/acs.analchem.3c00774.

During my PhD, I also co-authored a paper published in the journal Analytical Chemistry, which investigated the potential advantages of modifying the ablation grid in two-dimensional (2D) and three-dimensional (3D) laser ablation with inductively coupled plasma mass spectrometry (LA-ICP-MS) in single pulse mapping mode. The main objectives of the paper were to smooth the surface after ablation to facilitate layer-by-layer sampling, increase the precision of surface sampling for elemental distribution, improve image quality, and enable control of depth-based sampling. Since such a laser ablation stage is currently not available, a computational approach with geometric modeling was used to model its features. The approach is based on the compilation of experimentally derived round and square 3D crater profiles on variable hexagonal or orthogonal ablation grids. The computational approach optimizes the ablation grids to achieve minimum surface roughness as a function of average ablation depth, and consequently stimulates the post-ablation surface and corresponding image quality. The study has shown that reducing the ablation grid size in single-pulse LA-ICP-MS mapping improves post-ablation surface smoothness, spatial resolution and control over the depth of the ablation layer. Precise adjustment of the ablation grid and control of the 2D overlap of ablation points enables regulated ablation depth while maintaining surface smoothness. For optimal LA-ICP-MS mapping, symmetric contraction at a moderate level is recommended to minimize depth-related distribution discrepancies and reduce the risk of blurring. In addition, an online application (https://laICP-MS-apps.ki.si/webapps/home/) has been released that allows users to virtually experiment with the contraction/expansion of orthogonal and hexagonal ablation grids for generic 3D supergaussian laser crater profiles. For the future, it is crucial to emphasize that practical LA-ICP-MS mapping with contracted orthogonal and hexagonal ablation grids raises concerns about stage inaccuracies, especially for hexagonal mapping. The next step will involve the development of piezoelectric stages arranged in both orthogonal and hexagonal configurations so that the advantages of ablation grid adaptations can be fully realized.

References

[1] A. L. Gray, "Solid sample introduction by laser ablation for inductively coupled plasma source mass spectrometry," *Analyst,* 10.1039/AN9851000551 vol. 110, no. 5, pp. 551-556, 1985, doi: 10.1039/AN9851000551.

[2] H. P. L. S. E. Jackson, G. R. Dunning, B. J. Freyer, "The application of laser-ablation microprobe; inductively coupled plasma-mass spectrometry (LAM-ICP-MS) to in situ trace-element determinations in minerals," *The Canadian Mineralogist,* vol. 30, no. 4, pp. 1049-1064, 1992.

[3] B. J. Fryer, S. E. Jackson, and H. P. Longerich, "The application of laser ablation microprobe-inductively coupled plasma-mass spectrometry (LAM-ICP-MS) to in situ (U) • Pb geochronology," *Chemical Geology,* vol. 109, no. 1, pp. 1-8, 1993/10/25/ 1993, doi: https://doi.org/10.1016/0009-2541(93)90058-Q.

[4] D. Cardinal, L. Y. Alleman, J. De Jong, K. Ziegler, and L. André, "Isotopic composition of silicon measured by multicollector plasma source mass spectrometry in dry plasma mode," *Journal of Analytical Atomic Spectrometry,* Article vol. 18, no. 3, pp. 213-218, 2003, doi: 10.1039/b210109b.

[5] J. Karasinski, E. Bulska, M. Wojciechowski, L. Halicz, and A. A. Krata, "High precision direct analysis of magnesium isotope ratio by ion chromatography/multicollector-ICPMS using wet and dry plasma conditions," *Talanta,* vol. 165, pp. 64-68, 2017/04/01/ 2017, doi: https://doi.org/10.1016/j.talanta.2016.12.033.

[6] T. Van Acker *et al.*, "Analytical figures of merit of a low-dispersion aerosol transport system for high-throughput LA-ICP-MS analysis," *Journal of Analytical Atomic Spectrometry,* 10.1039/D1JA00110H vol. 36, no. 6, pp. 1201-1209, 2021, doi: 10.1039/D1JA00110H.

[7] S. J. M. Van Malderen, J. T. van Elteren, and F. Vanhaecke, "Development of a fast laser ablation-inductively coupled plasma-mass spectrometry cell for sub-μm scanning of layered materials," *Journal of Analytical Atomic Spectrometry,* vol. 30, no. 1, pp. 119-125, 2015, doi: 10.1039/c4ja00137k.

[8] A. Gundlach-Graham *et al.*, "High-speed, high-resolution, multielemental laser ablation-inductively coupled plasma-time-of-flight mass spectrometry imaging: part I. Instrumentation and two-dimensional imaging of geological samples," *Anal Chem,* vol. 87, no. 16, pp. 8250-8, Aug 18 2015, doi: 10.1021/acs.analchem.5b01196.

[9] G. Craig, A. J. Managh, C. Stremtan, N. S. Lloyd, and M. S. A. Horstwood, "Doubling Sensitivity in Multicollector ICPMS Using High-Efficiency, Rapid

Response Laser Ablation Technology," *Analytical Chemistry,* vol. 90, no. 19, pp. 11564-11571, 2018/10/02 2018, doi: 10.1021/acs.analchem.8b02896.

[10] J. T. van Elteren, V. S. Šelih, and M. Šala, "Insights into the selection of 2D LA-ICP-MS (multi)elemental mapping conditions," *J. Anal. At. Spectrom,* vol. 34, no. 9, pp. 1919-1931, 2019, doi: https://doi.org/10.1039/c9ja00166b.

[11] J. T. van Elteren, D. Metarapi, M. Šala, V. S. Šelih, and C. C. Stremtan, "Fine-tuning of LA-ICP-QMS conditions for elemental mapping," *Journal of Analytical Atomic Spectrometry,* vol. 35, no. 11, pp. 2494-2497, 2020, doi: 10.1039/d0ja00322k.

[12] M. Šala, V. S. Šelih, C. C. Stremtan, T. Tămaş, and J. T. van Elteren, "Implications of laser shot dosage on image quality in LA-ICP-QMS imaging," *J. Anal. At. Spectrom,* vol. 36, no. 1, pp. 75-79, 2021, doi: https://doi.org/10.1039/d0ja00381f.

[13] O. B. Bauer *et al.*, "LA-ICP-TOF-MS for rapid, all-elemental and quantitative bioimaging, isotopic analysis and the investigation of plasma processes," *J. Anal. At. Spectrom.,* 10.1039/C8JA00288F vol. 34, no. 4, pp. 694-701, 2019, doi: 10.1039/C8JA00288F.

[14] M. Balcerzak, "An Overview of Analytical Applications of Time of Flight-Mass Spectrometric (TOF-MS) Analyzers and an Inductively Coupled Plasma-TOF-MS Technique," *Anal. Sci.,* vol. 19, no. 7, pp. 979-989, 2003, doi: 10.2116/analsci.19.979.

[15] M. Vázquez Peláez, J. M. Costa-Fernández, and A. Sanz-Medel, "Critical comparison between quadrupole and time-of-flight inductively coupled plasma mass spectrometers for isotope ratio measurements in elemental speciation," *J. Anal. Atom. Spectrom.,* 10.1039/B202748H vol. 17, no. 8, pp. 950-957, 2002, doi: 10.1039/B202748H.

[16] M. Burger, G. Schwarz, A. Gundlach-Graham, D. Käser, B. Hattendorf, and D. Günther, "Capabilities of laser ablation inductively coupled plasma time-of-flight mass spectrometry," *J. Anal. Atom. Spectrom.,* 10.1039/C7JA00236J vol. 32, no. 10, pp. 1946-1959, 2017, doi: 10.1039/C7JA00236J.

[17] N. Miliszkiewicz, S. Walas, and A. Tobiasz, "Current approaches to calibration of LA-ICP-MS analysis," *Journal of Analytical Atomic Spectrometry,* 10.1039/C4JA00325J vol. 30, no. 2, pp. 327-338, 2015, doi: 10.1039/C4JA00325J.

[18] M. Guillong and D. Günther, "Effect of particle size distribution on ICP-induced elemental fractionation in laser ablation-inductively coupled plasma-mass spectrometry," *Journal of Analytical Atomic Spectrometry,* 10.1039/B202988J vol. 17, no. 8, pp. 831-837, 2002, doi: 10.1039/B202988J.

[19] J. Koch and D. Günther, "Review of the State-of-the-Art of Laser Ablation Inductively Coupled Plasma Mass Spectrometry," *Applied spectroscopy,* vol. 65, pp. 155-62, 05/01 2011, doi: 10.1366/11-06255.

[20] B. Rusk, "Laser Ablation ICP-MS in the Earth Sciences: Current Practices and Outstanding Issues.: Paul Sylvestor, Editor. Pp. 356. Mineralogical Association of Canada. Short Course Volume 40. 2008. ISBN: 9-0-921294-49-8. Price US$55.00 (nonmembers), US$44.00 (members)," *Economic Geology,* vol. 104, no. 4, pp. 601-602, 2009, doi: 10.2113/gsecongeo.104.4.601.

[21] V. Margetic, A. Pakulev, A. Stockhaus, M. Bolshov, K. Niemax, and R. Hergenröder, "A comparison of nanosecond and femtosecond laser-induced plasma spectroscopy of brass samples," *Spectrochimica Acta Part B: Atomic Spectroscopy,* vol. 55, no. 11, pp. 1771-1785, 2000/11/01/ 2000, doi: https://doi.org/10.1016/S0584-8547(00)00275-5.

[22] M. Guillong, I. Horn, and D. Günther, "A comparison of 266 nm, 213 nm and 193 nm produced from a single solid state Nd:YAG laser for laser ablation ICP-MS," *Journal of Analytical Atomic Spectrometry,* 10.1039/B305434A vol. 18, no. 10, pp. 1224-1230, 2003, doi: 10.1039/B305434A.

[23] I. Horn, D. Günther, and M. Guillong, "Evaluation and design of a solid-state 193 nm OPO-Nd:YAG laser ablation system," *Spectrochimica Acta Part B: Atomic Spectroscopy,* vol. 58, no. 10, pp. 1837-1846, 2003/10/17/ 2003, doi: https://doi.org/10.1016/S0584-8547(03)00163-0.

[24] C. C. Garcia, M. Wälle, H. Lindner, J. Koch, K. Niemax, and D. Günther, "Femtosecond laser ablation inductively coupled plasma mass spectrometry: Transport efficiencies of aerosols released under argon atmosphere and the importance of the focus position," *Spectrochimica Acta Part B: Atomic Spectroscopy,* vol. 63, no. 2, pp. 271-276, 2008/02/01/ 2008, doi: https://doi.org/10.1016/j.sab.2007.11.017.

[25] R. Hergenröder, "A model for the generation of small particles in laser ablation ICP-MS," *Journal of Analytical Atomic Spectrometry,* 10.1039/B604453K vol. 21, no. 10, pp. 1016-1026, 2006, doi: 10.1039/B604453K.

[26] D. Bleiner and A. Bogaerts, "Computer simulations of sample chambers for laser ablation-inductively coupled plasma spectrometry," *Spectrochimica Acta Part B: Atomic Spectroscopy,* vol. 62, no. 2, pp. 155-168, 2007/02/01/ 2007, doi: https://doi.org/10.1016/j.sab.2007.02.010.

[27] S. E. Jackson, "Calibration strategies for elemental analysis by LA-ICP-MS," in *Laser Ablation–ICP–MS in the Earth Sciences - current practices and outstanding issues*, vol. 40, P. Sylvester Ed., 2008.

[28] J. Qin, F. Huang, S. Zhong, D. Wang, and R. Seltmann, "Unraveling evolution histories of large hydrothermal systems via garnet U-Pb dating, sulfide trace element and isotopic analyses: A case study of Shuikoushan polymetallic ore field, South China," *Ore Geology Reviews,* vol. 149, p. 105063, 2022/10/01/ 2022, doi: https://doi.org/10.1016/j.oregeorev.2022.105063.

[29] X.-j. Zhao *et al.*, "LA-ICP-MS zircon U-Pb dating of tuffites in the Sachakou Pb-Zn mining area, Karakorum, Xinjiang and its establishment of Early Triassic strata," *China Geology,* vol. 7, no. 1, pp. 150-152, 2024/01/01/ 2024, doi: https://doi.org/10.31035/cg2023048.

[30] I. Bobos, H. Stein, X.-D. Deng, M. Sudo, and F. Noronha, "U–Pb LA-ICP-MS and Re–Os dating of wolframite and molybdenite: Constraints on multiple mineralization and cooling history (40Ar/39Ar) for the magmatic–hydrothermal system at Borralha, northern Portugal," *Ore Geology Reviews,* vol. 168, p. 106013, 2024/05/01/ 2024, doi: https://doi.org/10.1016/j.oregeorev.2024.106013.

[31] D. Chew, "Chapter 6 - U–Th–Pb phosphate geochronology by LA-ICP-MS," in *Methods and Applications of Geochronology*, J. G. Shellnutt, S. W. Denyszyn, and K. Suga Eds.: Elsevier, 2024, pp. 169-209.

[32] S. F. Durrant and N. I. Ward, "Recent biological and environmental applications of laser ablation inductively coupled plasma mass spectrometry (LA-ICP-MS)," *Journal of Analytical Atomic Spectrometry,* 10.1039/B502206A vol. 20, no. 9, pp. 821-829, 2005, doi: 10.1039/B502206A.

[33] I. Kroslakova and D. Günther, "Elemental fractionation in laser ablation-inductively coupled plasma-mass spectrometry: evidence for mass load induced matrix effects in the ICP during ablation of a silicate glass," *J. Anal. At. Spectrom,* 10.1039/B606522H vol. 22, no. 1, pp. 51-62, 2007, doi: https://doi.org/10.1039/B606522H.

[34] L. A. Runnalls and M. L. Coleman, "Record of natural and anthropogenic changes in reef environments (Barbados West Indies) using laser ablation ICP-MS and sclerochronology on coral cores," *Coral Reefs,* vol. 22, no. 4, pp. 416-426, 2003/12/01 2003, doi: 10.1007/s00338-003-0349-7.

[35] P. A. Hamer, G. P. Jenkins, and B. M. Gillanders, "Otolith chemistry of juvenile snapper Pagrus auratus in Victorian waters: natural chemical tags and their temporal variation," *Marine Ecology Progress Series,* vol. 263, pp. 261-273, 2003.

[36] K. H. Ek, G. M. Morrison, P. Lindberg, and S. Rauch, "Comparative Tissue Distribution of Metals in Birds in Sweden Using ICP-MS and Laser Ablation ICP-MS," *Archives of Environmental Contamination and Toxicology,* vol. 47, no. 2, pp. 259-269, 2004/08/01 2004, doi: 10.1007/s00244-004-3138-6.

[37] R. Idegawa, M. Ohata, N. Furuta, and K. Satake, "Analytical Chemistry represented by "super" and "ultra". Local analysis of trace elements and lead isotope ratios in bark and bark pockets by laser ablation/ICP-MS," *Bunseki Kagaku,* vol. 50, pp. 441-446, 06/01 2001, doi: 10.2116/bunsekikagaku.50.441.

[38] T. Punshon, B. P. Jackson, P. M. Bertsch, and J. Burger, "Mass loading of nickel and uranium on plant surfaces: application of laser ablation-ICP-MS," *Journal of Environmental Monitoring,* 10.1039/B310878C vol. 6, no. 2, pp. 153-159, 2004, doi: 10.1039/B310878C.

[39] T. Okuda *et al.*, "Daily concentrations of trace metals in aerosols in Beijing, China, determined by using inductively coupled plasma mass spectrometry equipped with laser ablation analysis, and source identification of aerosols," (in eng), no. 0048-9697 (Print).

[40] H. Reinhardt, M. Kriews, H. Miller, C. Lüdke, E. Hoffmann, and J. Skole, "Application of LA–ICP–MS in polar ice core studies," *Analytical and Bioanalytical Chemistry,* vol. 375, no. 8, pp. 1265-1275, 2003/04/01 2003, doi: 10.1007/s00216-003-1793-5.

[41] P. Bohleber, M. Roman, M. Šala, and C. Barbante, "Imaging the impurity distribution in glacier ice cores with LA-ICP-MS," *Journal of Analytical Atomic Spectrometry,* Article vol. 35, no. 10, pp. 2204-2212, 2020, doi: 10.1039/d0ja00170h.

[42] P. Bohleber *et al.*, "Quantitative Insights on Impurities in Ice Cores at the Micro-Scale From Calibrated LA-ICP-MS Imaging," *Geochemistry, Geophysics,*

Geosystems, Article vol. 25, no. 4, 2024, Art no. e2023GC011425, doi: 10.1029/2023GC011425.

[43] F. Alamilla, C. Galvez, M. Torre, and C. Garcia-Ruiz, "Applications of laser-ablation-inductively-coupled plasma-mass spectrometry in chemical analysis of forensic evidence," *TrAC, Trends in Analytical Chemistry,* vol. 42, pp. 1-34, 01/31 2013, doi: 10.1016/j.trac.2012.09.015.

[44] C. J. Scadding, R. J. Watling, and A. G. Thomas, "The potential of using laser ablation inductively coupled plasma time of flight mass spectrometry (LA-ICP-TOF-MS) in the forensic analysis of micro debris," *Talanta,* vol. 67, no. 2, pp. 414-424, 2005/08/15/ 2005, doi: https://doi.org/10.1016/j.talanta.2005.05.015.

[45] M. de Bruin-Hoegée, J. Schoorl, P. Zoon, M. J. van der Schans, D. Noort, and A. C. van Asten, "A novel standard for forensic elemental profiling of polymers by LA-ICP-TOF-MS," *Forensic Chemistry,* vol. 35, p. 100515, 2023/09/01/ 2023, doi: https://doi.org/10.1016/j.forc.2023.100515.

[46] P. Ramirez-Hereza, D. Ramos, J. Maroñas, S. A. Balanya, and J. Almirall, "Gaussianization of LA-ICP-MS features to improve calibration in forensic glass comparison," *Forensic Science International,* vol. 349, p. 111735, 2023/08/01/ 2023, doi: https://doi.org/10.1016/j.forsciint.2023.111735.

[47] Ž. Šmit *et al.*, "Analysis of medieval glass by X-ray spectrometric method," *Nuclear Instruments and Methods in Physics Research Section B: Beam Interactions with Materials and Atoms,* vol. 161-163, pp. 718-723, 03/01 2000, doi: 10.1016/S0168-583X(99)00947-7.

[48] I. De Raedt, K. Janssens, J. Veeckman, L. Vincze, B. Vekemans, and T. E. Jeffries, "Trace analysis for distinguishing between Venetian and façon-de-Venise glass vessels of the 16th and 17th century," *Journal of Analytical Atomic Spectrometry,* 10.1039/B102597J vol. 16, no. 9, pp. 1012-1017, 2001, doi: 10.1039/B102597J.

[49] R. J. Speakman and H. Neff, "Evaluation of Painted Pottery from the Mesa Verde Region Using Laser Ablation-Inductively Coupled Plasma-Mass Spectrometry (LA-ICP-MS)," *American Antiquity,* vol. 67, no. 1, pp. 137-144, 2002, doi: 10.2307/2694882.

[50] J. S. Becker and H.-J. Dietze, "State-of-the-art in inorganic mass spectrometry for analysis of high-purity materials," *International Journal of Mass Spectrometry,* vol. 228, no. 2, pp. 127-150, 2003/08/15/ 2003, doi: https://doi.org/10.1016/S1387-3806(03)00270-7.

[51] F. Kleiner, M. Decker, C. Rößler, H. Hilbig, and H.-M. Ludwig, "Combined LA-ICP-MS and SEM-EDX analyses for spatially resolved major, minor and trace element detection in cement clinker phases," *Cement and Concrete Research,* vol. 159, p. 106875, 2022/09/01/ 2022, doi: https://doi.org/10.1016/j.cemconres.2022.106875.

[52] R. Borges *et al.*, "Investigation of surface silver enrichment in ancient high silver alloys by PIXE, EDXRF, LA-ICP-MS and SEM-EDS," *Microchemical Journal,* vol. 131, pp. 103-111, 2017/03/01/ 2017, doi: https://doi.org/10.1016/j.microc.2016.12.002.

[53] S. J. Chingwaru, M. Tadie, and B. Von der Heyden, "Characterizing low-grade refractory gold ores using automated mineralogy coupled with LA ICP-MS," *Minerals Engineering,* vol. 210, p. 108674, 2024/05/01/ 2024, doi: https://doi.org/10.1016/j.mineng.2024.108674.

[54] P. Chen *et al.*, "Nanoplastics and nano-ZnO facilitate Cd accumulation in zebrafish larvae via a distinct pathway: Revelation by LA-ICP-MS imaging," *Chinese Chemical Letters,* p. 109908, 2024/04/18/ 2024, doi: https://doi.org/10.1016/j.cclet.2024.109908.

[55] O. Reifschneider *et al.*, "Revealing silver nanoparticle uptake by macrophages using SR-μXRF and LA-ICP-MS," *Chemical Research in Toxicology,* vol. 33, no. 5, pp. 1250-1255, 2020.

[56] G. Galbács, A. Kéri, A. Kohut, M. Veres, and Z. Geretovszky, "Nanoparticles in analytical laser and plasma spectroscopy–a review of recent developments in methodology and applications," *Journal of Analytical Atomic Spectrometry,* vol. 36, no. 9, pp. 1826-1872, 2021.

[57] I.-L. Hsiao *et al.*, "Quantification and visualization of cellular uptake of TiO 2 and Ag nanoparticles: comparison of different ICP-MS techniques," *Journal of nanobiotechnology,* vol. 14, pp. 1-13, 2016.

[58] S. Böhme, H.-J. Stärk, D. Kühnel, and T. Reemtsma, "Exploring LA-ICP-MS as a quantitative imaging technique to study nanoparticle uptake in Daphnia magna and zebrafish (Danio rerio) embryos," *Analytical and bioanalytical chemistry,* vol. 407, pp. 5477-5485, 2015.

[59] H. El Hadri, J. Gigault, S. Mounicou, B. Grassl, and S. Reynaud, "Trace element distribution in marine microplastics using laser ablation-ICP-MS," *Marine Pollution Bulletin,* vol. 160, p. 111716, 2020/11/01/ 2020, doi: https://doi.org/10.1016/j.marpolbul.2020.111716.

[60] P. Pořízka *et al.*, "Laser-based techniques: Novel tools for the identification and characterization of aged microplastics with developed biofilm," *Chemosphere,* vol. 313, p. 137373, 2023/02/01/ 2023, doi: https://doi.org/10.1016/j.chemosphere.2022.137373.

[61] R. Elseblani *et al.*, "Study of metal and organic contaminants transported by microplastics in the Lebanese coastal environment using ICP MS, GC-MS, and LC-MS," *Science of The Total Environment,* vol. 887, p. 164111, 2023/08/20/ 2023, doi: https://doi.org/10.1016/j.scitotenv.2023.164111.

[62] L. Brunnbauer, M. Jirku, C. D. Quarles, and A. Limbeck, "Capabilities of simultaneous 193 nm - LIBS/LA-ICP-MS imaging for microplastics characterization," *Talanta,* vol. 269, p. 125500, 2024/03/01/ 2024, doi: https://doi.org/10.1016/j.talanta.2023.125500.

[63] A. Limbeck, P. Galler, M. Bonta, G. Bauer, W. Nischkauer, and F. Vanhaecke, "Recent advances in quantitative LA-ICP-MS analysis: challenges and solutions in the life sciences and environmental chemistry," *Anal. Bioanal. Chem,* vol. 407, no. 22, pp. 6593-6617, 2015/09/01 2015, doi: https://doi.org/10.1007/s00216-015-8858-0.

[64] Q. Bian, C. C. Garcia, J. Koch, and K. Niemax, "Non-matrix matched calibration of major and minor concentrations of Zn and Cu in brass, aluminium and silicate glass using NIR femtosecond laser ablation inductively coupled plasma mass spectrometry," *Journal of Analytical Atomic Spectrometry,* 10.1039/B513690C vol. 21, no. 2, pp. 187-191, 2006, doi: 10.1039/B513690C.

[65] J. Pisonero, B. Fernández, and D. Günther, "Critical revision of GD-MS, LA-ICP-MS and SIMS as inorganic mass spectrometric techniques for direct solid analysis," *Journal of Analytical Atomic Spectrometry,* 10.1039/B904698D vol. 24, no. 9, pp. 1145-1160, 2009, doi: 10.1039/B904698D.

[66] C. C. Garcia, H. Lindner, and K. Niemax, "Laser ablation inductively coupled plasma mass spectrometry—current shortcomings, practical suggestions for improving performance, and experiments to guide future development," *Journal of Analytical Atomic Spectrometry,* 10.1039/B813124B vol. 24, no. 1, pp. 14-26, 2009, doi: 10.1039/B813124B.

[67] M. Ohata, H. Yasuda, Y. Namai, and N. Furuta, "Laser Ablation Inductively Coupled Plasma Mass Spectrometry (LA-ICP-MS): Comparison of Different Internal Standardization Methods Using Laser-induced Plasma (LIP) Emission and LA-ICP-MS Signals," *Analytical Sciences,* vol. 18, no. 10, pp. 1105-1110, 2002/10/01 2002, doi: 10.2116/analsci.18.1105.

[68] A. M. Leach and G. M. Hieftje, "Methods for shot-to-shot normalization in laser ablation with an inductively coupled plasma time-of-flight mass spectrometer," *Journal of Analytical Atomic Spectrometry,* 10.1039/B001968M vol. 15, no. 9, pp. 1121-1124, 2000, doi: 10.1039/B001968M.

[69] H. M. Pang, D. R. Wiederin, R. S. Houk, and E. S. Yeung, "High-repetition-rate laser ablation for elemental analysis in an inductively coupled plasma with acoustic wave normalization," *Analytical Chemistry,* vol. 63, no. 4, pp. 390-394, 1991/02/15 1991, doi: 10.1021/ac00004a017.

[70] H.-R. Kuhn and D. Günther, "A quantification strategy in laser ablation ICP-MS based on the transported aerosol particle volume determined by optical particle size measurement," *Journal of Analytical Atomic Spectrometry,* 10.1039/B607232A vol. 21, no. 11, pp. 1209-1213, 2006, doi: 10.1039/B607232A.

[71] E. Hoffmann, C. Lüdke, and H. Scholze, "Is laser-ablation-ICP-MS an alternative to solution analysis of solid samples?," *Fresenius' Journal of Analytical Chemistry,* vol. 359, no. 4, pp. 394-398, 1997/10/01 1997, doi: 10.1007/s002160050595.

[72] J.-H. Yuan *et al.*, "Investigation on Matrix Effects in Silicate Minerals by Laser Ablation-Inductively Coupled Plasma-Mass Spectrometry," *Chinese Journal of Analytical Chemistry,* vol. 39, no. 10, pp. 1582-1587, 2011/10/01/ 2011, doi: https://doi.org/10.1016/S1872-2040(10)60477-X.

[73] A. Raith, J. Godfrey, and R. C. Hutton, "Quantitation methods using Laser Ablation ICP-MS," *Fresenius' Journal of Analytical Chemistry,* vol. 354, no. 2, pp. 163-168, 1996/02/01 1996, doi: 10.1007/PL00012714.

[74] C. Austin *et al.*, "Factors affecting internal standard selection for quantitative elemental bio-imaging of soft tissues by LA-ICP-MS," *Journal of Analytical Atomic Spectrometry,* vol. 26, no. 7, 2011, doi: 10.1039/c0ja00267d.

[75] D. A. Frick and D. Günther, "Fundamental studies on the ablation behaviour of carbon in LA-ICP-MS with respect to the suitability as internal standard," *Journal of Analytical Atomic Spectrometry,* vol. 27, no. 8, 2012, doi: 10.1039/c2ja30072a.

[76] P. d. S. Moreau and M. A. Z. Arruda, "Direct analysis of tree rings using laser ablation-ICP-MS and quantitative evaluation of Zn and Cu using filter paper as a solid support for calibration," *Journal of Analytical Atomic Spectrometry,* 10.1039/D1JA00414J vol. 37, no. 4, pp. 795-804, 2022, doi: 10.1039/D1JA00414J.

[77] M. von Bremen-Kühne, H. Ahmadi, M. Sperling, U. Krämer, and U. Karst, "Elemental bioimaging of Zn and Cd in leaves of hyperaccumulator Arabidopsis halleri using laser ablation-inductively coupled plasma-mass spectrometry and referencing strategies," *Chemosphere,* vol. 305, p. 135267, 2022/10/01/ 2022, doi: https://doi.org/10.1016/j.chemosphere.2022.135267.

[78] J. Y. Kim, J. Park, J. Choi, and J. Kim, "Determination of Metal Concentration in Road-Side Trees from an Industrial Area Using Laser Ablation Inductively Coupled Plasma Mass Spectrometry," *Minerals,* vol. 10, no. 2, 2020, doi: 10.3390/min10020175.

[79] K. Chacón-Madrid and M. A. Zezzi Arruda, "Internal standard evaluation for bioimaging soybean leaves through laser ablation inductively coupled plasma mass spectrometry: a plant nanotechnology approach," *Journal of Analytical Atomic Spectrometry,* 10.1039/C8JA00254A vol. 33, no. 10, pp. 1720-1728, 2018, doi: 10.1039/C8JA00254A.

[80] J. A. Ko, N. Furuta, and H. B. Lim, "Quantitative mapping of elements in basil leaves (Ocimum basilicum) based on cesium concentration and growth period using laser ablation ICP-MS," *Chemosphere,* vol. 190, pp. 368-374, 2018/01/01/ 2018, doi: https://doi.org/10.1016/j.chemosphere.2017.10.003.

[81] D. Amarasiriwardena, M. Ahmed, and B. Arriaza, "Environmental arsenic exposure by ancient Andeans: Measurement of As in mummy hair using LA-ICP-MS," *Journal of Archaeological Science: Reports,* vol. 48, p. 103883, 2023/04/01/ 2023, doi: https://doi.org/10.1016/j.jasrep.2023.103883.

[82] Y.-N. Chan, J. T.-S. Lum, and K. S.-Y. Leung, "Development of a comprehensive method for hair and nail analysis using laser ablation-inductively coupled plasma-mass spectrometry," *Microchemical Journal,* vol. 188, p. 108503, 2023/05/01/ 2023, doi: https://doi.org/10.1016/j.microc.2023.108503.

[83] K. Rodiouchkina, I. Rodushkin, S. Goderis, and F. Vanhaecke, "Longitudinal isotope ratio variations in human hair and nails," *Science of The Total Environment,* vol. 808, p. 152059, 2022/02/20/ 2022, doi: https://doi.org/10.1016/j.scitotenv.2021.152059.

[84] P. Charapata *et al.*, "Whiskers provide time-series of toxic and essential trace elements, Se:Hg molar ratios, and stable isotope values of an apex Antarctic predator, the leopard seal," *Science of The Total Environment,* vol. 854, p. 158651, 2023/01/01/ 2023, doi: https://doi.org/10.1016/j.scitotenv.2022.158651.

[85] M. Arora *et al.*, "Fetal and postnatal metal dysregulation in autism," *Nature Communications,* vol. 8, no. 1, p. 15493, 2017/06/01 2017, doi: 10.1038/ncomms15493.

[86] A. L. Wright, E. T. Earley, C. Austin, and M. Arora, "Equine odontoclastic tooth resorption and hypercementosis (EOTRH): microspatial distribution of trace elements in hypercementosis-affected and unaffected hard dental tissues," *Scientific Reports,* vol. 13, no. 1, p. 5048, 2023/03/28 2023, doi: 10.1038/s41598-023-32016-6.

[87] A.-F. Maurer *et al.*, "Testing LA-ICP-MS analysis of archaeological bones with different diagenetic histories for paleodiet prospect," *Palaeogeography, Palaeoclimatology, Palaeoecology,* vol. 534, p. 109287, 2019/11/15/ 2019, doi: https://doi.org/10.1016/j.palaeo.2019.109287.

[88] A. Hanć, A. Olszewska, and D. Barałkiewicz, "Quantitative analysis of elements migration in human teeth with and without filling using LA-ICP-MS," *Microchemical Journal,* vol. 110, pp. 61-69, 2013/09/01/ 2013, doi: https://doi.org/10.1016/j.microc.2013.02.006.

[89] D. Günther, A. v. Quadt, R. Wirz, H. Cousin, and V. J. Dietrich, "Elemental Analyses Using Laser Ablation-Inductively Coupled Plasma-Mass Spectrometry (LA-ICP-MS) of Geological Samples Fused with Li2B4O7 and Calibrated Without Matrix-Matched Standards," *Microchimica Acta,* vol. 136, no. 3, pp. 101-107, 2001/06/01 2001, doi: 10.1007/s006040170038.

[90] V. R. Bellotto and N. Miekeley, "Improvements in calibration procedures for the quantitative determination of trace elements in carbonate material (mussel shells) by laser ablation ICP-MS," *Fresenius' Journal of Analytical Chemistry,* vol. 367, no. 7, pp. 635-640, 2000/07/01 2000, doi: 10.1007/s002160000421.

[91] C. P. Eze *et al.*, "Elemental composition of fly ash: a comparative study using nuclear and related analytical techniques/SkŁad Pierwiastkowy PopioŁÓw Lotnych: Studium Przypadku Z Wykorzystaniem Metod Nuklearnych I Analitycznych," *Chemistry-Didactics-Ecology-Metrology,* vol. 18, no. 1-2, pp. 19-29, 2013.

[92] M. Bonta, H. Lohninger, M. Marchetti-Deschmann, and A. Limbeck, "Application of gold thin-films for internal standardization in LA-ICP-MS imaging experiments," *Analyst,* 10.1039/C3AN01511D vol. 139, no. 6, pp. 1521-1531, 2014, doi: https://doi.org/10.1039/C3AN01511D.

[93] C. Austin, D. Hare, T. Rawling, A. M. McDonagh, and P. Doble, "Quantification method for elemental bio-imaging by LA-ICP-MS using metal spiked PMMA films," *J. Anal. At. Spectrom,* 10.1039/B911316A vol. 25, no. 5, pp. 722-725, 2010, doi: https://doi.org/10.1039/B911316A.

[94] F. Li *et al.*, "Direct multi-elemental analysis of whole blood samples by LA-ICP-MS employing a cryogenic ablation cell," *Journal of Analytical Atomic Spectrometry,* 10.1039/D2JA00282E vol. 38, no. 1, pp. 90-96, 2023, doi: 10.1039/D2JA00282E.

[95] N. Grijalba, A. Legrand, V. Holler, and C. Bouvier-Capely, "A novel calibration strategy based on internal standard–spiked gelatine for quantitative bio-imaging by LA-ICP-MS: application to renal localization and quantification of uranium," *Analytical and Bioanalytical Chemistry,* vol. 412, no. 13, pp. 3113-3122, 2020/05/01 2020, doi: 10.1007/s00216-020-02561-4.

[96] S. Hoesl *et al.*, "Internal standardization of LA-ICP-MS immuno imaging via printing of universal metal spiked inks onto tissue sections," *Journal of Analytical Atomic Spectrometry,* vol. 31, no. 3, pp. 801-808, 2016, doi: 10.1039/c5ja00409h.

[97] I. Moraleja *et al.*, "Printing metal-spiked inks for LA-ICP-MS bioimaging internal standardization: comparison of the different nephrotoxic behavior of cisplatin, carboplatin, and oxaliplatin," *Anal. Bioanal. Chem.,* vol. 408, no. 9, pp. 2309-2318, 2016/03/01 2016, doi: 10.1007/s00216-016-9327-0.

[98] B. Neumann, S. Hosl, K. Schwab, F. Theuring, and N. Jakubowski, "Multiplex LA-ICP-MS bio-imaging of brain tissue of a parkinsonian mouse model stained with metal-coded affinity-tagged antibodies and coated with indium-spiked commercial inks as internal standards," *J Neurosci Methods,* vol. 334, p. 108591, Jan 8 2020, doi: 10.1016/j.jneumeth.2020.108591.

[99] C. Giesen *et al.*, "Iodine as an elemental marker for imaging of single cells and tissue sections by laser ablation inductively coupled plasma mass spectrometry," *J. Anal. At. Spectrom.,* 10.1039/C1JA10227C vol. 26, no. 11, pp. 2160-2165, 2011, doi: 10.1039/C1JA10227C.

[100] L. Chen, Y. Liu, Z. Hu, S. Gao, K. Zong, and H. Chen, "Accurate determinations of fifty-four major and trace elements in carbonate by LA–ICP-MS using normalization strategy of bulk components as 100%," *Chemical Geology,* vol. 284, no. 3, pp. 283-295, 2011/05/24/ 2011, doi: https://doi.org/10.1016/j.chemgeo.2011.03.007.

[101] J. T. van Elteren, N. H. Tennent, and V. S. Šelih, "Multi-element quantification of ancient/historic glasses by laser ablation inductively coupled plasma mass spectrometry using sum normalization calibration," *Anal. Chim. Acta,* vol. 644, no. 1-2, pp. 1-9, Jun 30 2009, doi: https://doi.org/10.1016/j.aca.2009.04.025.

[102] C. Latkoczy, Y. Müller, P. Schmutz, and D. Günther, "Quantitative element mapping of Mg alloys by laser ablation ICP-MS and EPMA," *Applied Surface Science,* vol. 252, no. 1, pp. 127-132, 2005/09/30/ 2005, doi: https://doi.org/10.1016/j.apsusc.2005.02.040.

[103] V. L. Dressler *et al.*, "Biomonitoring of essential and toxic metals in single hair using on-line solution-based calibration in laser ablation inductively coupled plasma mass spectrometry," *Talanta,* vol. 82, no. 5, pp. 1770-1777, 2010/10/15/ 2010, doi: https://doi.org/10.1016/j.talanta.2010.07.065.

[104] L. Strnad, V. Ettler, M. Mihaljevic, J. Hladil, and V. Chrastny, "Determination of Trace Elements in Calcite Using Solution and Laser Ablation ICP-MS: Calibration to NIST SRM Glass and USGS MACS Carbonate, and Application to Real Landfill Calcite," *Geostandards and Geoanalytical Research,* vol. 33, no. 3, pp. 347-355, 2009/09/01 2009, doi: https://doi.org/10.1111/j.1751-908X.2009.00010.x.

[105] A. T. Phung, W. Baeyens, M. Leermakers, S. Goderis, F. Vanhaecke, and Y. Gao, "Reproducibility of laser ablation–inductively coupled plasma–mass spectrometry (LA–ICP–MS) measurements in mussel shells and comparison with micro-drill sampling and solution ICP–MS," *Talanta,* vol. 115, pp. 6-14, 2013/10/15/ 2013, doi: https://doi.org/10.1016/j.talanta.2013.04.019.

[106] T. Stehrer *et al.*, "LA-ICP-MS analysis of waste polymer materials," *Analytical and Bioanalytical Chemistry,* vol. 398, no. 1, pp. 415-424, 2010/09/01 2010, doi: 10.1007/s00216-010-3963-6.

[107] B. Wagner, A. Nowak, E. Bulska, J. Kunicki-Goldfinger, O. Schalm, and K. Janssens, "Complementary analysis of historical glass by scanning electron microscopy with energy dispersive X-ray spectroscopy and laser ablation inductively coupled plasma mass spectrometry," *Microchimica Acta,* vol. 162, no. 3, pp. 415-424, 2008/08/01 2008, doi: 10.1007/s00604-007-0835-7.

[108] P. Nadoll and A. E. Koenig, "LA-ICP-MS of magnetite: methods and reference materials," *Journal of Analytical Atomic Spectrometry,* 10.1039/C1JA10105F vol. 26, no. 9, pp. 1872-1877, 2011, doi: 10.1039/C1JA10105F.

[109] L. Zhang *et al.*, "Lead isotope analysis of melt inclusions by LA-MC-ICP-MS," *Journal of Analytical Atomic Spectrometry,* 10.1039/C4JA00088A vol. 29, no. 8, pp. 1393-1405, 2014, doi: 10.1039/C4JA00088A.

[110] B. Wagner, A. Nowak, E. Bulska, K. Hametner, and D. Günther, "Critical assessment of the elemental composition of Corning archeological reference glasses by LA-ICP-MS," *Analytical and Bioanalytical Chemistry,* vol. 402, no. 4, pp. 1667-1677, 2012/02/01 2012, doi: 10.1007/s00216-011-5597-8.

[111] T. Trejos, S. Montero, and J. R. Almirall, "Analysis and comparison of glass fragments by laser ablation inductively coupled plasma mass spectrometry (LA-ICP-MS) and ICP-MS," *Analytical and Bioanalytical Chemistry,* vol. 376, no. 8, pp. 1255-1264, 2003/08/01 2003, doi: 10.1007/s00216-003-1968-0.

[112] J.-H. Yuan *et al.*, "Quantitative Analysis of Sulfide Minerals by Laser Ablation-Inductively Coupled Plasma-Mass Spectrometry Using Glass Reference Materials with Matrix Normalization Plus Sulfur Internal Standardization Calibration," *Chinese Journal of Analytical Chemistry,* vol. 40, no. 2, pp. 201-207, 2012/02/01/ 2012, doi: https://doi.org/10.1016/S1872-2040(11)60528-8.

[113] J. Willner, L. Brunnbauer, S. Larisegger, M. Nelhiebel, M. Marchetti-Deschmann, and A. Limbeck, "A versatile approach for the preparation of matrix-matched standards for LA-ICP-MS analysis – Standard addition by the spraying of liquid standards," *Talanta,* vol. 256, p. 124305, 2023/05/01/ 2023, doi: https://doi.org/10.1016/j.talanta.2023.124305.

[114] L. Labeyrie, G. S. Vallverdu, D. Michau, S. Fontagné-Dicharry, and S. Mounicou, "Development of polymer films and biological matrices standards for selenium, mercury and endogenous elements quantitative LA-ICP MS imaging in entire rainbow trout fry," *Microchemical Journal,* vol. 194, p. 109204, 2023/11/01/ 2023, doi: https://doi.org/10.1016/j.microc.2023.109204.

[115] Z. Cui, M. He, B. Chen, and B. Hu, "In-situ elemental quantitative imaging in plant leaves by LA-ICP-MS with matrix-matching external calibration," *Analytica Chimica Acta,* vol. 1275, p. 341588, 2023/09/22/ 2023, doi: https://doi.org/10.1016/j.aca.2023.341588.

[116] C. K. Ooi *et al.*, "Development of matrix-specific standards for LA-ICP-MS zinc analysis in sand flathead (Platycephalus bassensis)," *Environmental Pollution,* vol.

344, p. 123415, 2024/03/01/ 2024, doi: https://doi.org/10.1016/j.envpol.2024.123415.

[117] D. J. Bellis, K. M. Hetter, J. Jones, D. Amarasiriwardena, and P. J. Parsons, "Calibration of laser ablation inductively coupled plasma mass spectrometry for quantitative measurements of lead in bone," *Journal of Analytical Atomic Spectrometry,* 10.1039/B603435G vol. 21, no. 9, pp. 948-954, 2006, doi: 10.1039/B603435G.

[118] D. S. Gholap *et al.*, "Comparison of laser ablation-inductively coupled plasma-mass spectrometry and micro-X-ray fluorescence spectrometry for elemental imaging in Daphnia magna," *Analytica Chimica Acta,* vol. 664, no. 1, pp. 19-26, 2010/04/01/ 2010, doi: https://doi.org/10.1016/j.aca.2010.01.052.

[119] J. Cizdziel, K. Bu, and P. Nowinski, "Determination of elements in situ in green leaves by laser ablation ICP-MS using pressed reference materials for calibration," *Analytical Methods,* 10.1039/C1AY05577A vol. 4, no. 2, pp. 564-569, 2012, doi: 10.1039/C1AY05577A.

[120] M. L. Praamsma and P. J. Parsons, "Characterization of calcified reference materials for assessing the reliability of manganese determinations in teeth and bone," *Journal of Analytical Atomic Spectrometry,* 10.1039/C4JA00049H vol. 29, no. 7, pp. 1243-1251, 2014, doi: 10.1039/C4JA00049H.

[121] C.-F. Wang, S.-L. Jeng, C. C. Lin, and P.-C. Chiang, "Preparation of airborne particulate standards on PTFE-membrane filter for laser ablation inductively coupled plasma mass spectrometry," *Analytica Chimica Acta,* vol. 368, no. 1, pp. 11-19, 1998/07/17/ 1998, doi: https://doi.org/10.1016/S0003-2670(98)00028-2.

[122] A. Stankova, N. Gilon, L. Dutruch, and V. Kanicky, "Comparison of LA-ICP-MS and LA-ICP-OES for the analysis of some elements in fly ashes," *Journal of Analytical Atomic Spectrometry,* 10.1039/C0JA00020E vol. 26, no. 2, pp. 443-449, 2011, doi: 10.1039/C0JA00020E.

[123] T. Uryu, J. Yoshinaga, Y. Yanagisawa, M. Endo, and J. Takahashi, "Analysis of Lead in Tooth Enamel by Laser Ablation–Inductively Coupled Plasma–Mass Spectrometry," *Analytical Sciences,* vol. 19, no. 10, pp. 1413-1416, 2003/10/01 2003, doi: 10.2116/analsci.19.1413.

[124] M. Pakieła, M. Wojciechowski, B. Wagner, and E. Bulska, "A novel procedure of powdered samples immobilization and multi-point calibration of LA ICP MS," *Journal of Analytical Atomic Spectrometry,* 10.1039/C0JA00201A vol. 26, no. 7, pp. 1539-1543, 2011, doi: 10.1039/C0JA00201A.

[125] D. Garbe-Schönberg and S. Müller, "Nano-particulate pressed powder tablets for LA-ICP-MS," *J. Anal. At. Spectrom,* 10.1039/C4JA00007B vol. 29, no. 6, pp. 990-1000, 2014, doi: https://doi.org/10.1039/C4JA00007B.

[126] M. Ødegård, J. Mansfeld, and S. H. Dundas, "Preparation of calibration materials for microanalysis of Ti minerals by direct fusion of synthetic and natural materials: Experience with LA–ICP–MS analysis of some important minor and trace elements in ilmenite and rutile," *Fresenius' Journal of Analytical Chemistry,* vol. 370, no. 7, pp. 819-827, 2001/08/01 2001, doi: 10.1007/s002160100844.

[127] M. Kołodziej *et al.*, "Analysis of mercury levels in historical bone material from syphilitic subjects - Pilot studies (short report)," *Anthropologischer Anzeiger; Bericht über die biologisch-anthropologische Literatur,* vol. 69, pp. 367-77, 07/01 2012, doi: 10.1127/0003-5548/2012/0163.

[128] S. Dewaele, P. Muchez, and J. Hertogen, "Production of a matrix-matched standard for quantitative analysis of iron sulphides by laser ablation inductively coupled plasma-mass spectrometry by welding: A pilot study," *Geologica Belgica,* vol. 10, pp. 109-119, 12/01 2007.

[129] P. Cheajesadagul, W. Wananukul, A. Siripinyanond, and J. Shiowatana, "Metal doped keratin film standard for LA-ICP-MS determination of lead in hair samples," *Journal of Analytical Atomic Spectrometry,* 10.1039/C0JA00082E vol. 26, no. 3, pp. 493-498, 2011, doi: 10.1039/C0JA00082E.

[130] A. Ugarte, N. Unceta, C. Pécheyran, M. A. Goicolea, and R. J. Barrio, "Development of matrix-matching hydroxyapatite calibration standards for quantitative multi-element LA-ICP-MS analysis: application to the dorsal spine of fish," *Journal of Analytical Atomic Spectrometry,* 10.1039/C1JA10037H vol. 26, no. 7, pp. 1421-1427, 2011, doi: 10.1039/C1JA10037H.

[131] M. Bonta and A. Limbeck, "Metal analysis in polymers using tandem LA-ICP-MS/LIBS: eliminating matrix effects using multivariate calibration," *Journal of Analytical Atomic Spectrometry,* 10.1039/C8JA00161H vol. 33, no. 10, pp. 1631-1637, 2018, doi: 10.1039/C8JA00161H.

[132] C. Arnaudguilhem *et al.*, "Toward a comprehensive study for multielemental quantitative LA-ICP MS bioimaging in soft tissues," *Talanta,* vol. 222, p. 121537, 2021/01/15/ 2021, doi: https://doi.org/10.1016/j.talanta.2020.121537.

[133] O. Reifschneider *et al.*, "Quantitative bioimaging of platinum in polymer embedded mouse organs using laser ablation ICP-MS," *Metallomics,* 10.1039/C3MT00147D vol. 5, no. 10, pp. 1440-1447, 2013, doi: 10.1039/C3MT00147D.

[134] T. Gao, T. Ren, Y. Zhou, P. Song, and S. Wang, "The production of polymer reference materials for microanalysis with high homogeneity by a 3D printing method," *J. Anal. At. Spectrom.,* 10.1039/D2JA00415A vol. 38, no. 4, pp. 893-901, 2023, doi: 10.1039/D2JA00415A.

[135] R. D. Deegan, O. Bakajin, T. F. Dupont, G. Huber, S. R. Nagel, and T. A. Witten, "Capillary flow as the cause of ring stains from dried liquid drops," *Nature,* vol. 389, no. 6653, pp. 827-829, 1997/10/01 1997, doi: 10.1038/39827.

[136] R. D. Deegan, O. Bakajin, T. F. Dupont, G. Huber, S. R. Nagel, and T. A. Witten, "Contact line deposits in an evaporating drop," *Physical Review E,* vol. 62, no. 1, pp. 756-765, 07/01/ 2000, doi: 10.1103/PhysRevE.62.756.

[137] M. Šala, V. S. Šelih, and J. T. van Elteren, "Gelatin gels as multi-element calibration standards in LA-ICP-MS bioimaging: fabrication of homogeneous standards and microhomogeneity testing," *Analyst,* 10.1039/C7AN01361B vol. 142, no. 18, pp. 3356-3359, 2017, doi: 10.1039/C7AN01361B.

[138] A. Schweikert *et al.*, "Micro-droplet-based calibration for quantitative elemental bioimaging by LA-ICPMS," *Anal. Bioanal. Chem.,* vol. 414, pp. 485-495, 2021/05/05 2022, doi: 10.1007/s00216-021-03357-w.

[139] M. Costas-Rodríguez *et al.*, "Laser ablation-inductively coupled plasma-mass spectrometry for quantitative mapping of the copper distribution in liver tissue sections from mice with liver disease induced by common bile duct ligation," *J. Anal. At. Spectrom.,* 10.1039/C7JA00134G vol. 32, no. 9, pp. 1805-1812, 2017, doi: 10.1039/C7JA00134G.

[140] A. Schweikert *et al.*, "Quantification in elemental bioimaging - evaluation of different calibration strategies enabled by micro-droplets," *Anal. Chim. Acta,* vol. 1223, p. 340200, 2022, doi: 10.1016/j.aca.2022.340200.

[141] S. J. M. Van Malderen, E. Vergucht, M. De Rijcke, C. Janssen, L. Vincze, and F. Vanhaecke, "Quantitative Determination and Subcellular Imaging of Cu in Single Cells via Laser Ablation-ICP-Mass Spectrometry Using High-Density Microarray Gelatin Standards," *Anal. Chem.,* vol. 88, no. 11, pp. 5783-5789, 2016/06/07 2016, doi: 10.1021/acs.analchem.6b00334.

[142] O. Hachmöller *et al.*, "Element bioimaging of liver needle biopsy specimens from patients with Wilson's disease by laser ablation-inductively coupled plasma-mass spectrometry," *Journal of Trace Elements in Medicine and Biology,* vol. 35, pp. 97-102, 2016/05/01/ 2016, doi: https://doi.org/10.1016/j.jtemb.2016.02.001.

[143] J. Liu *et al.*, "Quantitative imaging of trace elements in brain sections of Alzheimer's disease mice with laser ablation inductively coupled plasma-mass spectrometry," *Microchemical Journal,* vol. 172, p. 106912, 2022/01/01/ 2022, doi: https://doi.org/10.1016/j.microc.2021.106912.

[144] M. Cruz-Alonso, B. Fernandez, A. Navarro, S. Junceda, A. Astudillo, and R. Pereiro, "Laser ablation ICP-MS for simultaneous quantitative imaging of iron and ferroportin in hippocampus of human brain tissues with Alzheimer's disease," *Talanta,* vol. 197, pp. 413-421, 2019/05/15/ 2019, doi: https://doi.org/10.1016/j.talanta.2019.01.056.

[145] M. T. Westerhausen *et al.*, "Low background mould-prepared gelatine standards for reproducible quantification in elemental bio-imaging," *Analyst,* 10.1039/C9AN01580A vol. 144, no. 23, pp. 6881-6888, 2019, doi: 10.1039/C9AN01580A.

[146] K. Billimoria *et al.*, "The potential of bioprinting for preparation of nanoparticle-based calibration standards for LA-ICP-ToF-MS quantitative imaging," *Metallomics,* vol. 14, no. 12, p. mfac088, 2022, doi: 10.1093/mtomcs/mfac088.

[147] J. S. Becker, M. V. Zoriy, M. Dehnhardt, C. Pickhardt, and K. Zilles, "Copper, zinc, phosphorus and sulfur distribution in thin section of rat brain tissues measured by laser ablation inductively coupled plasma mass spectrometry: possibility for small-size tumor analysis," *J. Anal. At. Spectrom.,* 10.1039/B504978B vol. 20, no. 9, pp. 912-917, 2005, doi: 10.1039/B504978B.

[148] D. J. Hare, J. Lear, D. Bishop, A. Beavis, and P. A. Doble, "Protocol for production of matrix-matched brain tissue standards for imaging by laser ablation-inductively coupled plasma-mass spectrometry," *Analytical Methods,* vol. 5, no. 8, 2013, doi: 10.1039/c3ay26248k.

[149] K. Jurowski *et al.*, "A standard sample preparation and calibration procedure for imaging zinc and magnesium in rats' brain tissue by laser ablation-inductively

coupled plasma-time of flight-mass spectrometry," *J. Anal. At. Spectrom.,* vol. 29, no. 8, pp. 1425-1431, 2014, doi: 10.1039/c3ja50378j.

[150] K. Billimoria, D. N. Douglas, G. Huelga-Suarez, J. F. Collingwood, and H. Goenaga-Infante, "Investigating the effect of species-specific calibration on the quantitative imaging of iron at mg kg−1 and selenium at μ g kg−1 in tissue using laser ablation with ICP-QQQ-MS," *Journal of Analytical Atomic Spectrometry,* vol. 36, no. 5, pp. 1047-1054, 2021, doi: 10.1039/d1ja00042j.

[151] A. E. Egger *et al.*, "Quantitative bioimaging by LA-ICP-MS: a methodological study on the distribution of Pt and Ru in viscera originating from cisplatin- and KP1339-treated mice," *Metallomics,* 10.1039/C4MT00072B vol. 6, no. 9, pp. 1616-1625, 2014, doi: 10.1039/C4MT00072B.

[152] C. R. VanderSchee, D. Frier, D. Kuter, K. K. Mann, B. P. Jackson, and D. S. Bohle, "Quantification of local zinc and tungsten deposits in bone with LA-ICP-MS using novel hydroxyapatite-collagen calibration standards," *J Anal At Spectrom,* vol. 36, no. 11, pp. 2431-2438, Nov 2021, doi: 10.1039/d1ja00211b.

[153] M. L. Praamsma and P. J. Parsons, "Calibration strategies for quantifying the Mn content of tooth and bone samples by LA-ICP-MS," *Accreditation and Quality Assurance,* vol. 21, no. 6, pp. 385-393, 2016, doi: 10.1007/s00769-016-1234-8.

[154] M. T. Westerhausen *et al.*, "Preparation of matrix-matched standards for the analysis of teeth via laser ablation-inductively coupled plasma-mass spectrometry," *Anal. Meth.,* 10.1039/D2AY02015G vol. 15, no. 6, pp. 797-806, 2023, doi: 10.1039/D2AY02015G.

[155] D. Pozebon, V. L. Dressler, A. Matusch, and J. S. Becker, "Monitoring of platinum in a single hair by laser ablation inductively coupled plasma mass spectrometry (LA-ICP-MS) after cisplatin treatment for cancer," *International Journal of Mass Spectrometry,* vol. 272, no. 1, pp. 57-62, 2008/04/15/ 2008, doi: https://doi.org/10.1016/j.ijms.2008.01.001.

[156] S. Byrne *et al.*, "Were Chinchorros exposed to arsenic? Arsenic determination in Chinchorro mummies' hair by laser ablation inductively coupled plasma-mass spectrometry (LA-ICP-MS)," *Microchemical Journal,* vol. 94, no. 1, pp. 28-35, 2010/01/01/ 2010, doi: https://doi.org/10.1016/j.microc.2009.08.006.

[157] U. Kumtabtim, A. Matusch, S. Ulhoa Dani, A. Siripinyanond, and J. Sabine Becker, "Biomonitoring for arsenic, toxic and essential metals in single hair strands by laser ablation inductively coupled plasma mass spectrometry," *International Journal of Mass Spectrometry,* vol. 307, no. 1, pp. 185-191, 2011/10/01/ 2011, doi: https://doi.org/10.1016/j.ijms.2011.03.007.

[158] R. Luo, X. Su, W. Xu, S. Zhang, X. Zhuo, and D. Ma, "Determination of arsenic and lead in single hair strands by laser ablation inductively coupled plasma mass spectrometry," *Sci Rep,* vol. 7, no. 1, p. 3426, Jun 13 2017, doi: 10.1038/s41598-017-03660-6.

[159] C. O' Connor, B. L. Sharp, and P. Evans, "On-line additions of aqueous standards for calibration of laser ablation inductively coupled plasma mass spectrometry: theory and comparison of wet and dry plasma conditions," *Journal of Analytical*

Atomic Spectrometry, 10.1039/B600916F vol. 21, no. 6, pp. 556-565, 2006, doi: 10.1039/B600916F.

[160] D. Pozebon, V. L. Dressler, M. F. Mesko, A. Matusch, and J. S. Becker, "Bioimaging of metals in thin mouse brain section by laser ablation inductively coupled plasma mass spectrometry: novel online quantification strategy using aqueous standards," *Journal of Analytical Atomic Spectrometry,* vol. 25, no. 11, 2010, doi: 10.1039/c0ja00055h.

[161] H. Sela, Z. Karpas, M. Zoriy, C. Pickhardt, and J. S. Becker, "Biomonitoring of hair samples by laser ablation inductively coupled plasma mass spectrometry (LA-ICP-MS)," *International Journal of Mass Spectrometry,* vol. 261, no. 2, pp. 199-207, 2007/03/15/ 2007, doi: https://doi.org/10.1016/j.ijms.2006.09.018.

[162] G. Zhang, Q. Li, Y. Zhu, and Z. Wang, "Solution-based calibration strategy for laser ablation–inductively coupled plasma–mass spectrometry using desolvating nebulizer system," *Spectrochimica Acta Part B: Atomic Spectroscopy,* vol. 145, pp. 51-57, 2018/07/01/ 2018, doi: https://doi.org/10.1016/j.sab.2018.04.004.

[163] C.-K. Yang, P.-H. Chi, Y.-C. Lin, Y.-C. Sun, and M.-H. Yang, "Development of an on-line isotope dilution laser ablation inductively coupled plasma mass spectrometry (LA–ICP-MS) method for determination of boron in silicon wafers," *Talanta,* vol. 80, no. 3, pp. 1222-1227, 2010/01/01/ 2010, doi: https://doi.org/10.1016/j.talanta.2009.09.013.

[164] C. Pickhardt, J. S. Becker, and H.-J. Dietze, "A new strategy of solution calibration in laser ablation inductively coupled plasma mass spectrometry for multielement trace analysis of geological samples," *Fresenius' Journal of Analytical Chemistry,* vol. 368, no. 2, pp. 173-181, 2000/09/01 2000, doi: 10.1007/s002160000485.

[165] C. Pickhardt, A. V. Izmer, M. V. Zoriy, D. Schaumlöffel, and J. Sabine Becker, "On-line isotope dilution in laser ablation inductively coupled plasma mass spectrometry using a microflow nebulizer inserted in the laser ablation chamber," *International Journal of Mass Spectrometry,* vol. 248, no. 3, pp. 136-141, 2006/02/15/ 2006, doi: https://doi.org/10.1016/j.ijms.2005.11.001.

[166] D. N. Douglas, J. O'Reilly, C. O'Connor, B. L. Sharp, and H. Goenaga-Infante, "Quantitation of the Fe spatial distribution in biological tissue by online double isotope dilution analysis with LA-ICP-MS: a strategy for estimating measurement uncertainty," *Journal of Analytical Atomic Spectrometry,* vol. 31, no. 1, pp. 270-279, 2016, doi: 10.1039/c5ja00351b.

[167] L. Feng, J. Wang, H. Li, X. Luo, and J. Li, "A novel absolute quantitative imaging strategy of iron, copper and zinc in brain tissues by Isotope Dilution Laser Ablation ICP-MS," *Anal. Chim. Acta,* vol. 984, pp. 66-75, 2017/09/01/ 2017, doi: https://doi.org/10.1016/j.aca.2017.07.003.

[168] I. Moraleja *et al.*, "An approach for quantification of platinum distribution in tissues by LA-ICP-MS imaging using isotope dilution analysis," *Talanta,* vol. 178, pp. 166-171, 2018/02/01/ 2018, doi: https://doi.org/10.1016/j.talanta.2017.09.031.

[169] L.-N. Zheng *et al.*, "Single-Cell Isotope Dilution Analysis with LA–ICP–MS: A New Approach for Quantification of Nanoparticles in Single Cells," *Analytical*

Chemistry, vol. 92, no. 21, pp. 14339-14345, 2020/11/03 2020, doi: 10.1021/acs.analchem.0c01775.

[170] J. Liu *et al.*, "Isotope dilution LA-ICP-MS for quantitative imaging of trace elements in mouse brain sections," *Anal. Chim. Acta,* vol. 1273, p. 341524, 2023/09/08/ 2023, doi: https://doi.org/10.1016/j.aca.2023.341524.

[171] H. Pan, L. Feng, Y. Lu, Y. Han, J. Xiong, and H. Li, "Calibration strategies for laser ablation ICP-MS in biological studies: A review," *TrAC Trends in Analytical Chemistry,* vol. 156, p. 116710, 2022/11/01/ 2022, doi: https://doi.org/10.1016/j.trac.2022.116710.

[172] D. Metarapi *et al.*, "Semiquantitative Analysis for High-Speed Mapping Applications of Biological Samples Using LA-ICP-TOFMS," *Analytical Chemistry,* 2023/04/25 2023, doi: 10.1021/acs.analchem.3c01439.

Bibliography

Publications Related to the Thesis

Journal Articles

A. Jerše, K. Mervič, J. T. van Elteren, V. S. Šelih, in M. Šala, „Quantification anomalies in single pulse LA-ICP-MS analysis associated with laser fluence and beam size“, Analyst (London), let. 147, št. 23, str. 5293–5299, 2022, doi: 10.1039/d2an01172g.

J. T. van Elteren, D. Metarapi, K. Mervič, in M. Šala, „Exploring the Benefits of Ablation Grid Adaptation in 2D/3D Laser Ablation Inductively Coupled Plasma Mass Spectrometry Mapping through Geometrical Modeling“, Analytical chemistry (Washington), let. 95, št. 26, str. 9863–9871, 2023, doi: 10.1021/acs.analchem.3c00774.

K. Mervič, J. T. van Elteren, M. Bele, in M. Šala, „Utilizing ablation volume for calibration in LA-ICP-MS mapping to address variations in ablation rates within and between matrices“, Talanta (Oxford), let. 269, str. 125379–125379, 2023, doi: 10.1016/j.talanta.2023.125379.

T. Van Helden, K. Mervič, I. Nemet, J. T. van Elteren, F. Vanhaecke, S. Rončević, M. Šala, T. Van Acker, “Evaluation of two-phase sample transport upon ablation of gelatin as a proxy for soft biological matrices using nanosecond laser ablation - inductively coupled plasma - mass spectrometry“, Analytica chimica acta, let. 1287, str. 342089–342089, 2024, doi: 10.1016/j.aca.2023.342089.

K. Mervič, V. S. Šelih, M. Šala, in J. T. van Elteren, „Non-matrix-matched calibration in bulk multi-element laser ablation - Inductively coupled plasma - Mass spectrometry analysis of diverse materials“, Talanta (Oxford), let. 271, 2024, doi: 10.1016/j.talanta.2024.125712.

K. Mervič, M. Šala, in S. Theiner, „Calibration approaches in laser ablation inductively coupled plasma mass spectrometry for bioimaging applications“, TrAC, Trends in analytical chemistry (Regular ed.), 2024, doi: 10.1016/j.trac.2024.117574.

Conference Papers

K. Mervič, A. Jerše, M. Šala, J. T. van Elteren, in V. S. Šelih, „Laser fluence and beam size influence on precision in single pulse LA-ICP-MS analysis“, in Abstract Book: European workshop on laser ablation (EWLA 2022), Bern, Switzerland, 12.07. - 15.07.2022.

V. S. Šelih, M. Šala, K. Mervič, in J. T. van Elteren, „Laser ablation ICP-MS - where do we come from and where do we go?“, SAAS22: 1. Simpozij analitičke atomske spektrometrije, str. 14, 2022.

K. Mervič, A. Jerše, M. Šala, J. T. van Elteren, in V. S. Šelih, „Influence of laser fluence and beam size on aerosol formation and effect on precision in LA-ICP-MS analysis“, in Abstract Book: European Winter Conference on Plasma Spectrochemistry (EWCPS 2023), Ljubljana, Slovenia, 29.01. - 03.02.2023.

D. Metarapi, J. T. van Elteren, K. Mervič, in M. Šala, „Enhancing LA-ICP-MS image quality through ablation grid optimization“, in Abstract Book: North American workshop on laser ablation (NAWLA 2023), South Bend, Indiana, USA, 05.06. - 09.06.2023.

K. Mervič, J. T. van Elteren, V. S. Šelih, in M. Šala, „Ablation volume-aided calibration in 2D LA-ICP-MS mapping to correct for differences in ablated mass“, in Abstract Book: North American workshop on laser ablation (NAWLA 2023), South Bend, Indiana, USA, 05.06. - 09.06.2023.

K. Mervič, J. T. van Elteren, V. S. Šelih, in M. Šala, „Exploring the Impact of Laser Ablation Energy Density on Biological Samples Analysis via LA-ICP-MS “, in Abstract Book: 9th International Symposium on Metallomics (ISM9), London, UK, 17.06. - 21.06.2024

K. Mervič, J. T. van Elteren, V. S. Šelih, in M. Šala, „Correcting Ablated Mass Differences in 2D LA-ICP-MS Mapping through Ablation Volume-Assisted Calibration“, in Abstract Book: European workshop on laser ablation (EWLA 2024), Ghent, Belgium, 02.07. - 05.07.2024.

Biography

The author of this thesis, Kristina Mervič, began her higher education at the Faculty of Pharmacy at the University of Ljubljana, specializing in cosmetology. She completed her academic bachelor's degree in 2018 with a thesis on "In silico evaluation of irritation and sensitization potential of selected cosmetic ingredients, structurally related to cinnamic acid". During her bachelor's degree, she spent six months researching hair care at the Department of Cosmetic Science at the University of Arts in London. After graduating, she continued her education at Liverpool John Moores University, where she completed her Master's degree in Cosmetic Science with distinction in 2019. Her Master's thesis project was carried out in collaboration with Unilever and focused on the development of an HPLC analytical approach for the analysis of active ingredients in cosmetic formulations; for confidentiality reasons, the title is not disclosed. She then remained at Unilever in the Research and Technology department until 2020. During this time, her research focused on the development of a new sweat management formulation. The formulation was filed for patent in 2022 in the field of cosmetic compositions and their use as sweat management compositions, in particular as aluminum-free sweat management compositions, and has since been patented under the name Cosmetic sweat management compositions (WO2023117481A1) in collaboration with Unilever.

In October 2020, she started her work at the National Institute of Chemistry as a Young Researcher under the supervision of Dr. Vid Simon Šelih and Dr. Martin Šala. She was part of the laser ablation group in the Department of Analytical Chemistry. In the meantime, she also enrolled in doctoral studies at the Jožef Stefan International Postgraduate School, Ecotechnologies program. During her doctoral studies, she published four first-author and two co-author papers in high-ranking journals. She presented her research work at numerous international conferences (*e.g.* EWLA 2022, EWCPS 2023, NAWLA 2023, EWLA 2024, ISM9 2024) and was awarded EWLA 2024 upcoming talent award. She was also part of the organizing group of the European Winter Conference on Plasma Spectrochemistry. Before finishing her PhD, she spent two months in Berlin, where she worked on a microplastics research in collaboration with the BAM Institute in the group of Björn Meermann. In September 2024, she successfully completed all courses and experimental work required to complete the PhD program, resulting to this dissertation.